THERMODYNAMIC MODELLING OF INDUSTRIAL RELEVANT ELECTROLYTE SOLUTIONS.

DISSERTATION ZUR ERLANGERUNG DES DOKTORGRADES
DER NATURWISSENSCHAFTEN (DR. RER. NAT.)
DER NATURWISSENSCHAFTLICHEN FALKULTÄT IV
CHEMIE & PHARMAZIE
DER UNIVERSITÄT REGENSBURG

Vorgelegt von

Nicolas Papaiconomou aus Paris, Frankreich

2003

Promotiongesuch angereicht am:	1. Juni 2003
Die Arbeit wurde angeleitet vom:	Professor Doktor Werner Kunz
Prüfungsauschuss:	Herr Prof. Doktor Gerd Maurer
	Herr Doktor Christophe Monnin
	Herr Prof. Doktor Pierre Turq
	Herr Doktor Jean-Pierre Simonin
	Herr Prof. Doktor Werner Kunz

Remerciements

Cette dissertation est le fruit d'un travail de thèse réalisé en coopération entre deux laboratoires, situés en France et en Allemagne. En Allemagne d'abord, ou plus exactement en Bavière, où le laboratoire de Chimie physique et théorique de l'Université de Regensburg dirigé par le Professeur Werner Kunz m'a accueilli pendant toute la durée de cette thèse. Ayant véritablement vécu pendant toute cette période à Regensburg, mes remerciements iront d'abord aux collaborateurs allemands que j'ai cotoyés.

Je remercie Werner Kunz, pour le soutien et l'accueil si chaleureux qui m'a été réservé. Accueil francophone qui plus est, ce qui m'a largement facilité la prise de contact avec mon environnement. Je le remercie également pour sa direction de thèse, ses conseils vis-à-vis du sujet, et sur nos nombreuses discussions toujours fructueuses, tant sur le plan scientifiques que culturelles.

Je remercie également la petite équipe francaise du laboratoire. Patrick d'abord, qui a eu la responsabilité de m'aider à régler les tracasseries administratives dés mon arrivée à Regensburg. Didier également pour ses avis et sa vision plus expérimentale de la chimie. Merci aussi à Pierre pour sa vivacité et sa connaissance de la chimie pratique. Nos discussions scientifiques furent toujours passionnées et riches d'enseignement. Merci aussi à sa compagne Audrey pour sa gentillesse et nos discussions toujours à contre-courant, et donc, intéressantes.

Je remercierai ensuite l'équipe d'électrochimie de l'institut que j'ai côtoyé au quotidien et avec qui j'ai pu si bien me changer les idées, en particulier après 19 heures… Je remercie spécialement Heiner Gores pour sa chaleur, son amitié, son enthousiasme pour la chimie et ses échanges scientifiques toujours enrichissants, mais également pour son goût des « bonnes choses ».
Merci également à Roland Neuder pour son aide à chacune de mes interrogations sur la thermodynamique, et pour sa bonne humeur.

Je remercie également Wolfgang Simon pour sa jovialité et son enseignement des finesses de la langue bavaroise…
Merci et bon courage également à tous ceux du labo qui commencent (courage Julia et Stefen), sont en train ou ont fini leur thèse et grâce à qui mon séjour a été aussi enrichissant qu'instructif.

Je finirai en remerciant Sharka et John qui sont devenus de véritables amis, et avec qui nous avons partagé autant notre vie professionnelle que privée. Je n'oublierai pas notre collaborateur japonais Takahaki à la compagnie très chaleureuse, et avec qui j'ai passé de si bons moments.

Merci enfin à tout ceux que j'ai pu côtoyer de près ou de loin, et que je n'ai pas pu citer ici.

Le laboratoire Li2C m'a accueilli dés mon stage DEA voilà plus de 4 ans. En tant que directeur du laboratoire, je voulais remercier Pierre Turq pour le soutien qu'il m'a toujours apporté. Merci aussi pour sa chaleur et sa bonne humeur, et également pour ses conseils aussi bien sur le plan scientifique que professionnel.

Merci ensuite à mon directeur de stage de DEA puis de thèse, Jean-Pierre Simonin qui est parvenu à m'inculquer la rigueur nécessaire à la réalisation de tout travail scientifique. Merci aussi pour son objectivité scientifique, et son soutien au quotidien.

Ce travail n'aurait pas non plus été possible sans l'aide d'Olivier Bernard, dont les valeurs tant scientifiques qu'humaines ne sont plus à démontrer. Merci pour toute l'aide qu'il a pu m'apporter pour comprendre un peu plus le monde de la mécanique statistique en particulier, et toute la bonne humeur qu'il a pu me communiquer.

Merci à Jean Chevalet, qui a toujours su m'encourager et me motiver à persévérer dans la recherche. Merci à Marie Jardat et à Serge Vidal, Eric Balnois pour leur bonne humeur et leur accueil chaleureux à chacun de mes passages au laboratoire.

Merci aussi à Yann, Jean-Francois, Virginie et Antony pour leur présence qui a facilité ma réintégration chronique dans le labo, et pour les discussions intéréssantes que nous avons pu avoir.

J'achèverai en remerciant les secrétaires des deux labos qui m'ont tant aidé dans les tâches administratives, tant en France qu'en Allemagne.

Et merci à mon petit frère, devenu si grand maintenant, à mon père qui me fit l'honneur d'être présent à ma thèse, et de remettre le pied sur le sol parisien, délaissé 20 ans auparavant. Merci enfin à ma mère pour son soutien de tous les instants, et tout ce qu'elle a fait pour moi depuis… 27ans. Merci enfin à tous deux pour ces retrouvailles familiales auxquelles Hugo et moi avons pu assister en cette douce soirée du 18 juillet 2003.

TABLE OF CONTENTS

Chapter I- Introduction

The theoretical study of electrolyte theory goes back to the 19th century with the work of Kohlrausch who was the first to establish alaw for the conductivity as a function of the square root of concentration. Later, Debye and Hückel, and Onsager, brought theoretical justifications of the Kohlrausch law. Debye and Hückel calculated the departure from ideality of electrolyte solutions with a linearised Poisson-Boltzmann equation by assuming that in diluted solutions, ions could be regarded as point charges surrounded by an ionic atmosphere. They established the infinite dilution limiting law, called the Debye-Hückel limiting law (the point charge assumption is justified at very low concentrations). This important expression is however not applicable to electrolytes solutions at concentration above 0.01 M.

Later, other types of models have been developed to extend the Debye-Hückel law to higher concentrations. The first extension was of to impose a closest approach distance to ions. Precisely, the ions in the cloud could not approach the central ion by more than some distance.

Since that time, other semi-empirical models have been developed, such as the Bromley model, the Davis model or the Pitzer model. This latter model took the expressions of the osmotic coefficient obtained from the extended Debye-Hückel law and applied a virial expansion in molality, as recommended by other theories (Guggenheim).

The success of the Pitzer model lies in the fact that it opens the way to the description of highly concentrated solutions, up to 6 or 10 mol/kg, with only a few parameters. Nevertheless, these parameters have a very limited physical meaning, since the virial expansion was empirically introduced in the model.

Another way of investigation has also been explored by using the statistical mechanics in order to obtain thermodynamic quantities for ionic solutions. This has been carried out with the help of the Ornstein-Zernicke (OZ) equation which will be detailed in Chapter III, and by treating the solution in the McMillan Mayer formalism.

The OZ equation treats statistically and rigorously the interactions between particles by taking into account the direct interaction between 1 and 2 for example, and also the indirect interactions between 1 and 2 due to the presence of a particle 3 and 4, indirectly interacting on 1 and 2.

The MM formalism considers the solvent as a continuum characterised by its permittivity ε, in which the solute is immersed. This solute can be considered in this case as a gas of solute in the sense of Van't Hoff.

Different closure relations to the OZ equation have been worked out, such as HNC, MSA, or PY. The MSA model, that has been utilised in our work, is adequate to the description of charged hard spheres in a continuum, and has the main advantage of giving simple analytical expressions.

These statistical models have been mostly applied, until now, to simple aqueous electrolyte solutions, such as ions in water solvent, and rarely to complex chemical solutions. Such solutions are composed of many neutral and charged species exhibiting chemical equilibria, and vapour-liquid equilibria.

Besides, these models, built in the MM framework, do not explicitely take into account the solvent effect on the thermodynamic properties of solutions. This poses a problem in many cases, such as multi-solvent solutions, or for the description of solutions over the whole mole fraction scale (from pure solvent to pure fused salts).

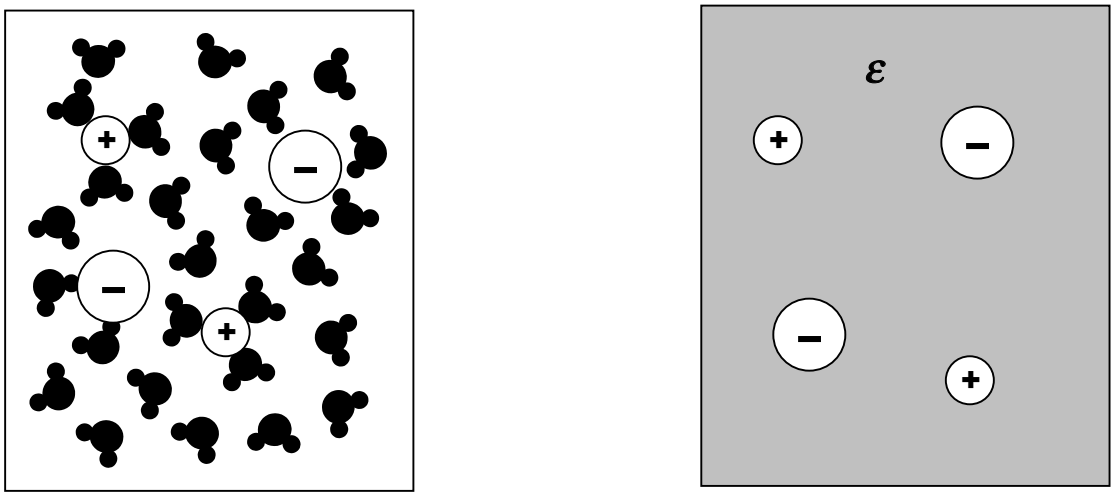

Figure 1.1- Representation of a solution in the experimental referential and in the McMillan Mayer framework. Left picture: description of an electrolyte solution with discrete solvent. Right picture: description of an electrolyte solutions in the McMillan Mayer framework. The solvent is no more discrete, and is caracterised by its permittivity ε.

A gap has then appeared between the industrial needs of describing the thermodynamic properties of complex chemical solutions and available theoretical models.

Various applied and engineering oriented models have been developed in order to describe or predict the thermodynamic properties of industrially relevant solutions. These empirical models were mostly designed for the description of solution of neutral solutes. The expectations for these models are, unlike theoretical models, to give the general behaviour of solutions and the shape of

thermodynamic properties curves. Unlike MM models, these models are for example the Wilson mode, the Wohl's expansion, the NRTL model or the UNIQUAC model. These models, in which the solvent is not explicitely taken into account) calculate the excess Gibbs energy of solutions, yielding equation of state in the experimental level of description (constant temperature and pressure).

Such models have been well optimised for the description of multi-component systems of neutral species. But since the equations are empirical and based on neutral solute solutions, they do not originally follow the DH Limiting Law, and are therefore unable to describe the effects of charges in a solution. This limitation is rather restrictive since electrolytes greatly influence the properties of a system. For instance, the solubility pressure of carbon dioxide (CO_2) in water depends on the nature of the salt introduced in the solution, resulting in a strong extra-solubilisation (salting-in effect), or, on the contrary, in a desolubilisation (salting-out effect) of the CO_2. Electrolytes also favour the mixing of originally immiscible solvents, and vice-versa.

Since electrostatic interactions are long range interactions, and neutral solute interactions are short-ranged, the simplest way for extending empirical models for neutral solutes to electrolyte solutions, is to consider the excess Gibbs energy as the sum of two contributions, namely a long-range and a short-range interaction, respectively.

$$G^{ex} = G^{LR} + G^{SR}$$

with G^{LR} the long-range electrostatic Gibbs energy and G^{SR} the short-range excess Gibbs energy as given by empirical models for neutral solute solutions.

The short-trange contribution is calculated with the help of empirical models for neutral solute solutions, and the long-range contribution is calculated with the help of electrolyte models.

Until now, the long-range term has been calculated with the Pitzer-Debye-Hückel term, as introduced by Pitzer. It is an extended Debye-Hückel term adapted to the Gibbs energy formalism. Such models yield general expressions of the Gibbs energy of neutral solutes and of solutions of electrolytes. When no ion is present in the solution, we have simply $G^{LR}=0$.

The adaptation of statistical mechanics models to the needs of chemical engineering correspond to the main idea concerning this thesis. We first tried to apply already existing theoretical models to the description of industrially relevant systems, and second to develop semi-empirical models with improved electrostatic terms, relating empirical and theoretical models, in order to obtain more physical but still flexible equations.

DISSERTATION PLAN

Chapter II will be devoted to the basic thermodynamics required for the knowledge and the description of the macroscopic behaviour of chemical solutions. Also an overview of the various and most well-known empirical models used in chemical engineering is given.

Chapter III gives the basics of the statistical MSA model. We will introduce the Ornstein Zernicke equation, and the different closure realtions. After that, the MSA model is introduced, first by summarising the different extensions brought to this model in order to extend it to highly concentrated solutions, and second by detailing the temperature dependence introduced by us in the MSA model in order to apply the model to the description of solutions at temperatures above 298K.

Chapters IV and V will be devoted to two new applications of the MSA model. First, the case of the solubility of LiCl hydrates will be detailed, for which we predict the thermodynamic properties, such as ΔH, ΔS and Cp. Second, the solubility pressure of carbon dioxide over aqueous electrolyte CO_2-containing solutions will be considered. The description of such complex solutions is done here for the first time with the MSA model.

Chapter VI of this dissertation contains to the study of a new semi-empirical electrolyte model, the MSA-NRTL, in which we used the well-known NRTL model, adapted to highly concentrated electrolyte solutions, and the electrostatic contribution of the MSA model, replacing the classical PDH term. This model has been successfully applied to aqueous electrolyte solutions, to solutions composed of one salt and two solvents, and to the description of thermodynamic properties of electrolyte solutions at high temperatures.

Finally, a short conclusion of our work is given.

Chapter II- Description of solutions

Thermodynamics is the science of the properties (i.e., temperature, pressure, volume) of systems at equilibrium. It was first developed during the 19th century with the works of Sadi Carnot for instance on new heat machines. Since this time, thermodynamics has been applied and extended to all science fields, such as biology, physics, chemistry and even astronomy. This science has been successfully applied in the domain of chemistry and is indeed the most helpful tool for analysing and optimising a chemical reaction.

About thermodynamics, Einstein said:

"A theory is the more impressive the greater the simplicity of its premises is, the more different kinds of things it relates, and the more extended is its area of applicability. Therefore, the deep impression which classical thermodynamics made upon me. It is the only physical theory of universal content concerning which I am convinced that, within the framework of the applicability of its basic concepts, it will never be overthrown."[1]

Firstly developed for macroscopic systems to determine the efficiency of machines, thermodynamics did not require any knowledge on the microscopic "molecular" state of the system for establishing its laws. Thermodynamic laws are thus of "universal content" because they are independent of the nature and the size of the system. The thermodynamic principles and expressions are gathered under the term "classical thermodynamics".

The coming out of the atomic theory at the end of the 19th century opened the doors to another thermodynamics, known as "statistical thermodynamics". This science, in opposition to "classical thermodynamics" developed for macroscopic systems, applies the thermodynamic principles to a molecular scale, bringing a microscopic notion to the classical thermodynamic properties, as pressure for instance.

The aim of the following chapter is not to make an exhaustive review of thermodynamics but to summarise the main concepts and models used nowadays in chemical thermodynamics. To that end, we will follow the book written by Prausnitz, Lichtenthaler and de Azevedo [1].

[1] From „Albert Einstein: Philosopher-Scientist" edited by P. A. Schlipp, Open Court Publishing company, La Salle, IL (1973).

The first section will be devoted to a simple summary of the basic variables and coefficients of a thermodynamic system. The second section will be devoted to the empirical description of non-ionic solutions.

A. Fundamentals of thermodynamics

1. Homogeneous closed systems

A closed system is a system that does not exchange matter with its surrounding, but it may exchange energy. A homogeneous system is a system with uniform properties, in a macroscopic sense. The density for instance has the same value in any point of the system.
There are four variables, which are divided in two groups.

- The extensive variables are variables that depend on the nature of the system. These are the volume V and the entropy S.
- The intensive variables are variables that are not dependent on the size of the system. These are the pressure P and the temperature T.

A small change in the internal energy function U, is defined as follows

$$dU = TdS - PdV \tag{2.1}$$

That is, U is a function of only two independent variables, S and V. Since there are four variables, three other energy functions are defined

$$dF = -SdT - PdV \tag{2.2}$$

$$dH = TdS + VdP \tag{2.3}$$

$$dG = -SdT + VdP \tag{2.4}$$

F is called the Helmholtz free energy, *H* the enthalpy and *G* the Gibbs energy. These functions are state functions, which means that the integration of the differential form of these functions is independent of the way of integration.

The definitions of these four state functions are:

$$F = U - TS \tag{2.5}$$

$$H = U + PV \tag{2.6}$$

$$G = U - TS + PV \tag{2.7}$$

Regarding eqns. (2.1) to (2.4), the different T, P, S and V variables correspond to the partial differentials of the state functions. This can be obtained by writing the mathematic derivative expression of each state function. The free Helmholtz energy is here used as an example:

$$dF = -\left.\frac{\partial F}{\partial T}\right|_V dT - \left.\frac{\partial F}{\partial V}\right|_T dV \tag{2.8}$$

Combined to eqn. (2.2) one obtains the relations for S and P:

$$S = -\left.\frac{\partial F}{\partial T}\right|_V \qquad P = -\left.\frac{\partial F}{\partial V}\right|_T \tag{2.9}$$

These relations are part of the so-called Maxwell relations and are collected in Table 2.1.

Table 2.1- Maxwell relations and identities for a homogeneous closed system.

Fundamental Equations

$dU = TdS - PdV$ $\qquad$ $dH = TdS + VdP$

$dF = -SdT - PdV$ $\qquad$ $dG = -SdT + VdP$

Maxwell Relations

$$\left.\frac{\partial T}{\partial V}\right|_S = -\left.\frac{\partial P}{\partial S}\right|_V \qquad \left.\frac{\partial S}{\partial V}\right|_T = \left.\frac{\partial P}{\partial T}\right|_V$$

$$\left.\frac{\partial T}{\partial P}\right|_S = \left.\frac{\partial V}{\partial S}\right|_P \qquad \left.\frac{\partial S}{\partial P}\right|_T = -\left.\frac{\partial V}{\partial T}\right|_P$$

Identities

$$T = \left.\frac{\partial U}{\partial S}\right|_V = -\left.\frac{\partial H}{\partial S}\right|_P \qquad V = \left.\frac{\partial H}{\partial P}\right|_S = -\left.\frac{\partial G}{\partial P}\right|_T$$

$$-P = \left.\frac{\partial U}{\partial V}\right|_S = \left.\frac{\partial F}{\partial V}\right|_T \qquad -S = \left.\frac{\partial F}{\partial T}\right|_V = \left.\frac{\partial G}{\partial T}\right|_P$$

$$\left.\frac{\partial U}{\partial V}\right|_T = T\left.\frac{\partial P}{\partial T}\right|_V - P \qquad \left.\frac{\partial H}{\partial P}\right|_T = V - S\left.\frac{\partial V}{\partial T}\right|_P$$

2. Homogeneous open systems

An open system can exchange matter and energy with its surroundings. We now consider how laws of thermodynamics for a closed system can be extended to apply to an open system. For a closed system, we considered U to be a function of *S* and *V*

$$U = U(S,V) \tag{2.10}$$

In an open system, however, there are additional independent variables. For these, we can use the mole numbers of the various components present. Hence, *U* is the function

$$U = U\left(S, V, n_1, n_2, \ldots n_m\right) \tag{2.11}$$

where m is the number of components. The mole number n_i, is an extensive variable. The total differential form is then

$$dU = \left.\frac{\partial U}{\partial S}\right|_{V,n_i} dS - \left.\frac{\partial U}{\partial V}\right|_{S,n_i} dV + \sum_i \left.\frac{\partial U}{\partial n_i}\right|_{S,V,n_j} dn_i \tag{2.12}$$

where subscript n_i and n_j refer to all mole numbers. Because the first two derivatives in eqn. (2.12) refers to a closed system, we may use the identities of table 1.1. Further, the function μ_i is defined as

$$\mu_i = \left.\frac{\partial U}{\partial n_i}\right|_{S,V,n_j} \tag{2.13}$$

And eqn. (2.13) may be rewritten in the form

$$dU = TdS - PdV + \sum_i \mu_i dn_i \tag{2.14}$$

As for closed systems, the three other state functions that are F, G and H may be written as

$$dF = -SdT - PdV + \sum_i \mu_i dn_i \tag{2.15}$$

$$dH = TdS + VdP + \sum_i \mu_i dn_i \tag{2.16}$$

$$dG = -SdT + PdV + \sum_i \mu_i dn_i \tag{2.17}$$

The variable μ_i is the so-called chemical potential. It is an intensive quantity, depending on pressure, temperature and composition of the system. Eqn. (2.13) for the chemical potential can also be considerer as a differential of A, H, and G state functions and be written as follows

$$\mu_i = \left.\frac{\partial F}{\partial n_i}\right|_{T,V,n_j} = \left.\frac{\partial H}{\partial n_i}\right|_{S,P,n_j} = \left.\frac{\partial G}{\partial n_i}\right|_{T,P,n_j} \tag{2.18}$$

The chemical potential is an important function because it is the basic variable defining the chemical equilibrium of a system composed of one or more species.

As for eqns. (2.5) to (2.7), the expressions of the different state functions are then:

$$F = U - TS + \sum_i n_i \mu_i \tag{2.19}$$

$$H = U + PV + \sum_i n_i \mu_i \tag{2.20}$$

$$G = U - TS + PV + \sum_i n_i \mu_i \tag{2.21}$$

3. The chemical potential

The chemical potential of species *i* is usually written in the following way:

$$\mu_i = \mu_i^0 + RT \ln a_i \tag{2.22}$$

The activity a_i has been characterised by Lewis as a quantity defining how active a solution is compared to its ideal behaviour. In an ideal solution, the activity is equal to the number of moles of species *i*, defined on the appropriate concentration scale (molality, molarity or mole fraction), as will be seen in the next subsection.

For solute species for instance, if the quantity of species *i* is defined in molality (moles of species *i* per kilo of solvent), the ideal activity is:

$$a_i = m_i$$

For real solutions, one inserts the activity coefficient to the above equation resulting in:

$$a_i = m_i \gamma_i \tag{2.23}$$

This relation is general. For ideal solutions, the γ_i is equal to one, which is coherent with the relation $a_i=m_i$. γ_i is dimensionless. Thus, the activity has the dimension of the mole amount in which it is defined (here, molality). Besides, the chemical potential is independent of the scale used to define the moles of species *i*. Thus, the activity coefficients are dependent on the scale in which the mole quantity of species *i* are expressed. The conversion expressions required for changing from a scale to another (molality to molarity for example), requiring knowledge of the standard state chemical potential μ^0, will be given in the next subsection.

The notion of ideality introduced by the activity in the chemical potential allows us to write the chemical potential in another form:

$$\mu_i = \mu_i^{id} + \mu_i^{ex} \tag{2.24}$$

and

$$\mu_i^{id} = \mu_i^{0,id} + RT \ln m_i \tag{2.25}$$

$$\mu_i^{ex} = RT \ln \gamma_i \tag{2.26}$$

assuming the particle number is expressed on molality scale.

Eqns. (2.18) and (2.24)-(2.26) yield

$$\mu_i = \left.\frac{\partial G}{\partial n_i}\right|_{T,P,n_j} = \left.\frac{\partial G^{id}}{\partial n_i}\right|_{T,P,n_j} + \left.\frac{\partial G^{ex}}{\partial n_i}\right|_{T,P,n_j} \tag{2.27}$$

with

$$G_i = G_i^{id} + G_i^{ex} \tag{2.28}$$

$$\left.\frac{\partial G^{ex}}{\partial n_i}\right|_{T,P,n_j} = RT\ln\gamma_i \qquad (2.29)$$

μ_i is also related to *U*, *F* and *H* in the same way as in eqn. (2.29). The relations are gathered in Table 1.1.

4. The Gibbs-Duhem equation

The total differential form of equations (2.23) is

$$dG = dU - SdT - TdS + PdV + VdP + \sum_i \mu_i dn_i + \sum_i n_i d\mu_i \qquad (2.30)$$

Eqn. (2.30) and eqn. (2.17) are both exact, which implies

$$0 = SdT - VdP + \sum_i n_i d\mu_i \qquad (2.31)$$

This relation is the so-called Gibbs-Duhem (GD) relation. It is a necessary condition for the self-coherence of a model for μ_i. This relation is usually used as a test for the models of excess functions. We will use the GD relation to test the models developed in this work.
This equation is of course can be established with the three other state functions.

We will see in the next subsections other writings of eqn. (2.31).

5. The thermodynamic coefficients

a) The activity coefficient and the reference state

A first thermodynamic data available from the experiments is the activity coefficient of a species *i*. Modelling of vapor liquid equilibrium or of conductivity of salts requires information on the activity coefficient of species in the liquid phase. This coefficient has already been introduced earlier (see eqn. (2.23)).

By convention, when species *i* is a solvent, the reference state is the pure solution of species *i*. When species *i* is a solute, the reference state is the infinite dilute state. These two different states are defined respectively with the exponents * (γ^*) and ∞(γ^∞) on the activity coefficient. These two different reference states considering the different nature of species in solution are gathered in the so-called unsymmetrical convention.

$$\gamma_1 \to 1 \quad as \quad x_1 \to 1 \qquad (2.32)$$

$$\gamma_2 \to 1 \quad as \quad x_2 \to 0 \tag{2.33}$$

with notation 1 for the solvent and 2 for the solute.

When the excess function (G^{ex} for instance) is defined in the symmetrical convention, i.e. when both solute and solvent have the pure solution as reference state, one has

$$\gamma_1 \to 1 \quad as \quad x_1 \to 1 \tag{2.34}$$

$$\gamma_2 \to 1 \quad as \quad x_2 \to 1 \tag{2.35}$$

Comparison between theory and experiment is first possible when the solute reference state is the same. The conversion relation is

$$ln\,\gamma_i = \left.\frac{\partial G^{ex}}{\partial n_i}\right|_{T,P,n_j} - \lim_{x\to 0}\left.\frac{\partial G^{ex}}{\partial n_i}\right|_{T,P,n_j} \tag{2.36}$$

In the case of electrolyte solutions, one should obtain the activity coefficient of each ion, according to the development made before. Eqn. (2.29) for the cation is here rewritten for clarity:

$$\gamma_+ = \left.\frac{\partial G^{ex}}{\partial n_+}\right|_{T,P,n_-,n_w} \tag{2.37}$$

where n_+, n_- and n_w are the mole number of cations, ions and solvent particles, respectively.
The last equation implies the addition of a cation (dn_+) without the addition of an anion, which is physically not possible. Consequently, one rather calculates the mean ionic activity coefficient, and the mean ionic activity of the salt. On the molality scale, the relations are [2]

$$\nu \ln \gamma_\pm = \nu_+ \ln \gamma_+ + \nu_- \ln \gamma_- \tag{2.38}$$

with ν_i is the stoechiometric number of ion i, and $\nu = \nu_+ + \nu_-$.
For the mean ionic activity coefficient, the relation given in eqn. (2.36) reads

$$ln\,\gamma_\pm = \frac{1}{\nu}\left(\nu_+ \left.\frac{\partial G^{ex}}{\partial n_+}\right|_{T,P,n_-} + \nu_- \left.\frac{\partial G^{ex}}{\partial n_-}\right|_{T,P,n_+}\right) - \lim_{x\to 0}\frac{1}{\nu}\left(\nu_+ \left.\frac{\partial G^{ex}}{\partial n_+}\right|_{T,P,n_-} + \nu_- \left.\frac{\partial G^{ex}}{\partial n_-}\right|_{T,P,n_+}\right) \tag{2.39}$$

b) The osmotic coefficient

Let us consider the case of NaCl in water up to 5 mol.kg^{-1}. The experimental values of the activity coefficients of both solute and solvent are collected in Table 2.2. As it can be noticed, the variation of the activity coefficient of water is very small compared to the mean ionic activity coefficient of the solute. The departure from ideality revealed with the mean ionic activity coefficient is not clearly to see with the values of solvent activity coefficient.

This problem is bypassed introducing another quantity, the osmotic coefficient, the variations of which are far bigger than the activity coefficient of the solvent. This osmotic coefficient has also the big advantage to be a measurable data by osmotic pressure experiments. The osmotic coefficient is defined on the molality scale by:

$$\phi = -\frac{x_1}{x_2}\ln a_1 = -\frac{1}{\nu m M_1}\ln a_i \qquad (2.40)$$

with m the molality of the salt in mol kg^{-1} of solvent and M_1 the molar mass of solvent in units of kg mol^{-1}.

This definition is given in the experiment referential. That is, with mole amounts given in mole per kilogram of solvent, at the real pressure P of the solution and temperature T. The next subsection elaborates on this reference system, known as the Lewis-Randall framework.

Table 2.2- Values of solvent activity, mean ionic solvent and osmotic coefficient for aqueous NaCl solutions at 298K.

Molality [a]	$\gamma_\pm$	a_w	ϕ
0.1	0.779	0.9495	0.933
0.5	0.681	0.9501	0.921
1.0	0.657	0.9494	0.936
2.0	0.668	0.9482	0.984
2.5	0.688	0.9453	1.013
3.0	0.714	0.9436	1.045
4.0	0.783	0.9399	1.116
5.0	0.874	0.9360	1.191

[a]: Units of mol kg^{-1}.

c) Conversion of activity coefficients between different concentration scales

The definition of the activity depends on the different concentration scale used. The scales in common are:

- The molality *m*, is the number of moles of species *i* per kilogram of solvent *m*. The unit is $mol.kg^{-1}$. This scale is the most convenient scale for experimentalists.
- The concentration *c*, is the number of mole of species *i* per unit of volume of the solution. Unit is $mol.dm^{-3}$. Concentration is practical for models built in the MacMillan Mayer level since in this formalism, the solvent is not explicitely taken into account.
- The mole fraction scale *x* is the most widely used scale in classical thermodynamics. This scale has no unit as it is a ratio of species *i* to the overall mole amount of species in the solution (including the solvent)

$$x_i = \frac{n_i}{\sum_j n_j} \tag{2.41}$$

where the sum is made over all species, solvent included.

Its advantage is that the solute *i* and solvent *m* are totally symmetric; when $x_i = 0$, then $x_m = 1$, and vice versa. Moreover, this scale is independent of the mole amount of solvent *m* or of solute *i*.

These three scales are related together, because they express the same mole amount of species *i* n_i in the solution.

In the case of one salt s composed of two ions (+ and -) and a solvent *w*, the conversion from one scale to another is given by [2]

$$x_i = \frac{\nu m}{\nu m + 1/M_w} \tag{2.42}$$

$$c = \frac{md}{1 + mM_s} \tag{2.43}$$

with ν, *m*, *d*, M_w the sum of ions, the molality of solute, the density of solution and the molar mass of solvent, respectively. M_s is the molar mass of solute. $\nu = \nu_+ + \nu_-$ and ν_+ and ν_- are the cation and anion stoechiometric numbers, respectively.

Three different activity coefficients are used. The molal (γ), molar (y) and rational (f) activity coefficients correspond to the activity coefficients on the molal, molar and mole fraction scale, respectively.

The activity of solute *i* in a solution can be written in the different concentration scales as following

$$a_i(m) = m_i \gamma_i \tag{2.44}$$

$$a_i(c) = c_i y_i$$

$$a_i(x) = x_i f_i$$

The mean ionic acitivity is given by the relation:

$$\nu \ln a_\pm = \nu_+ \ln a_+ + \nu_- \ln a_- \tag{2.45}$$

which leads to the following expression for the mean ionic activity in the molality scale

$$\nu \ln a_\pm = \sum_{i=+,-} \nu_i \ln(m_i \gamma_i) \tag{2.46}$$

with

$$m_i = \nu_i m$$

One often needs to convert activity coefficients from one scale to another. For instance, theoretical thermodynamic quantities are often calculated on the molarity scale, and must be converted in the molality scale on which the experimental measurements are made.

The conversion between molarity and molality scales will now be detailed. The equations for the conversion between mole fraction and molality and between molarity and mole fraction will then be summarized.

As for activity, a mean ionic chemical potential can be defined

$$\mu_{\pm} = \mu_{\pm}^{0}(m) + RT \ln a_{\pm}(m) \tag{2.47}$$

with $\mu_{\pm}^{0}$ the reference state chemical potential in the molality scale. $\mu_{\pm}$ is independent of the concentration scale used. Thus,

$$\mu_{\pm} = \mu_{\pm}^{0}(c) + RT \ln a_{\pm}(c) \tag{2.48}$$

Comparison between eqns. (2.47) and (2.48) yields

$$\mu_{\pm}^{0}(m) + RT \ln a_{\pm}(m) = \mu_{\pm}^{0}(c) + RT \ln a_{\pm}(c) \tag{2.49}$$

The question is how to find the values of μ^{0} in both scales. This is done by recalling the properties of the standard state. The standard state is defined at c→0 (m→0). In this case, $y_{\pm}$→1 ($\gamma_{\pm}$→1), and we have also the limit c/m→d_0, d_0 being the pure solvent density. This yields

$$\mu_{\pm}^{0}(m) - \mu_{\pm}^{0}(c) = RT \ln d_0 \tag{2.50}$$

Leading the final conversion expression between molality and molarity scales

$$\ln \gamma_{\pm} = \ln \frac{c}{m d_0} + \ln y_{\pm} \tag{2.51}$$

The conversion relations for the mean ionic activity coefficient in the different scale are

$$f_i = \gamma_i (1 + m M_w) \tag{2.52}$$

$$\gamma_i = \frac{d - cMs}{d_0} y_i = \frac{c}{m d_0} y_i \tag{2.53}$$

$$y_i = (1 + m M_s) \frac{d_0}{d} \gamma_i = \frac{m d_0}{c} \gamma_i \tag{2.54}$$

These relations will be useful for the comparison between calculated and experimental thermodynamic coefficients. The MSA model, for example,gives activity coefficients on the concentration scale, whereas the experimental activity coefficients are on the molality scale.

d) The Gibbs-Duhem relation for electrolyte solutions

Let us consider the case of a chemical reaction in liquid phase. The solution is thermostated, that is T is held constant. The reaction is made at atmospheric pressure, P, a constant. Eqn. (2.31) then reduces to:

$$\sum_i n_i d\mu_i = 0 \tag{2.55}$$

Using eqns. (2.22) and (2.45), one can write eqn. (2.55) as follows:

$$n_w d\ln a_w + \nu n_s d\ln a_\pm = 0 \tag{2.56}$$

since $\mu_i^0(T,P)$ is constant. Here, n_w is the number of moles of solvent in one kilo of solvent and n_s is the number of moles of salt. Combining eqn. (2.56) with (2.40) and (2.46) yields:

$$-\nu d(m\phi) + \nu m d\ln(m\gamma_\pm) = 0 \tag{2.57}$$

since $n_w = 1/M_w$ and $n_s = m$. The resulting equation of Gibbs-Duhem is written as

$$\ln\gamma_\pm = \phi - 1 + \int_o^m (\phi - 1) d\ln m \tag{2.58}$$

or

$$\phi = 1 + \frac{1}{m}\int_o^m m\, d\ln\gamma_\pm \tag{2.59}$$

and gives the mathematical relation between ϕ and $\gamma_\pm$. One can calculate directly ϕ from $\gamma_\pm$, (and vice-versa) provided one has precise values of $\gamma_\pm$, at low concentrations (due to the integration between 0 and m). This equation should always be used to test the thermodynamic coherence of theoretical calculation of ϕ and $\gamma_\pm$.

6. The Lewis-Randall and McMillan Mayer scales

All thermodynamic coefficients exposed in this section have been calculated by differentiating the energy state function. The excess Gibbs energy has been taken as an example. This state function is, as it has been shown in the previous section, the energy state function defined with T, P and n as independent variables. These are the three natural variables in which a chemical experiment is done. The pressure on solution is the experimental pressure *P*. This level of representation of a solution is called the Lewis-Randall level of description. The practical unit used for calculating the number of mole of species *i* in this formalism is the molality (or the mole fraction scale).

Another possible representation, widely used in theoretical chemistry is the so-called McMillanMayer (MM) formalism. The name comes from MacMillan and Mayer who studied ways of representing chemical solutions considering the solvent as a continuum characterised by its sole dielectric constant ε. MacMillan Mayer theory states that the thermodynamic properties of a solution can be reduced to those of an imperfect gas, constituted by the solute species, provided that the chemical potential of the solvent be held constant [3].

The calculation of thermodynamic quantities within a theoretical model built in the MM framework yields values at the MM level of description. The comparison to experimental values

(necessary for testing the model) is not straightforward, since experimental quantities are not defined at the same level of description. To overcome this conceptual problem, one uses conversion expressions between the MM and LR level of description. This conversion is problematic though since it requires the knowledge of density or peculiar properties of solution which are not always known. Fortunately, approximations can be done, yielding simple and usable analytical expressions.

Two main parts will be discussed here. Firstly, the description of a solution within the MM framework will be detailed. And secondly the MM-to-LR conversion, as developed by Simonin [4, 5], will be explained.

a) The continuous solvent model

The complete classical and theoretical description of a system composed of solvent molecules and solute particles is based on a Hamiltonian in which all particle interactions are expressed [6].

$$H = \sum_i \frac{p_i^2}{2m_j} + V_{ions}(\{\mathrm{r}_i\}) + \sum_\alpha \frac{p_\alpha^2}{2m_\alpha} + V_{solvent}(\{\mathrm{r}_\alpha\}) + V_{solvent/ions}(\{\mathrm{r}_\alpha, \mathrm{r}_i\}) \qquad (2.60)$$

where *i* stands for solute and a for solvent particles. The position of each particle is given by $\boldsymbol{r}_i$ and $\boldsymbol{r}_\alpha$ for the solute and solvent, respectively. The canonical variables are here the movement quantities $\boldsymbol{p}_\alpha$ and $\boldsymbol{p}_i$. For convenience, the case of one electrolyte in one solvent will be considered below. The generalisation to more electrolytes is straightforward.

Instead of studying the Hamiltonian of eqn. (2.60), MacMillan and Mayer [3] proposed to deal only with solutes. The effect is then to reduce the "space of phases" from { $\boldsymbol{r}_\alpha$, $\boldsymbol{p}_\alpha$, $\boldsymbol{r}_i$, $\boldsymbol{p}_i$} to {$\boldsymbol{r}_i$, $\boldsymbol{p}_i$}. The partition function for this system is calculated in the grand-canonical ensemble, since one can vary the number of particles in this ensemble.

$$\begin{aligned}
\Xi(T,V,\mu_\alpha,\mu_i) &= \sum_{states} e^{\beta\mu_\alpha N_\alpha + \beta\mu_i N_i - \beta H} \\
&= \sum_{N_\alpha=0}^{+\infty} \sum_{N_i=0}^{+\infty} \frac{e^{\beta\mu_\alpha N_\alpha + \beta\mu_i N_i}}{N_\alpha!\, N_i!\, h^{3(N_\alpha+N_i)}} \int\!\!\ldots\!\int e^{-\beta H(\{\boldsymbol{r}_\alpha,\boldsymbol{p}_\alpha,\boldsymbol{r}_i,\boldsymbol{p}_i\})} d\boldsymbol{r}_\alpha^{N_\alpha} d\boldsymbol{r}_i^{N_i} d\boldsymbol{p}_\alpha^{N_\alpha} d\boldsymbol{p}_i^{N_i} \qquad (2.61) \\
&= \sum_{N_\alpha,N_i} \frac{e^{\beta\mu_\alpha N_\alpha + \beta\mu_i N_i}}{N_\alpha!\, N_i!\, \lambda_\alpha^{3N_\alpha} \lambda_i^{3N_i}} \int\!\!\ldots\!\int e^{-\beta V(\{\boldsymbol{r}_\alpha,\boldsymbol{r}_i\})} d\boldsymbol{r}_\alpha^{N_a} d\boldsymbol{r}_i^{N_i}
\end{aligned}$$

with $\beta=1/kT$, *k* the Boltzmann constant, T the temperature, V the volume and *h* the Planck constant. μ_a or μ_i and N_α or N_t are the chemical potentials and the particle numbers of solvent and solute, respectively. V({**r**a, **r**i}) is the total interaction potential $V_{ions}(\{\mathbf{r}_i\})$ + $V_{solvant}(\{\mathbf{r}_\alpha\})$ +

$V_{solvant/ions}(\{\mathbf{r}_\alpha,\mathbf{r}_i\})$. λ_α and λ_i are the de Broglie wavelengths associated with the solvent and solute, respectively. They are calculated by integration on the positions. For a particle of mass m, the de Broglie wavelength is $\frac{h}{\sqrt{2\pi mkT}}$. One finally obtains

$$\Xi(T,V,\mu_\alpha,\mu_i)=\sum_{N_\alpha,N_i}\frac{z_i^{N_i}z_\alpha^{N_\alpha}}{N_i!\,N_\alpha!}\int\!\!\ldots\!\int e^{-\beta V(\{r_\alpha,r_i\})}dr_\alpha^{N_\alpha}\,dr_i^{N_i} \tag{2.62}$$

with z_i and z_α being the fugacity of solute and solvent, respectively.

MacMillan and Mayer assumed that the solute and solvent terms of the partition function could be separated:

$$\Xi(T,V,\mu_\alpha,\mu_i)=\sum_{N_i}\frac{z_i^{N_i}}{N_i!}\int\!\!\ldots\!\int d\mathbf{r}_i^{N_{ii}}\sum_{N_\alpha}\frac{z_\alpha^{N_\alpha}}{N_\alpha!}\int\!\!\ldots\!\int e^{-\beta V(\{\mathbf{r}_\alpha,\mathbf{r}_i\})}d\mathbf{r}_\alpha^{N_\alpha} \tag{2.63}$$

This expression is similar to the partition function for pure species, considering the integration term on the solvent space of phases as an effective potential acting between the solute particles. One obtains

$$\Xi(T,V,\mu_\alpha,\mu_i)=\Xi_{MM}(T,V,a)\times\Xi_{pur}(T,V,\mu_\alpha) \tag{2.64}$$

with $\Xi_{pur}(T,V,\mu_\alpha)$ the pure solvent partition function when it has the same chemical potential μ_α as in the solution. This is calculated by considering the case $\Xi_{pur}(T,V,\mu_\alpha,\mu_i=-\infty)$. $\Xi_{MM}(T,V,a)$ is the Mac-Millan Mayer partition function which is formally written as

$$\Xi_{MM}(T,V,a_i)=\sum_{N_i}\frac{a_i^{N_i}}{N_i!}\int\!\!\ldots\!\int e^{-\beta V_{eff}(\{\mathbf{r}_i\})}d\mathbf{r}_i^{N_\alpha} \tag{2.65}$$

The effective potential between solute particles is defined by

$$V_{eff}(\{\mathbf{r}_i\})=-kT\ln g_{N_i}(\{\mathbf{r}_i\}) \tag{2.66}$$

where $g_{N_i}(\{\mathbf{r}_i\})$ is the solute correlation function at N_i bodies in the limit $z_i\rightarrow 0$, *i.e.* at infinite dilution. The activity a_i is defined in this case defined by

$$a_i=z_i\lim_{z_i\to 0}\frac{\rho_i}{z_i} \tag{2.67}$$

with ρ_i the solute number density at equilibrium. Its chemical potential is written as

$$\begin{aligned}\mu_i &= kT\ln\lambda_i^3+kT\ln z_i\\ &= kT\ln\lambda_i^3+kT\ln\gamma_i+kT\ln a_i\end{aligned} \tag{2.68}$$

where $\gamma_i = \lim_{z_i \to 0} \frac{\rho_i}{z_i}$.

b) The Van't Hoff idea:

The preceding calculations give us all necessary thermodynamic quantities. The grand potential Ω is

$$\begin{aligned} \Omega &= -PV = -kT \ln \Xi \left(T, V, \mu_\alpha, \mu_i\right) \\ &= -kT \ln \Xi_{pur} \left(T, V, \mu_\alpha\right) - kT \ln \Xi \left(T, V, a\right) \\ &= \Omega_{pur} + \Omega_{MM} \end{aligned} \tag{2.69}$$

Ω is the sum of the pure solvent grand potential and the one obtained with the help of the MM partition function. The latter is formally equal to the grand potential for a real gas in which only the solute space of phases is taken into account, and with an effective potential given by (2.66). This is the so-called *gas of solute*, introduced by Van't Hoff in 1887 [7].

The different thermodynamic equilibrium quantities are calculated with the help of the classical thermodynamic identities.

$$d\Omega = -PdV - SdT - N_\alpha d\mu_\alpha - \sum_i N_i d\mu_i \tag{2.70}$$

The pressure is thus,

$$P = P_{pure} + P_{osm} \tag{2.71}$$

In this expression, P_{pure} is the pressure for the pure solvent in equilibrium with the solution, at same temperature and chemical potential. P_{osm} is the osmotic pressure calculated with the help of the solute gas partition function.

For the description of electrolytes, the preceding calculation has proved that it is possible to treat exactly the statistical physics of the solution considering only the variables associated to ions, assuming these interact through an effective potential averaged on the solvent as given in eqn. (2.66). In this representation of the solution however, the effect of the solvent is actually hidden in the effective potential. If the interactions are pair-wise in the exact Hamiltonian in the discrete solvent, the effective potential between solute particles is not necessarily so. N body effects must be taken into

account. Since eqn. (2.66) does not yield an explicit expression of the effective potential, some further assumptions are needed, leading to approximated results.

As stated earlier in the chapter, the quantities calculated in the MM framework can not be directly compared to experimental values, as the osmotic pressure for instance. These quantities need be converted to the experimental level of description, the Lewis-Randall framework. To that end, a conversion expression, called from now on *MM-to-LR conversion*, is required.

c) MM-to-LR conversion

Eqn. (2.71) has a direct consequence on the osmotic coefficient, since we can write

$$\phi = \frac{P_{osm}^{real}}{P_{osm}^{id}} \tag{2.72}$$

where P_{osm} is the osmotic pressures of the solution considered as a real or an ideal solution, respectively. The osmotic pressure of an ideal solution is defined by

$$P^{id} = \frac{N}{V} kT = \rho_{tot} kT \tag{2.73}$$

with

$$\rho_{tot} = \sum_i \rho_i \tag{2.74}$$

ρ_i being the number density of species i (molecule per volume unit, here m^3) and is related to the molarity of species i by the relation

$$\rho_i = 10^3 N_A c_i \tag{2.75}$$

with N_A the Avogadro's constant and c_i the molarity in mol L^{-1}.

The osmotic coefficient is then defined by the relation

$$\phi = \frac{\beta P^{osm}}{\rho_{tot}} \tag{2.76}$$

The osmotic coefficient calculated by eqn. (2.72) is the one calculated by using theoretical models, such as the MSA for ionic solutions.

This coefficient has to be compared to the experimental osmotic coefficient, which is obtained with the help of eqn. (2.45). In the same way, the solute activity coefficient or mean activity coefficient is calculated at the MM level, and has to be converted to the LR scale in order to be compared with the experimental values.

This MM-to-LR conversion has been studied in detail [3, 8]. An approximate relation for this conversion has been given by Simonin [5] and is summarised here. The following results will be used below.

The conversion formula used is an approximate conversion, holding as long as compressibility of the solution at P_{osm} can be neglected

$$\phi_{LR} = \phi_{MM}\left(1 - c_t V_{\pm}\right) \tag{2.77}$$

$$ln\, y_{\pm}^{LR} = ln\, y_{\pm}^{MM} - c_t V_{\pm} \phi^{MM} \tag{2.78}$$

in which y denotes an activity coefficient on the molarity scale, $V_{\pm}$ is the mean solute partial molar volume and c_t is the total solute molarity

$$c_t = m/V$$

And

$$m \equiv \sum_i m_i$$

m_i the molality of ion I and V the total volume of the solution.

$$V = \frac{1 + \sum_i m_i M_i}{d} \tag{2.79}$$

with M_i the molar weight of ion i and d the density of solution.

For conversion of activity coefficients in the molarity scale to the experimental molality scale one writes

$$y_{\pm}^{LR} = \gamma_{\pm}^{LR} V d_w \tag{2.80}$$

with γ the experimental activity coefficient on the molality scale, and d_w the density of solvent w.

The mean solute partial molal volume V_{+-} can be defined as:

$$V_{\pm} = \sum_i x_i V_i \tag{2.81}$$

in which x_i is the mole fraction of species i

$$x_i = m_i / m \tag{2.82}$$

and

$$V_i \equiv \frac{\partial V}{\partial m_i} \tag{2.83}$$

Eqn. (2.83) implies that

$$dV = \sum_i V_i dm_i \tag{2.84}$$

from which we get, by virtue of eqns. (2.81) and (2.82)

$$V_{\pm} = \left.\frac{\partial V}{\partial m}\right|_{x_i} \tag{2.85}$$

with x_i define in eqn. (2.82). Eqn.(2.85), with the help of eqn.(2.79) leads to

$$V_{\pm} = \frac{M - d'}{d - c_t d'} \tag{2.86}$$

where

$$M = \sum_i x_i M_i$$

M_i is its molar mass, m_i its molality and

$$d' \equiv \left.\frac{\partial d}{\partial c_t}\right|_{x_i} \tag{2.87}$$

Eqn. (2.79) involves the density of solution. In the case of one solute, this quantity has been calculated by using the following expression found in the literature [9]:

$$d = d_w + d_1 c_s - d_2 c_s^{3/2} \tag{2.88}$$

Here, c_s is the molar concentration of the solute and d_1 and d_2 are parameters that have been determined by a least-square adjustment of experimental data.

We managed to get approximate equations for converting quantities from a framework to another. These equations, although requiring the density of the solution, are simple and can be used in theoretical models built in the MM framework.

B. Description of solutions of neutral solutes

As stated above, the experimental level of description is the LR level. In this description, the adequate state function is the Gibbs energy as referef to earlier in section 6.

Many empirical models have been used to describe the Gibbs energy of mixtures of solvent and neutral solutes. Some simple equations, or simple representations of these solutions, have been found to be able to describe roughly their thermodynamic properties.

These models, of course, were mostly unpredictive and their validity ranges were restricted. Nevertheless, the development of such models is until today a major topic of theoretical research.

In neutral solutions, particles interact in several ways. For instance, through excluded volume interactions, dipole-dipole interactions and dispersion forces.

The common point between these interactions is that all them are "short-ranged". That is, their range never exceeds one or two neighbour particles. In this case, one can assume that average interactions occur only between a particle and its immediate neighbour.

Considering this, empirical models have been developed in order to bring some theoretical description and applied expressions to the excess energy functions of solutions of neutral solutes. These models utilise the notion of pair wise interactions between particles to calculate the excess functions. These empirical interactions undergo an empirical effective short-range potential.

The models presented that follow below express energy functions in the LR formalism, *i.e.* excess Gibbs energies. The development of Gibbs energy models allows straightforward calculations of several thermodynamic properties such as the activity and osmotic coefficients, the vapor pressures of solutions, and the calorific heat capacities.

The excess Gibbs energy is usually written in the following format

$$G^{ex} = n_t g^{ex} \qquad (2.89)$$

with

$$g^{ex} = \sum_i x_i \ln f_i \qquad (2.90)$$

g^{ex} is the molecular Gibbs energy and f_i the activity coefficient of species i on the mole fraction scale.

In a binary mixture, the molar excess Gibbs energy g^{ex} obeys to the boundary conditions:

$g^{ex}=0$ when $x_i=0$

where the subscript i stands for both solute and solvent.

The classical models used in thermodynamic modelling will be now described.

1. Wohl's expansion

According to the boundary conditions as fixed above, a very simple equation may be established for binary systems: $g^{ex}=A*x_1*x_2$, which corresponds to the so-called two-Margules equation. Departing from this expression, many g^{ex} equations can be constructed, depending on the mathematical form given to the factor A. A practical expression for A, found by Wohl and allowing the description of many binary systems, corresponds to the general series expansion

$A=(B_{12}^{(n)} (x1-x2)^n)$

The resulting expression for g^{ex} is known as the Redlich-Kister equation. This equation will not be detailed here. Another expansion, known as the Wohl's expansion will be rather detailed. Wohl modified the Redlich-Kister expression by substituting x_i with z_i and generalised it to multi-component systems, yielding the Wohl's expansion for g^{ex}:

$$\frac{g^{ex}}{RT\left(\sum_i x_i q_i\right)} = \sum_i \sum_j a_{ij} z_i z_j + \sum_i \sum_j \sum_k a_{ijk} z_i z_j z_k + \sum_i \sum_j \sum_k \sum_l a_{ijkl} z_i z_j z_k z_l + \ldots\ldots \quad (2.91)$$

where

$$z_i = \frac{x_i q_i}{\sum_j x_j q_j}$$

$$a_{ij} = a_{ji}$$

The advantage of this expansion is the rough physical significance assignable to the parameters. The *q* terms are effective volumes of the molecules and a measure of the size of the molecule. The *a* terms are interaction parameters whose significance is similar to the virial coefficients.

Two models are directly related to the Wohl's expansion: the van Laar equation and the Margules equations, which shall be seen now.

a) Van Laar equation

The Van Laar equation corresponds to the Wohl's expansion truncated after the first term (see eqn. (2.91)). The Van Laar equation reads:

$$\frac{g^{ex}}{RT} = \frac{\sum_i \sum_j a_{ij} q_i q_j x_i x_j}{\left(\sum_k x_k q_k\right)} \quad (2.92)$$

The differentiation of g^E leads to the activity coefficients of species *i*

$$ln\, f_i = \frac{2q_i \sum_{j\neq i} \sum_{k\neq i} q_j q_k x_j x_k \left(a_{ki} - a_{kj}\right)}{\left(\sum_j x_j q_j\right)^2} \quad (2.93)$$

In the case of a binary system composed of two species 1 and 2, the activity coefficient of species 1 can be written as:

$$ln\, f_1 = \frac{A'}{\left(1 + \frac{A' x_1}{B' x_2}\right)^2}$$

with

$$A' = 2q_1 a_{12}$$

$$B' = 2q_2 a_{21}$$

In this case, only two parameters, A' and B' are required. One observes that the parameter A' is nothing else than the infinite dilution activity coefficient of species 1.

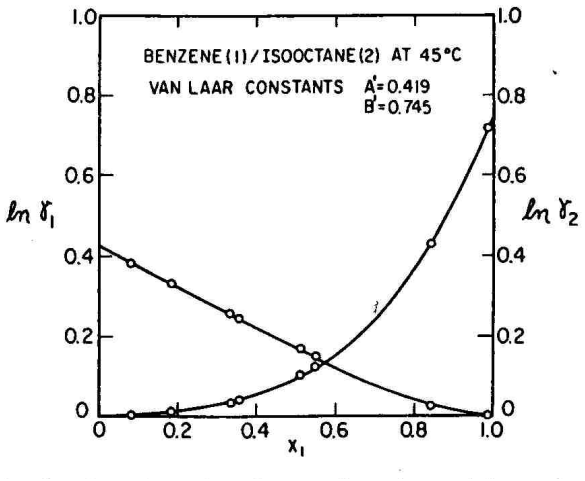

Figure 2.1 Application of van Laar's equations to a mixture whose components differ appreciably in molecular size. Data taken from ref 10.

The Van Laar equation should be applied for simple, non-polar systems. But because of its simplicity and its flexibility, this equation is widely used for describing activity coefficients of complex mixtures.

Since it does not require any ternary parameter, Van Laar can describe multi-component systems, provided that the behaviour of species in the multi-component mixtures will vary little from the one observed in the binary mixture.

b) Margules equations

Another derivation of the Wohl's expansion is the so-called Margules equations. Assuming the components in the solution are not too varied in size, it may be written as $q=q_i=q_j$, one obtains the following expression for g^{ex}:

$$\frac{g^{ex}}{RT} = \sum_i \sum_j q x_i x_j + \sum_i \sum_j \sum_k q x_i x_j x_k + \sum_i \sum_j \sum_k \sum_l q x_i x_j x_k x_l + \ldots\ldots \qquad (2.94)$$

Different equations can be found, depending on which terms of the equation (2.92) are neglected.

i) Two-suffix Margules equation:

Neglecting the term of third order and higher, one obtain the so-called "Two-suffix Margules equation":

$$\frac{g^{ex}}{RT} = \sum_i \sum_j q x_i x_j \qquad (2.95)$$

The differentiation of the excess Gibbs energy gives the activity coefficients:

$$ln\, f_i = 2q\sum_j a_{ij} x_j (1 + x_i) + 2q\sum_j \sum_k a_{jk} x_j x_k \qquad (2.96)$$

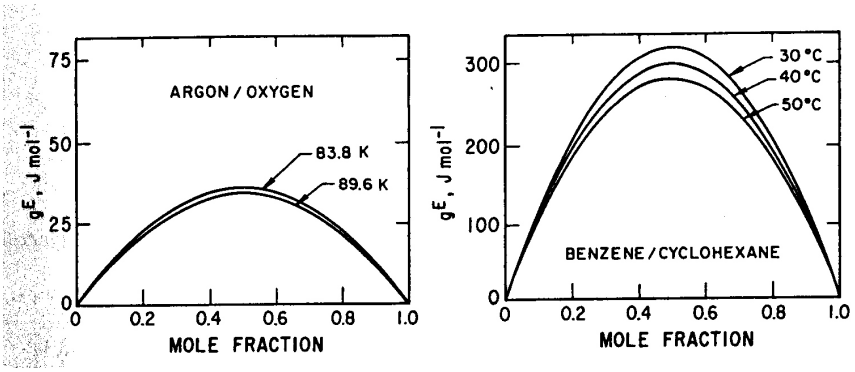

Figure 2.2- Applicability of two-suffix Margules equations to simple binary mixtures. Data taken fromm refs 11 and 12.

This equation is a second order polynomial expression for the activity coefficient. It is able to describe systems for which the g^{ex} and the activity coefficients of each species are parabolic functions of the mole fraction.

The Figure 2.2 shows the g^{ex} curves obtained for the two system argon/oxygen [11] and benzene/cyclohexane [12]. One observes the parabolic form of g^{ex} for both systems which are accurately describes by the two-suffix Margules.

This model, although appropriate for solutions of species that have similar sizes, is widely used for systems composed with species of different sizes. An advantage of this particular model, is that only parameter for the binary systems are needed to describe multi-component systems.

The two-suffix Margules equation, as well as the Van Laar equation, is often used for interpolating and extrapolating data with respect to composition or smoothing data curves when experimental points are scarce.

ii) Three-suffix Margules equation:

Neglecting the term of fourth order and higher, one obtains the so-called "three-suffix Margules equation":

$$\frac{g^{ex}}{RT} = \sum_i \sum_j q a_{ij} x_i x_j + \sum_i \sum_j \sum_k q a_{ijk} x_i x_j x_k \qquad (2.97)$$

Then, the activity coefficients are:

$$\ln f_i = 2q\sum_j a_{ij}x_j(1+x_i)+2q\sum_j\sum_k a_{jk}x_jx_k+3q\sum_j\sum_k a_{ijk}x_jx_k-2q\sum_j\sum_k\sum_l a_{jkl}x_jx_kx_l \quad (2.98)$$

For ternary systems the three suffix Margules coefficient activity is often rewritten as:

$$\ln f_i = A'_{12}\,x_2^2(1-2x_1)+2A'_{21}\,x_1x_2(1-x_1)+A'_{13}\,x_3^2(1-2x_1)+2A'_{31}\,x_1x_3(1-x_1)$$
$$-2A'_{23}\,x_2x_3^2-2A'_{32}\,x_2^2x_3+\left(\frac{A'_{21}+A'_{12}+A'_{13}+A'_{23}+A'_{32}}{2}-Q'\right)(x_2x_3-2x_1x_2x_3) \quad (2.99)$$

with

$$A'_{12}=q(2a_{12}+3a_{122}) \qquad A'_{21}=q(2a_{12}+3a_{112}) \qquad A'_{31}=q(2a_{13}+3a_{113})$$
$$A'_{13}=q(2a_{13}+3a_{133}) \qquad A'_{23}=q(2a_{23}+3a_{233}) \qquad A'_{32}=q(2a_{23}+3a_{223})$$

$$Q'=\frac{3q}{2}(a_{122}+a_{112}+a_{133}+a_{113}+a_{233}+a_{223}-4a_{123})$$

The advantage of this notation is that the *Q'* parameter is at this point the only ternary parameter.

With this equation, multi-component system can no longer be described only with binary system parameters, except *Q'* is set to zero.

	A'	B'
Acetone (1)/chloroform (2)	-0.553	-0.276
Acetone (1)/methanol (2)	0.334	0.368
Chloroform (1)/methanol (2)	2.89	-2.17

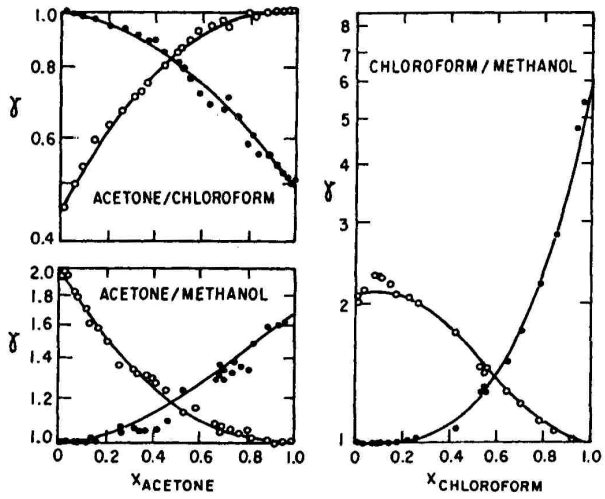

Figure 2.3. Activity coefficients for three binary systems at 50°C. Lines calculated from three-suffix Margules equations. Data taken from ref 13.

The three-Margules equation has been used for describing vapor-liquid equilibrium of various binary or ternary systems. Its flexibility makes it accurate even for strongly non-ideal systems.

The Figure 2.3 shows the description of activity coefficients of three binary systems with the three-suffix Margules equation. One notices here that these three systems are well described over the

whole range of mole fraction. Some deviations are nevertheless observed in the chloroform/ methanol system for small mole fractions of chloroform. All three systems exhibit strong deviations from ideality.

The description of three non-ideal ternary systems by the three-suffix Margules equation is shown in Table 2.3 [13]. The first system presented is composed of acetone, methyl acetate and methanol. This system can be described without the presence of a ternary parameter, when *Q'* is set to zero. In the second system, composed of acetone, chloroform and methanol, the *Q'* has a value of –0.368 which is smaller than the A_{ij} values. Setting *Q'* to zero in this case would lead to a less precise but still acceptable description of the presented system. In the last system presented in Table 2.3, and composed of acetone, carbon tetrachloride and methanol, the description by the three-suffix Margules equation is only possible with a ternary parameter. The value of *Q'* is 1.15, which is of the same order as the A_{ij} constants.

Table 2.3. Three-suffix Margules constants for three ternary systems at 50°C. Data taken from ref. [13]

System	Margules constants
Acetone (1)/methyl acetate (2)/methanol (3)	$A'_{12} = 0.149$ $A'_{21} = 0.115$
	$A'_{13} = 0.701$ $A'_{31} = 0.519$
	$A'_{23} = 1.07$ $A'_{32} = 1.02$
	$Q' = 0$
Acetone (1)/chloroform (2)/methanol (3)	$A'_{12} = 0.83$ $A'_{21} = -0.69$
	$A'_{13} = 0.701$ $A'_{31} = 0.519$
	$A'_{23} = 0.715$ $A'_{32} = 1.80$
	$Q' = -0.368$
Acetone (1)/carbon tetrachloride (2)/methanol (3)	$A'_{12} = 0.715$ $A'_{21} = 0.945$
	$A'_{13} = 0.701$ $A'_{31} = 0.519$
	$A'_{23} = 1.76$ $A'_{32} = 2.52$
	$Q' = 1.15$

2. The Wilson model

The Wilson model is based on molecular considerations [14]. It can be seen as a model derivated from the Flury Hugins model. Firstly, the free Gibbs energy of mixing is assumed to be of the form:

$$\frac{g^{tot}}{RT} = \sum_i x_i \ln \xi_i \qquad (2.100)$$

where x_i is the local volume fraction of component *i* about a central molecule of the same type. Secondly, the local distribution of particles *j* around a central particle *i* is assumed to be given by the relation

$$\frac{x_{ij}}{x_{ki}} = \frac{x_j e^{-g_{ii}/kT}}{x_k e^{-g_{ki}/kT}} \tag{2.101}$$

with x_{ij} the local mole fraction of *j* around *i*, and g_{ij} proportionnal to the interation energy between *i* and *j*. This notion of local mole fraction and distribution are also used in the NRTL model, and will be detailed in the next subsection. The expression for ξ_i according to the assumption made above is then

$$\xi_i = \frac{x_i v_i e^{-g_{ii}/kT}}{\sum_j x_j v_j e^{-g_{ij}/kT}} \tag{2.102}$$

with v_i the molar volume of component i.

The resulting Gibbs energy of mixing is

$$\frac{g^{tot}}{RT} = \sum_i x_i \, ln \sum_j \frac{x_i v_i e^{-g_{ii}/kT}}{\sum_j x_j v_j e^{-g_{ji}/kT}} \tag{2.103}$$

and

$$G^{tot} = G^{ex} + G^{id}$$

The final expression for g^{ex} reads

$$\frac{g^{ex}}{RT} = \sum_i x_i \, ln \sum_j x_j \frac{v_i}{v_j} e^{-\left(g_{ij} - g_{ii}\right)/kT} \tag{2.104}$$

The general Wilson expression for the molecular excess Gibbs energy is:

$$\frac{g^{ex}}{RT} = \left[\sum_i x_i \, ln \left(\sum_j x_j \Lambda_{ij} \right) \right] \tag{2.105}$$

And the activity coefficients are

$$ln \, f_k = -ln\left(\sum_j \Lambda_{kj} x_j \right) + 1 - \sum_i \frac{x_i \Lambda_{ik}}{\sum_j x_j \Lambda_{ij}} \tag{2.106}$$

The adjustable parameters are the Λ_{ij} parameters whose expressions are

$$\Lambda_{ij} = \frac{v_i}{v_j} e^{\left(-\frac{g_{ij} - g_{ii}}{RT}\right)}$$

$$\Lambda_{ji} = \frac{v_j}{v_i} e^{\left(-\frac{g_{ji}-g_{jj}}{RT}\right)}$$

with v_i the partial molar volume of species i and g_{ij} the interaction parameter between i and j.
The parameters Λ_{ij} are only binary parameters. Thus, the Wilson model can represent multi-component systems with only binary system parameters.

The Wilson model can describe mixtures of polar and non-polar systems that are not accurately described by the Wohl's expansion models. It is also suitable for solutions that exhibit strong deviations from ideality.

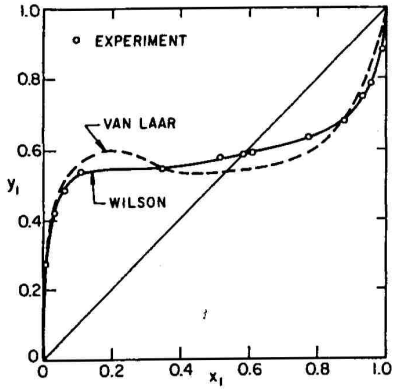

Figure 2.4. Vapor-liquid equilibrium for the ethanol (1)/ isooctane (2) system at 50°C. Lines calculated from *P-x* data. The van Laar equations erroneously predict partial immiscibility. Data taken from ref 15.

As an example, the description of the vapor liquid equilibrium of the binary system ethanol/isooctane is given in Figure 2.4. The vapor-liquid equilibrium has been calculated twice. Once with the Wilson model, and once with the Van Laar model. For this system the Wilson model gives a precise description of the equilibrium, whereas the Van Laar model predicts partial immiscibility.

The observed and calculated vapor compositions for the system acetone/methyl acetate/ methanol are shown in Figure 2.5. The curves obtained with the Wilson model and the Van Laar equation are also plotted below in Figure 2.5. The Wilson model gives in this case a much more accurate description of the data than the Van Laar's proposal.

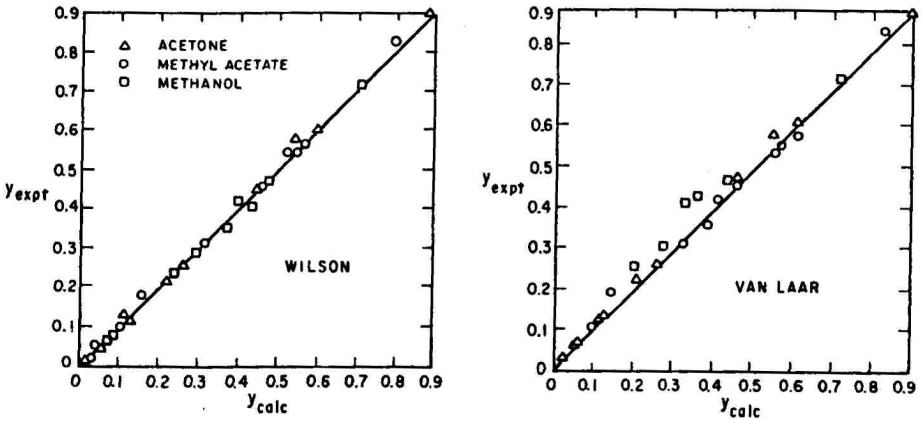

Figure 2.5. Experimental and calculated vapor compositions for the ternary system acetone/ methyl acetate/ methanol at 50°C. Calculations use only binary data. Data taken from ref 16.

Nevertheless, the Wilson model has two discerning disadvantages. It is not suitable for systems where the logarithm of the activity coefficients exhibit maxima or minima when plotted against the mole fraction. And the Wilson model is not suitable for the descripütion of systems exhibiting partial immiscibilty. This is a mathematical limitation of the modeldue tot the form of the equations. Phase instability is calculated with the help of the following relation:

$$\frac{\partial\left(g^{tot}\right)^2}{\partial^2 x_i} = 0 \tag{2.107}$$

with

$$g^{tot} = RT\left(\sum_i x_i \ln x_i\right) + g^{ex} - \sum_i x_i g_{i,pure} \tag{2.108}$$

with g^{ex} defined in eqn. (2.105).

This yields

$$\frac{\partial\left(g^{ex}\right)^2}{\partial^2 x_i} + RT\left(\sum_j \frac{1}{x_j}\right) = 0 \tag{2.109}$$

In the case of a binary system, the derivation of g^{ex} in eqn. (2.108) in respect to first component component (denoted by the subscript 1) yields the following expression

$$\frac{\Lambda_{21}^2}{x_1\left(x_1 + x_2\Lambda_{21}\right)^2} + \frac{\Lambda_{12}^2}{x_2\left(x_2 + x_1\Lambda_{12}\right)^2} = 0 \tag{2.110}$$

This equation can never be satisfied, since Λ_{21} and Λ_{12} are always positive. Therefore, the unadequacy of the Wilson model for partially immiscible systems.

3. The NRTL model

In the NRTL model, interaction energies between species are taken into account. This is made by considering different types of cells centred on a specific species. We will examine the case of a ternary system composed of two species 1 and 2 [17].

Two different types of arrangement may exist (see Figure 1) that correspond to central A or B particle, as shown in Figure 2.6. Denoting by g_{ji} ($=g_{ij}$) the interaction energy between two species *i* and *j*, the following quantities are generally introduced:

$$\tau_{ji} = \beta(g_{ji} - g_{ii}) \tag{2.111}$$

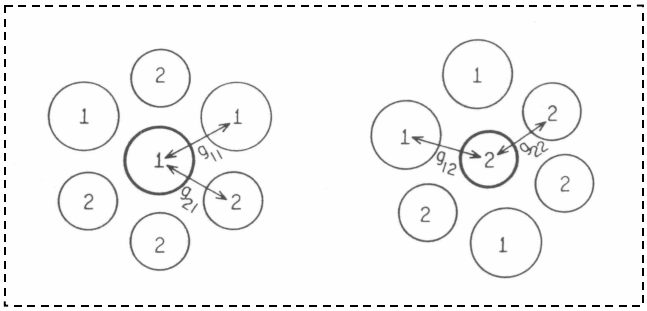

Fig.2.6 The 2 types of cells according to like-ion repulsion and local electroneutrality of the classical e-NRTL model. Left cell: cell with solvent 1 as central particle. Right cell: cell with solvent 2 as central particle.

For the binary system presented in Figure 2.6 eqn. (2.111) reads

$$\tau_{12} = \beta(g_{12} - g_{22}) \tag{2.112}$$

$$\tau_{21} = \beta(g_{21} - g_{11})$$

for the differences between interaction energies.

The probability P_{ji} (the symbol P_{ji} is used here in place of G_{ji} [17]) of finding a particle of species *j* in the immediate neighbour of a central particle of species *i* is assumed to obey a Boltzmann distribution as

$$P_{ji} = \exp(-\alpha\tau_{ji}) \tag{2.113}$$

Yielding for the binary mixture

$$P_{12} = exp(-\alpha\tau_{12}) \tag{2.114}$$

$$P_{21} = exp(-\alpha\tau_{21})$$

In these equations, α is the so-called non-randomness parameter (assumed to be identical for P_{ji} in eqn. (2.113) and (2.114)). The inverse of the latter parameter represents the typical number of particles surrounding a central particle [17].

The last (closure) equation relates the local mole fractions of species j and k, X_{ji} and X_{ki}, around central species i, to the probabilities as

$$\frac{X_{ji}}{X_{ki}} = \frac{x_j}{x_k}\frac{P_{ji}}{P_{ki}} \tag{2.115}$$

where j and i are ions or solvent. The relations between local mole fractions are

$$\sum_j X_{ji} = 1 \tag{2.116}$$

From eqns. (2.113) and (2.115), one gets

$$X_{ji} = x_j P_{ji} / \sum_k x_k P_{ki} \tag{2.117}$$

with x_j the mole fraction of species j in solution.

For the binary mixture,

$$X_{12} = \frac{x_1 P_{12}}{x_1 P_{12} + x_2} \tag{2.118}$$

$$X_{21} = \frac{x_2 P_{21}}{x_2 P_{21} + x_1} \tag{2.119}$$

with these definitions, the NRTL contribution to the Gibbs energy per molecule of species i, $g_i^{ex,NRTL}$ (often denoted by $g^{(i)}$), averaged on the different possible configurations, can be calculated according to

$$g_i^{NRTL} = \sum_j X_{ji} g_{ji}$$

which yields, using eqn. (2.115),

$$g_i^{NRTL} = \sum_j x_j P_{ji} g_{ji} / \sum_j x_j P_{ji} \tag{2.120}$$

In order to calculate the excess Gibbs energy, the reference state values, g_i^{ref}, must be specified. The reference state is a pure solvent for the solvent. Then, one has

$$\overline{G_i}^{ref,NRTL} = g_{ii}$$

and

$$g^{ref,NRTL} = \sum_k x_k g_k^{ref,NRTL} \tag{2.121}$$

Consequently, the NRTL deviation of the excess Gibbs energy of the solution (per molecule), averaged over all species, is given by

$$g^{ex,NRTL} = \sum_k x_k \left(g_k^{NRTL} - g_k^{ref} \right) \tag{2.122}$$

In the case of the ternary solution composed of 1 and 2 the expression for the excess Gibbs energy of the solution per molecule is then

$$g^{ex,NRTL} = x_1 \left(g_1^{NRTL} - g_1^{ref} \right) + x_2 \left(g_2^{NRTL} - g_2^{ref} \right) \tag{2.123}$$

$$\frac{g^{ex,NRTL}}{RT} = x_1 \tau_{12} X_{12} + x_2 \tau_{21} X_{21} \tag{2.124}$$

in the case of two solvents A and B

The generalisation to *n* species is straightforward. The NRTL equation for multi-components is:

$$\frac{g^{ex,NRTL}}{RT} = \sum_i \sum_{j \neq i} \left[x_i \frac{x_j P_{ji}}{\sum_k x_k P_{ki}} \tau_{ij} \right] \tag{2.125}$$

The activity coefficients in the symmetric convention are then obtained using eqn. (2.29)

$$ln\, f_i = \frac{\sum_j x_j \tau_{ji} P_{ji}}{\sum_k x_k P_{ki}} + \sum_j \frac{x_j P_{ji}}{\sum_k x_k P_{kj}} \left(\tau_{ij} - \frac{\sum_m x_m \tau_{mj} P_{mj}}{\sum_l x_l P_{lj}} \right) \tag{2.126}$$

The idea of local composition used in the NRTL model is similar to the Wilson model, to which the NRTL model is close. It can be noted that the derivative of the excess Gibbs energy with respect to temperature leads, in the two models, to the same final relation.

The NRTL model, as the Wilson model, describes multi-component systems only with the help of binary parameters. Renon et al. [17] used NRTL for predicting vapor-liquid equilibrium of ternary systems, and compared the results to the ones obtain with the Wohl's expansion. The predictions of

NRTL are in all cases as good if not better than the description of Wohl's expansion, even with the use of a ternary parameter.

The NRTL model is widely used in engineering chemistry for describing vapor-liquid equilibrium of multi-component systems because it provides accurate description of systems with few parameters. Another main advantage of the model is that it exhibits very low variance from the collected experimented data.

Table 2.4- Comparison of NRTL and Wohl's equations for prediction of ternary vapor-liquid equilibrium. NRTL calculations are made without any ternary parameter. Wohl's calculation are carried out with ternary constant. Data taken from ref. 17.

System	*NRTL deviation in individual vapor mole fraction* $\times 10^3$	*Wohl's deviation in vapor mole fraction* $\times 10^3$
Chloroform (1)	-3	11
Acetone (2)	-5	-11
Methanol (3)	-8	0
Benzene (1)	-3	-15
Carbon tetrachloride (2)	-2	7
Methanol (3)	5	8
Acetone (1)	-4	-9
Methanol (2)	1	8
Methyl acetate (3)	3	1
n-Heptane(1)	-5	8
Toluene (2)	-3	-2
Methanol (3)	8	6

From a theoretical point of view, the NRTL model is more adapted to the description of excess enthalpy h^{ex} than of excess Gibbs energy. This is due to the fact that entropic effects are not taken into account in the model. The competition between entropic and energetic interaction is hidden behind the values of the τ_{ij} parameters corresponding to the interaction resulting from this competition. This can pose a problem when the entropic interaction between *i* and *j*, such as steric effects or excluded volume effects, changes as another species is introduced in the solution. In this case, the sign of interaction (repulsive or attractive) are erroneously described by the τ_{ij} parameter.

4. Other models

a) The UNIQUAC model

The UNIQUAC equation (universal quasi-chemical model) [18], is a two parameter equation for g^{ex} that can be seen to a certain point as an extension of the quasichemical theory of Guggenheim [19] for nonramdom mixtures to solutions containing molecules of different size.

UNIQUAC considers two types of interactions to determine the excess energy: the size and shape of molecules (resulting in surface fractions and areas fractions per molecule), and the interaction energies to determine the excess Gibbs energy. The construction of the model is empirical, although the meaning of the parameters used is physical. One should notice that all molecules parameters are taken relative to the parameters of a CH_2 group in a high-molecular-weight paraffin.

The excess Gibbs free energy is divided in two parts. The combinatorial part $g^{ex}{}_{comb}$ corresponds mainly to entropic effects and require information on the surface fraction and on area fraction of a molecule. The residual part $g^{ex}{}_{resid}$ arises from intermolecular forces that are responsible for the enthalpy of mixing. This latter part requires adjustable parameters parameters since it is due to intermolecular forces.

$$g^{ex} = g^{ex}_{comb} + g^{ex}_{resid} \tag{2.127}$$

And

$$g^{ex}_{comb} / RT = \sum_i x_i \, ln \frac{\Phi^*_i}{x_i} + \frac{z}{2} \sum_i q_i x_i \, ln \frac{\theta_i}{\Phi^*_i} \tag{2.128}$$

$$g^{ex}_{resid} / RT = -\sum_i x_i q'_i \, ln \left(\sum_j \theta'_j \, \tau_{ji} \right) \tag{2.129}$$

where z is the coordination number set to 10. Φ^* is the segment fraction, q and q' are the area fractions. They are related to the different mole fractions as following

$$\Phi^*_i = \frac{r_i x_i}{\sum_j q_j x_j}, \quad \theta_i = \frac{q_i x_i}{\sum_j q_j x_j}, \quad \theta'_i = \frac{q'_i \, x_i}{\sum_j q'_j \, x_j} \tag{2.130}$$

and

$$\tau_{ij} = e^{-\frac{a_{ij}}{T}} \quad \text{and} \quad \tau_{ji} = e^{-\frac{a_{ji}}{T}} \tag{2.131}$$

τ_{ij} are the adjustable binary parameters. R_i, q_i and q'_i are the pure-component molecular-structure constant depending on molecular size and surface areas. q_i and q'_i are the surface interaction and the the geometric external surface, respectively. Except for water and lower alcohols, $q=q'$.

The resulting activity coefficient of species i requires only pure-component and binary parameters and is written as

$$ln\ f_i = ln\frac{\Phi_i^*}{x_i} + \frac{z}{2} ln\frac{\theta_i}{\Phi_i^*} + l_i - \frac{\Phi_i^*}{x_i}\sum_j x_j l_j - q'_i\left(1 + ln\left(\sum_j \theta'_j \tau_{ji}\right) - \sum_j \frac{\theta'_j \tau_{ij}}{\sum_k \theta'_k \tau_{kj}}\right) \quad (2.132)$$

$$l_j = \frac{z}{2}(r_j - q_j) - (r_j - 1)$$

UNIQUAC is widely utilised in applied chemistry in modelling or predicting the thermodynamic behaviour of chemical mixtures. It is applicable to a wide variety of non-electrolyte mixtures. Polar or non-polar solvents, such as alcohols, ketones, hydrocarbons or nitriles can be accurately described with the UNIQUAC model, including partially miscible mixtures, which can't be described by the Wilson model for example.

An initial example is presented in this dissertation with the n-hexane/nitroethane system at 45°C [20] shown in Figure 2.7, showing a VLE curve. The pressure of the vapor phase is plotted against the mole fraction of acetonitrile in the liquid phase, exhibiting a strong deviation from ideality. Despite this deviation, the experimental points are very well described within the UNIQUAC model.

Results for multicomponent systems are collected in Table 2.5. Here, the VLE for different temperatures of a quaternary and several ternary systems are presented. The accuracy of the results is in all cases satisfactory. The largest error occurs for the system acetic acid/ formic acid/ water for where experimental uncertainties are greater than for the other systems. For the system chloroform/ acetone/ methanol, the moderate deviation in vapor composition is due to the unusual deviations from ideality arising from strong hydrogen bonding between chloroform and alcohol. In this situation, the activity coefficient demonstrates an extremum, which are usually not well described with the UNIQUAC equation.

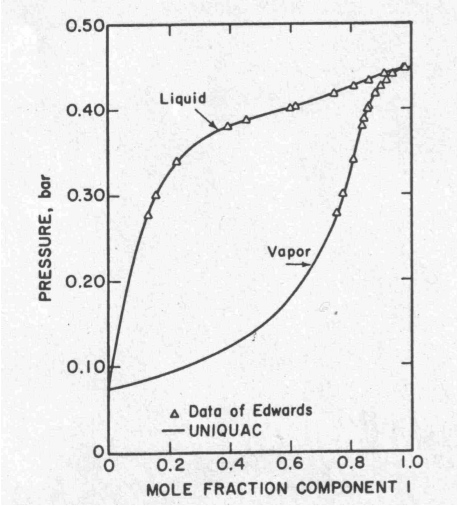

Figure 2.7- Strong positive deviations fron ideality. Vapor-liquid equilibrium for the n-hexane (1)/ nitroethane (2) system at 45°C. Data taken from ref. 20.

Table 2.5- Prediction of multi-component vapor-liquid equilibrium with UNIQUAC equations using binary data only. Data taken from ref. 21.

System	*Number of data points*	*Pressure[a] or Temperature[b]*	*Deviation in vapor composition [c]*
Aceitc acid (1)	40	1.013	1.00
Formic acid (2)		102-110	1.60
Water (3)			2.18
Chloroform (1)	29	0.6179-0.8599	0.86
Acetone (2)		50	0.77
Methanol (3)			0.81
Chloroform (1)	72	1.013	0.74
Methanol (2)		56-72	1.11
Ethyl acetate (3)			0.80
MethylCycloPentane (1)	48	1.013	0.51
Ethanol (2)		60-71	0.55
Benzene (3)			0.35
n-Hexane (1)	10	1.013	0.31
MethylCycloPentane (2)		60-65	0.44
Ethanol (3)			0.55
Benzene (4)			0.44

[a]: Units in bar. [b]: Units in K. [c]: Units in mol %

b) The group contribution method

The group contribution method has been developed to qualitatively describe thermodynamic properties of systems rather than quantitatively.

The principle of this method is to consider a molecule as an ensemble of functional groups. The whole solution is then regarded as a mixture of functional groups and no more in molecules mixture. That is, a molecule A is divided in groups 1, 2, 3, etc, and a molecule B is divided in groups 1', 2', 3', etc. Interactions between 1 and 1', 1 and 2', 1 and 3' and so on, are now considered, and no more interaction between two A or between A and B.

The consideration of molecules as ensemble of functional groups requires, of course, many more parameters than in the case where molecules are considered. But considering the infinite number of existing molecules, and the finite number of functional groups, the number of parameters is *in fine* much smaller.

This method requires, however, that many systems are fitted together in order to differenciate the effect of each functional group on the thermodynamic properties and a big parameter table. This has been done and keep on being done by the ASOG (analytical solution of groups) method.

The UNIQUAC model is a model that required many molecule parameters, as stated ebove in the last section. Therefore, the development of a new model, called UNIFAC (universal functionnal activity

coefficient), in which the group contribution method is applied to the UNIQUAC model. In the UNIFAC model, the activity coefficients are calculated in the same way as with the UNIQUAC model, except made from the parameters that are now group specific and no longer molecule specific. In the UNIQUAC model , the residual part of the activity coefficient (see eqns. (2.129) and (2.132)) requires knowledge of the surface areas, mole fractions of molecules and interaction energies between molecules. In the UNIFAC model, the activity coefficient is calculated with surface areas and mole fractions of the functional groups, and interaction energies between these groups.

This model, though requiring more parameters for a single molecule, allows the description of numerous systems, and predict thermodynamic properties of systems that are not experimentally studied. Therefore, it is today one of the most popular model used in chemical engineering.

References

[1] J. M. Prausnitz, R. N. Lichtenthaler and E. Gomes de Azevedo, in *Molecular Thermodynamics of Fluid-Phase Equilibrium*, Prentice Hall, Upper Saddle River, New Jersey, 1999.

[2] R. A. Robinson and R. H. Stokes, in *Electrolyte Solutions, 2nd ed.*, ed. Butterworths: London, 1959.

[3] W. G. McMillan and J. E. Mayyer, *J. Chem. Phys.*, 1945, **13**, 276.

[4] J. P. Simonin, *J. Chem. Soc., Faraday Trans.*, 1996, **92**, 3519.

[5] J. P. Simonin, *Fluid Phase Equilibrium*, 1999, **165**, 41.

[6] J. F. Dufrèche, Ph.D. dissertation, Université Pierre et Marie Curie, 2002.

[7] Van't Hoff, 1887,

[8] H. L. Friedman, in *Ionic Solution Theory*, Interscience, New York, 1962.

[9] P. Novotný and O. Sohnel, *J. Chem. Eng. Data*, 1988, **33**, 49.

[10] S. Weissmann and S. E. Wood, *J. Chem. Phys.*, 1960, **32**, 1153.

[11] R. A. H pool, G. Saville, T. M. Herrington, B. D. C. Shields and L. A. K. Staveley, *Trans. Faraday Soc.*, 1962, **58**, 1962.

[12] G. Scatchard, S. E. Wood and J. M. Mochel, *J. Phys. Chem.*, 1939, **43**, 119.

[13] W. H. Severns, A. Sesonske, R. H. Perry and R. L. Pigford, *AIChE J.*, 1955, **1**, 401.

[14] G. M. Wilson, *J. Am. Chem. Soc.*, 1964, **86**, 127.

[15] C. B. Kretschmer, *J. Am. Chem. Soc.*, 1948, **70**, 1785.

[16] R. V. Orye and J. M. Prausnitz, *Ind. Eng. Chem.*, 1965, **57**, 19.

[17] H. Renon and J. M. Prausnitz, *AIChE J.*, 1968, **14**, 135.

[18] AbramsD. Abrams and J. M. Prausnitz, *Ind. Eng. Chem. Process Des. Dev.*, 1978, **17**, 552.

[19] E. A. Guggenheim, in *Mixtures*, Oxford: Oxford University press, 1952.

[20] J. B. Edwards, Ph.D. Dissertation, Georgie Institue of technology, 1962.

[21] T. F. Anderson and J. M. prausnitz, *Ind. Eng. Chem. Process Des. Dev.*, 1978, **17**, 552

Chapter III- The MSA model

This section is devoted to the theoretical description of ionic solutions with the help of statistical mechanics. The MM framework, in which the models are developed, has been introduced in the preceding chapter. The first section will be devoted to the statistical mechanical description of ionic solutions. In the second section we will focus on the different available versions of the MSA model. Finally, our work will be presented on applying the MSA model to ionic solutions at high temperatures.

A. Description of ionic solutions

1. The primitive model for electrolyte solutions

As seen in the preceding chapter, the description of a solution in the MacMillan Mayer framework requires only the solute-solute (solvent averaged) effective interaction potential. The simplest model is the so-called primitive model in which the ions are regarded as charged hard spheres. The effective potential between two ions *i* and *j* separated from a distance *r* iswritten as:

$$V_{ij}(r) = V_{HS}(r) + \frac{z_i z_j e^2}{4\pi\varepsilon_0\varepsilon_s r} \tag{3.1}$$

with z_i, the charge of ion *i*, *e* the proton charge, ε_0 the permittivity of a vacuum and ε_s the dielectric constant of solvent. $V_{HS}(r)$, the hard sphere interaction potential, reads.

$$\begin{cases} V_{HS}(r) = +\infty & \textbf{\textit{if}} \quad r < \dfrac{\sigma_i + \sigma_j}{2} \\ V_{HS}(r) = 0 & \textbf{\textit{if}} \quad r > \dfrac{\sigma_i + \sigma_j}{2} \end{cases} \tag{3. 2}$$

where σ_i and σ_j denote the diameters of ion *i* and *j*, respectively. For ions of equal size (cations and anions), one speaks of the *restricted primitive model*.

The electrostatic term of this effective potential corresponds to a charged particle immersed in a continuous solvent characterised by its sole permittivity ε_s. This permittivity is related to the mean force between ions, and thus is an effective permittivity of solvent between ions. At low concentration, ions being far from antother, the premittivity is similar to the one of pure solvent [1]. At high concentrations, the interactions between ions and solvent particles yielding the reorientation of the solvent molecules, and thus the reorientation of dipole moments of solvent. This results in a change of thevalue of the effective permittivity value [2].

2. Method of solution in the primitive model

a) Integral equations of statistical mechanics

A way of calculating thermodynamic equilibrium quantities for a given potential is to use simulation methods [3], such as Monte Carlo or molecular dynamics. These methods do not lead to analytical expressions, and require long computation times. Other methods are then used for the calculation of such quantities, generallybased on the so-called integral equations, which are briefly summarised here.

In the case of the continuous solvent model, one of the characteristic quantities of the solution is the total pair correlation function $h_{ij}(r_{ij})$. It is related to the pair correlation function as follows

$$g_{ij}(r_{ij}) = 1 + h_{ij}(r_{ij}) \tag{3. 3}$$

with g_{ij} the probability density of finding a *j* particle particle around an *i* particle, when separated from a distance r_{ij} (g_{ij} is normalised to 1 when $r_{ij} \to \infty$). If g_{ij} is explicitly known, one may obtain the pressure and the internal energy of the system:

$$\Delta U^{ex} = \frac{1}{2}\sum_i \rho_i \rho_j \int_0^\infty 4\pi V_{ij}(r) h_{ij}(r) r^2 dr \tag{3. 4}$$

$$\beta P_{osm} = \sum_i \rho_i - \frac{2}{3}\beta\pi \sum_{i,j} \rho_i \rho_j \int_0^\infty \frac{\partial V_{ij}(r)}{\partial r} g_{ij}(r) r^3 dr \tag{3. 5}$$

with ΔU^{ex} the exces internal energy of the system, and βP_{osm} the osmotic pressure. Integrating these quantities yields afterwards the other thermodynamic quantities [4, 5].

In 1914, Ornstein and Zernicke proposed an equation expressing the total correlation function as a function of a direct correlation function c_{ij}, describing only the two-body interactions,

$$h_{ij}(r_{ij}) = c_{ij}(r_{ij}) + \sum_k \rho_k \int c_{ik}(r_{ik}) h_{kj}(r_{kj}) d\mathbf{r}_k \qquad (3.\ 6)$$

with ρ_k the number density of species k. For calculating the pair correlation function and the equilibrium thermodynamic quantities of the system, one needs a supplementary equation for $h_{ij}(r_{ij})$ (or $g_{ij}(r_{ij})$ or $c_{ij}(r_{ij})$) called *closure relation*. Many approximated relations have been proposed that can be obtained with the help of mathematical techniques as the diagram developments or functional derivatives [4, 5].

i) The Hypernetted Chain equation (HNC)

The HNC equation relates $h_{ij}(r_{ij})$, $g_{ij}(r_{ij})$, and $c_{ij}(r_{ij})$ and the interaction potential $V_{ij}(r)$ through the relation

$$g_{ij}(r_{ij}) = exp(-\beta V_{ij}(r_{ij}) + h_{ij}(r_{ij}) - c_{ij}(r_{ij}) \qquad (3.\ 7)$$

The solution can only be obtained numerically. Writing the OZ equations in the Fourier space, one may find the function $g_{ij}(r_{ij})$.

The HNC equation is well adapted to the coulomb potential [6]. In the case of low charge electrolytes, the pair correlation function is nearly equal to the one obtained by simulation [7]. It also allows to describe the correlation functions for polyelectrolytes [8]. Its main default is that the solution algorithm for the HNC equation will not converge if the system is highly charged and the particles are small. In such cases, one is close to the spinodal line, HNC is unable to describe the phase separation domain [9].

ii) Percus Yevick (PY) and other closure relations

There are several other closure relations. The Percus-Yevick (PY), for instance, reads:

$$g_{ij}(r_{ij}) = e^{-\beta V_{ij}(r)}\left(1 + h_{ij}(r_{ij}) - c_{ij}(r_{ij})\right) \qquad (3.\ 8)$$

It is very well adapted to the hard-sphere model, for which it yields analytical results [10], but it cannot be used for ionic systems.

Other closure relations have been proposed, whether by combining the preceding relations or forcing the self consistence of the results, setting for instance the pressure obtained by the virial theorem equal to the one obtained by the compressibility equation [10, 11].
Another closure relation will be used in our work, the Mean Spherical Approximation (MSA), which will now be detailed.

b) The MSA closure relation

The direct correlation function $c_{ij}(r_{ij})$ has an exact limit when $r_{ij} \rightarrow +\infty$

$$c_{ij}(r_{ij}) = -\beta V_{ij}(r_{ij}) \qquad (3.9)$$

The MSA assumption is to apply this equation for all r_{ij} greater than the distance of closest approach. Due to the repulsion between particles at small r, one explicitly writes that particles cannot penetrate each other. The MSA closure relation thus reads

$$\begin{cases} g_{ij}(r_{ij}) = 0 & \text{for} \quad r_{ij} < \dfrac{\sigma_i + \sigma_j}{2} \\ c_{ij}(r_{ij}) = -\beta V_{ij}(r) & \text{for} \quad r_{ij} > \dfrac{\sigma_i + \sigma_j}{2} \end{cases} \qquad (3.10)$$

For distances $r_{ij}<(\sigma_i+\sigma_j)/2$, the MSA closure relation is exact. For distances $r_{ij}>(\sigma_i+\sigma_j)/2$, the MSA closure relation can be found by linearising the HNC relation (eqn. 3.7).

The main advantage of MSA is that it yields an analytical solution for several potentials: hard sphere, hard sphere + square well, hard sphere + Yukawa, hard sphere + dipoles, and for electrolyte systems which will be studied below: charged hard spheres. Notice that the MSA is approximately correct only for potentials smaller than kT.

i) The primitive model solved with MSA

The first solution of the MSA equation for charged hard spheres was given by Waisman and Lebowitz [11]. Then, it was improved by several authors [12], especially Blum [13-15] who was the first to obtain explicit tractable equations.

For charged hard spheres, the thermodynamic quantities calculated within the MSA model involve two contributions. The first one is the hard sphere contribution and the second contribution is electrostatic. Thus in the MSA model, all quantities calculated are the sum of an electrostatic term and a hard sphere term. For example, the MSA equation of state may be formally written as

$$\frac{\beta P_{osm}^{MSA}}{\rho_t} = 1 + \frac{\beta \Delta P_{osm}^{el}}{\rho_t} + \frac{\beta \Delta P_{osm}^{HS}}{\rho_t} \qquad (3.\ 11)$$

with

$$\rho_t = \sum_i \rho_i$$

ΔP^{el} and ΔP^{HS} are the electrostatic and the hard sphere contribution to the pressure, respectively. In eqn. 3.11, the relation $\beta P/\rho_t$ is used.

One of the interesting features of the MSA model lies in the fact the electrostatic term provides a correction to the Debye-Hückel theory, by replacing the Debye screening parameter κ by Γ, which is written as [18]:

$$\Gamma = \left[\pi\lambda \sum_i \rho_i \left(\frac{z_i - \sigma_i^2 \eta}{1 + \Gamma\sigma_i} \right)^2 \right]^{1/2} \qquad (3.\ 12)$$

$$\lambda = \frac{\beta e^2}{4\pi\varepsilon_0 \varepsilon}$$

$$\eta = \frac{1}{\Omega} \frac{\pi}{2\Delta} \sum_i \frac{\rho_i \sigma_i z_i}{1 + \Gamma\sigma_i}$$

$$\Omega = 1 + \frac{\pi}{2\Delta} \sum_i \frac{\rho_i \sigma_i^3}{1 + \Gamma\sigma_i}$$

$$\Delta = 1 - \frac{\pi}{6} \sum_i \rho_i \sigma_i^3$$

Here, 2Γ has the same meaning in MSA as the parameter κ in the Debye-Hückel theory. Here, the ion size is explicitly taken into account in the ionic atmosphere. The equations for thermodynamic quantities are formally similar to those obtained with the Debye-Hückel theory. For instance, the electrostatic contribution to the equation of state in the MSA model is

$$\frac{\beta \Delta P_{osm}^{el}}{\rho_t} = -\frac{\Gamma^3}{3\pi\rho_t} - \frac{2\lambda}{\pi\rho_t} \eta^2 \qquad (3.\ 13)$$

and in the Debye Hückel theory:

$$\frac{\beta \Delta P_{osm}^{DH}}{\rho_t} = -\frac{(\kappa/2)^3}{3\pi\rho_t} \qquad (3.\ 14)$$

In the case where all ions are of equal size, one has η=0. The forms of eqns. (3.13) and (3.14) are then identical. The case of equal sized ions yields much simpler equations for the electrostatic expressions. This approximation has been used several times [19], and is also suitable for solutions of asymmetric ions. Nevertheless, it is not to be used for salts which ions are more than 5 times bigger than their counter-ion (σ_i/σ_j=5).

Let us now compare MSA with other theories, such as HNC. Consider a 1-1 and a 2-2 electrolytes at 25°C in water. The dielectric constant of solution is 78.3, σ_+=3Å, σ_-=5 Å, and the concentration of the salt is 1 mol/L. The osmotic coefficient $\phi = \beta P_{osm}/\rho_t$ is given in Table 3.1. HNC is here our reference model, since it gives the same results as simulations for 1-1 electrolytes and close results for 2-2 electrolytes [5].

Table. 3.1 – Osmotic coefficient of aqueous electrolyte solutions calculated using different theories. The electrolyte concentration is 1 mol/L, σ_+=3A and σ_-=5A.

Electrolyte	HNC (virial)	MSA (virial)	MSA (energy)
1-1	1,064	1,011	1,068
2-2	0,620	0,159	0,593

The HNC value for the osmotic coefficient is calculated with the help of the virial equation [4] (which gives the pressure as an integral of the pair correlation function). MSA calculations have been done in two ways: firstly with the virial theorem, and secondly by integrating the energy with respect to temperature. It is not surprising to get different values in the MSA when calculated in two different ways. Since the MSA closure relation is approximate, it leads to approximate expressions of $\beta\Pi$ and ΔE (see eqns. 3.4 and 3.5). As a result, the derivation of these thermodynamic quantities yield different expressions of the same quantity, such as osmotic or activity coefficients.

One notices that the MSA osmotic coefficient for 1-1 electrolyte, calculated via the energy is very close to the HNC result (and simulations). For the 2-2 salt, the result is close though less accurate. On the contrary, the virial theorem gives quite underestimated values of the osmotic coefficient. In our study, we will use the expressions for the thermodynamic quantities in the MSA model derived from the energy route.

Let us now conclude this section by studying the MSA pair correlation function $g_{ij}(r)$ for the 1-1 and 2-2 electrolytes used above as examples. The plots of $g_{ij}(r_{ij})$ as a function of r_{ij} calculated with the help of the HNC and the MSA models are shown in Figure 3.1. In the case of 1-1 salt, the MSA result is very close to HNC. For distances r_{ij} near contact however, the MSA pair correlation function is not very accurate. Moreover, it gives negative values for $g_{++}(r)$, in the two electrolyte cases. Furthermore, the value of $g_{\pm}(r)$ at contact is in the two cases far away from the HNC values. Hence, MSA does not account properly for short range effects.

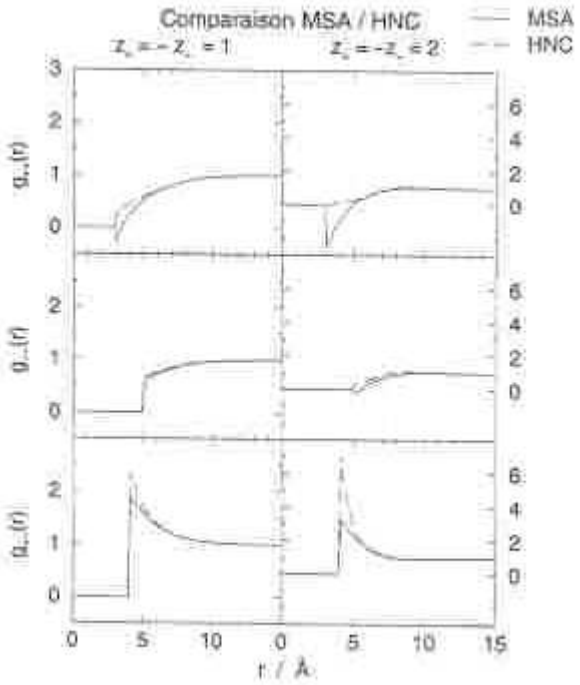

Figure 3.1- Comparison of the pair correlation function *g(r)* calculated with the HNC and the MSA models, in the case of two 1-1 and 2-2 electrolytes, at 1 mol L^{-1}.

Despite this bad description of the structure with the MSA model, the integration of the pair correlation functions lead to very accurate values of the thermodynamic quantities as it will be detailed now.

B. Thermodynamic quantities in the MSA model

1. The MSA primitive model

The resulting state function calculated within the MSA model in the MM framework is the excess free Helmholtz energy per volume unit of the system. This function results, as all thermodynamic quantities calculated within the MSA model, into the combination of a hard sphere and an electrostatic contributions.

$$\Delta F^{MSA} = \Delta F^{el} + \Delta F^{HS} \qquad (3.\ 15)$$

in which Δ means an excess quantity.

Each contribution results into an excess activity coefficient

$$\Delta \ln \gamma_i^X = \frac{\partial \beta \Delta F^X}{\partial \rho_i} \qquad (3.\ 16)$$

with X= *el*, *HS* and ρ_i being the number density of species *i* (number of particles per volume unit), and into a contribution to the osmotic coefficient

$$\Delta\phi^X = \rho_t \frac{\partial}{\partial\rho_t}\left[\frac{\beta\Delta F^X}{\rho_t}\right] \tag{3. 17}$$

with $\rho_t = \sum_i \rho_i$ (the summation being made over all solutes) and where the derivation is performed at constant mole fraction of each solute (ρ_i/ρ_t =constant). ρ_i is related to the concentration through the relation:

$$\rho_i = 10^3 N_A c_i \tag{3. 18}$$

The activity and osmotic coefficients are given by

$$ln\,\gamma_i = \Delta\, ln\,\gamma_i^{el} + \Delta\, ln\,\gamma_i^{HS} \tag{3. 19}$$

$$\phi = 1 + \Delta\phi^{el} + \Delta\phi^{HS} \tag{3. 20}$$

by virtue of the relations ϕ^{ideal} = 1 and $ln\gamma^{ideal}$ = 0.

a) Electrostatic term

i) The unrestricted primitive model

The electrostatic contribution to ΔF has been reviewed in several papers [18-20]. We will first consider the general case where the ions have different sizes, corresponding to the so-called unrestricted primitive model.

$$\beta\Delta F^{el} = -\lambda\sum_i \rho_i z_i \frac{\Gamma z_i + \eta\sigma_i}{1+\Gamma\sigma_i} + \frac{\Gamma^3}{3\pi} \tag{3. 21}$$

where $\beta=1/k_BT$. Γ is the above mentioned MSA screening parameter, given by eqn. (3.12).

The electrostatic contribution to the activity and the osmotic coefficients (see eqns. (3.16) and (3.15)) are

$$ln\,\gamma_i^{el} = -\lambda\left[\frac{\Gamma z_i^2}{1+\Gamma\sigma_i} + \eta\sigma_i\left(\frac{2z_i - \eta\sigma_i^2}{1+\Gamma\sigma_i} + \frac{\eta\sigma_i^2}{3}\right)\right] \tag{3. 22}$$

$$\Delta\phi^{el} = -\frac{\Gamma^3}{3\pi\rho_t} - \lambda\frac{2\eta^2}{\pi\rho_t} \tag{3. 23}$$

ii) Restricted Primitive model.

In the case of the restricted primitive model (RPM), all ions have the same size. This leads to $\sigma_i = \sigma_j = \sigma$ and η=0. The electrostatic contribution to the excess free Helmholtz energy is

$$\beta \Delta F^{RPM,el} = -\lambda \frac{\Gamma}{1+\Gamma\sigma} \sum_i \rho_i z_i^2 + \frac{\Gamma^3}{3\pi} \tag{3. 24}$$

where Γ is now written as:

$$\Gamma = \frac{1}{2\sigma}\left(\sqrt{1+2\kappa\sigma} - 1\right) \tag{3. 25}$$

The contribution to the thermodynamic coefficients is:

$$ln\,\gamma_i^{RPM,el} = -\lambda \frac{\Gamma z_i^2}{1+\Gamma\sigma_i} \tag{3. 26}$$

$$\Delta\phi^{RPM,el} = -\frac{\Gamma^3}{3\pi\rho_t} \tag{3. 27}$$

b) Hard sphere term

Different expressions can be used for the hard sphere term ΔF^{HS} , such as the Percus-Yevick (PY), or the Boublik-Mansoori-Carnahan-Starling-Leyland (BMCSL) expressions. The latter has been used in our work since it provides better values for the compressibility than the PY expression, as shown in Table 3.2.

$$\frac{\pi}{6}\beta\Delta F^{HS} = \left(\frac{X_2^3}{X_3^2} - X_0\right) ln(1-X_3) + \frac{3X_1X_2}{1-X_3} + \frac{X_2^3}{X_3(1-X_3)^2} \tag{3. 28}$$

where

$$X_n = \frac{\pi}{6}\sum_i \rho_i \sigma_i^n \tag{3. 29}$$

Combining eqns. (3.16) and (3.17) with eqn.(3.28) leads to

$$ln\,\gamma_i^{HS} = -ln(1-X_3) + \sigma_i F_1 + \sigma_i^2 F_2 + \sigma_i^3 F_3 \tag{3. 30}$$

$$\Delta\phi^{HS} = \frac{X_3}{1-X_3} + \frac{3X_1X_2}{X_3(1-X_3)^2} + \frac{X_3^2(3-X_3)}{X_0(1-X_3)^3} \tag{3. 31}$$

with

$$F_1 = \frac{3X_2}{1-X_3}$$

$$F_2 = \frac{3X_1}{1-X_3} + \frac{3X_2^2}{X_3(1-X_3)^2} + \frac{3X_2^2}{X_3^2} ln(1-X_3)$$

$$F_3 = \left(X_0 - \frac{X_2^3}{X_3^2} \right) \frac{1}{1-X_3} + \frac{3X_1X_2 - X_2^3/X_3^2}{(1-X_3)^2} + \frac{2X_2^3}{X_3(1-X_3)^3} - \frac{2X_2^3}{X_3^3} ln(1-X_3)$$

Table 3.2- Values for the compressibility of a hard sphere mixture calculated with various hard sphere equations. The values are here shown for a system of two hard sphere with following properties: $\rho_1=\rho_2=\rho/2$, $\sigma_2/\sigma_1=3$. X_3 is defined by eqn. (3.29). Z is the compressibility of a hard sphere mixture. Subscript *MD* stands for molecular dynamics, which give the reference values for the compressibility. The subscripts *CS*, *comp* and *virial* stand for Carnahan-Starling, compressibility and virial, respectively. It is clearly to see that the Carnahan Starling expression is closer to the MD values than either the compressibility or the virial values. MD values taken from ref. [21].

X_3	Z^{MD}	Z^{CS}	Z^{comp}	Z^{vir}
0.2333	2.37	2.368	2.386	2.332
0.2692	2.77	2.772	2.804	2.708
0.3106	3.36	3.356	3.414	3.239
0.3582	4.24	4.241	4.352	4.019
0.3808	4.76	4.764	4.912	4.467
0.4393	6.57	6.566	6.872	5.952
0.5068	9.77	9.896	10,588	8.512

c) Results

The unrestricted primitive model has been used by Ebeling et al. [22] for describing experimental mean ionic activity coefficients of various electrolyte solutions up to 1 mol kg^{-1} at 298 K. The mean ionic activity coefficients have been calculated with eqns. (3.19) and (3.30). The MSA activity coefficients, obtained in the MM framework, have been converted to the LR framework. Nevertheless, this conversion does not improve much the quality of fits, since it is known that the deviation between MM and LR quantities are small at low concentrations [23]. 15 salts have been fitted simultaneously in order to obtain a common set of 8 ion-specific ion diameters.

Parameter values are summarised in Table 3.3 and a plot is given in Figure 3.2. In this table the values of the crystallographic radii of ions are also collected. The sizes of the anions have been kept equal to their crystallographic value, since it is known that they are hardly solvated [24].

As it can be seen, the MSA radius is effectively bigger than the crystallographic radii for the three ions Li^+, Na^+ and K^+. This is due to the solvation sphere surrounding the ion which is included in the MSA effective ion diameter. For the last two cations, radii are smaller than Pauling ones due to the fact that these salt are associated, though not necessary in a chemical

way. An extra attractive force exists in the case of the Rubidium and Cesium salt that is not taken into account in the MSA model, yielding low values of $\gamma_{\pm}$ and hence low values of σ_{MSA}

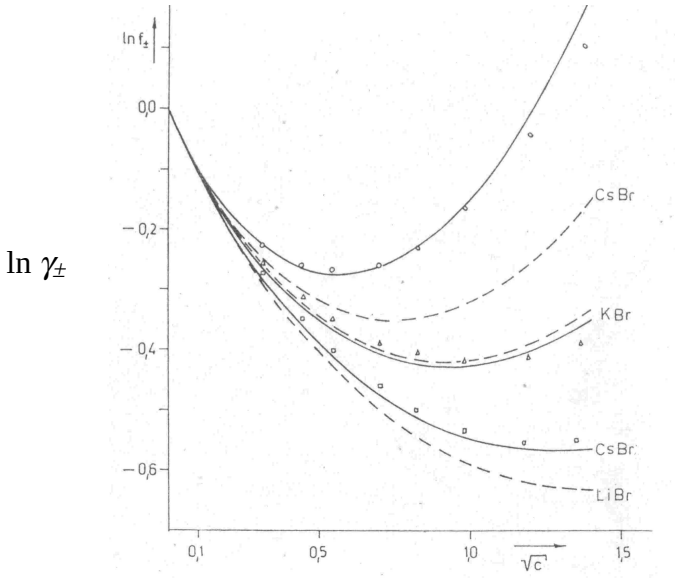

Figure 3.2- Mean activity coefficients $\gamma_{\pm}$ for aqueous alkali bromide solutions at 25°C. Curves are calculated using Pauli radii (---) or fitted radii (-) from table 3.3. Experimental values: (○): LiBr, (△): KBr, (□): CsBr. Experimental data taken from ref 25.

Despite the accurate description obtained with this version of the MSA model of the activity coefficients of earth-alcaline electrolyte solution up to 1 mol kg^{-1}, the latter model cannot be extended to high concentrations. Since the MSA diameter is an effective diameter including the hydration sphere, one has to consider the fact that this diameter decreases with salt concentration. The hydration sphere decreases with concentration, due to less relative free space and water molecules available. Furthermore, the permittivity of solution is also expected to vary with salt concentration, as detailed in the beginning of the chapter.

The extension of the MSA model to high concentrations then requires the introduction of a conversion relation between the MM and LR frameworks, as described in chapter 2 for example, and concentration dependences for the ion diameters σ and the solution permittivity ε .

Table 3.3- Values of the adjusted MSA parameters from the common fit of activity coefficients for the 15 earth-alcaline electrolytes. R_p stands for Pauli radius and R for the adjusted MSA radius. Results taken from ref. 22.

	R_p [a]	R [a]
Li^+	0.60	2.25
Na^+	0.95	1.69
K^+	1.33	1.36
Rb^+	1.48	1.08
Cs^+	1.69	0.84
Cl^-	1.81	1.78
Br^-	1.95	1.90
I^-	2.16	2.16

[a] In units of 10^{-10} m.

2. Applications of the primitive MSA model

a) Application to highly concentrated solutions

Several studies about the extension of the MSA model for high salt concentrations at 298K have been attempted. To this end, two corrections have been brought to the original MSA model. Firstly, a conversion between the MM and LR level of description had to be added to the calculations of the thermodynamic coefficients in order to compare them properly with the experimental values. Secondly, a concentration dependence was assumed for the two MSA parameters σ and ε. This assumption is reasonable for ε since it is known that the dielectric constant of a solution decreases when adding salt, by reducing the density of solvent dipole moments. The MSA diameter σ is also expected to vary as the solvation sphere depends on the salt concentration.

Sun and Teja [26] studied the extension of MSA to high concentrations. They introduced a concentration dependence in the MSA diameter, but not in the permittivity, and used an expression to convert osmotic coefficients calculated in the MM framework to values in the LR level of description. They also studied the ability of the MSA model to describe high temperatures solutions by introducing a temperature dependence into the MSA diameter.

The accuracy of the model was good in a wide range of temperature and concentrations. Nevertheless, the model did no longer fulfill the Gibbs-Duhem law, since the derivative of ΔF with respect to ρ (see eqns. (3.16) and (3.17)) was not calculated considering the concentration dependence of σ.

In the work of Simonin et al. [27, 28], the concentration dependence of σ and ε as correctly taken into account in the derivation of ΔF, so yielding thermodynamic coefficients that fulfill the GD relation. The concentration dependences were assumed to be linear for σ and ε^{-1}.

$$\sigma_+ = \sigma_+^{(0)} + \sigma_+^{(1)} c_s \qquad (3.32)$$

$$\varepsilon^{-1} = \varepsilon_w^{-1}\left(1 + \alpha c_s\right) \qquad (3.33)$$

where c_s is the salt concentration, ε_W the dielectric constant of pure water, and $\sigma_+^{(0)}$ the ion size at infinite dilution. $\sigma_+^{(1)}$ and α are adjustable parameters. Notice that $\sigma_+^{(0)}$ is a constant characteristic of a given cation. The size of anions was taken constant (crystallographic, or "optimum", size).

i) Electrostatic term

The proper derivation of ΔF yields for the electrostatic contribution [28]

$$\ln \gamma_i^{el} = -\lambda\left[\frac{\Gamma z_i^2}{1+\Gamma\sigma_i} + \eta\sigma_i\left(\frac{2z_i - \eta\sigma_i^2}{1+\Gamma\sigma_i} + \frac{\eta\sigma_i^2}{3}\right)\right] + \sum_j \rho_j q_j \frac{\partial\sigma_j}{\partial\rho_i} + \beta\Delta U^{el}\varepsilon\frac{\partial\varepsilon^{-1}}{\partial\rho_i} \tag{3. 34}$$

$$\Delta\phi^{el} = -\left[\frac{\Gamma^3}{3\pi\rho_t} + \lambda\frac{2\eta^2}{\pi\rho_t}\right] + \frac{1}{\rho_t}\sum_i \rho_i q_i D(\sigma_i) + \frac{\beta\Delta E^{el}}{\rho_t}\varepsilon D(\varepsilon^{-1}) \tag{3. 35}$$

$$q_i = \lambda\left[\frac{\Gamma^2 z_i^2}{(1+\Gamma\sigma_i)^2} + \eta\frac{\eta\sigma_i^2(2-\Gamma^2\sigma_i^2) - 2z_i}{(1+\Gamma\sigma_i)^2}\right] \tag{3. 36}$$

$$\Delta U^{el} = -\lambda\sum_i\left[\rho_i z_i\frac{\Gamma z_i + \eta\sigma_i}{1+\Gamma\sigma_i}\right] \tag{3. 37}$$

with $D(A) = \sum_k \rho_k \frac{\partial A}{\partial\rho_k}$ which yields using eqns. (3.14), (3.15)

$$D(\sigma_+) = \sigma_+ - \sigma_+^{(0)} \tag{3. 38}$$

$$\varepsilon D(\varepsilon^{-1}) = 1 - \varepsilon/\varepsilon_w \tag{3. 39}$$

ii) Hard sphere contribution

For the hard sphere term, the BMCSL expression of ΔF as given in eqn. (3.28) has been used. The proper derivation gives [28]

$$\ln \gamma_i^{HS} = -\ln(1-X_3) + \sigma_i F_1 + \sigma_i^2 F_2 + \sigma_i^3 F_3 + \sum_j Q_j\rho_j\frac{\partial\sigma_j}{\partial\rho_i} \tag{3. 40}$$

$$\Delta\phi^{HS} = \left[\frac{X_3}{1-X_3} + \frac{3X_1X_2}{X_3(1-X_3)^2} + \frac{X_3^2(3-X_3)}{X_0(1-X_3)^3}\right] + \frac{1}{\rho_t}\sum_j Q_j\rho_j D(\sigma_j) \tag{3. 41}$$

with

$$Q_i = F_1 + 2\sigma_i F_2 + 3\sigma_i^2 F_3$$

$$F_1 = \frac{3X_2}{1-X_3}$$

$$F_2 = \frac{3X_1}{1-X_3} + \frac{3X_2^2}{X_3(1-X_3)^2} + \frac{3X_2^2}{X_3^2}\ln(1-X_3)$$

$$F_3 = \left(X_0 - \frac{X_2^3}{X_3^2}\right)\frac{1}{1-X_3} + \frac{3X_1X_2 - X_2^3/X_3^2}{(1-X_3)^2} + \frac{2X_2^3}{X_3(1-X_3)^3} - \frac{2X_2^3}{X_3^3}\ln(1-X_3)$$

iii) MM-to-LR conversion.

A new approximated and justified MM-to-LR conversion is introduced, as explained in chapter 2. The resulting expressions for the thermodynamic coefficients are

$$\ln \gamma_i^{LR,calc} = \left(\ln \gamma_i^{el} + \ln \gamma_i^{HS}\right) - CV_i\left(1 + \Delta\phi^{el} + \Delta\phi^{HS}\right) \quad (3.\ 42)$$

$$\phi^{LR,calc} = \left(1 + \Delta\phi^{el} + \Delta\phi^{HS}\right)\left(1 - CV_{\pm}\right) \quad (3.\ 43)$$

with $V_{\pm}$ defined in chapter 2, section 6 (see eqn. (2.86)).

The calculation of V_i and $V_{\pm}$ requires the knowledge of the concentration dependence of the solution density. The expression used for the solution density is given by eqn. (2.88), as determined by Novotny and Sohnel [29].

iv) Results

The model has been applied to various salts at 298 K, for symmetric 1-1 salts and unsymmetric 1-2 salts [28]. Results have been here summarized in Table 3.4, and some plots have been given in Figure 3.3.

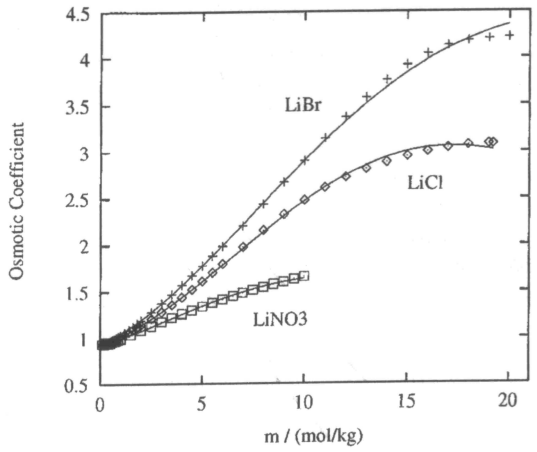

FIGURE 3.3- LR experimental and calculated osmotic coefficient for LiCl, LiBr, and $LiNO_3$ as a function of the salt molality. (◇) Experimental points for LiCl; (+) Experimental points for LiBr; (□) Experimental points for $LiNO_3$; (—) Calculated curves.

In all cases, the fitted parameter $\sigma_+^{(0)}$ was found to be greater or equal to the corresponding crystallographic value, which is coherent with the previous explanations given. The negative value of the concentration dependent parameter $\sigma^{(1)}$ is also coherent with the idea that the solvation sphere decreases with the concentration. Furthermore, the positive value of α is in agreement with the observation that solution permittivity decrease with the salt concentration.

The model was also used to describe mixtures of electrolytes. It was found to be predictive for mixtures with common cations. For mixtures without common cations, a supplementary cross parameter σ_{i-j} was introduced to describe the effect of cation *i* on cation *j*.

Table 3.4- Values of parameters from fit of osmotic coefficients for pure salts.

Salt	m_{max} [a]	$\sigma^{(0)}$ [b]	$10^2\,\sigma^{(1)}$ [c]	$10^2\,\alpha$ [d]	*AARD* [e]
HCl	16	5.040	-8.216	6.266	0.2
HBr	11	5.040	-8.132	2.921	0.9
HI		5.040	-9.502	3.216	0.9
LiCl	19.2	5.430	-9.147	15.45	0.5
LiBr	20	5.430	-9.676	14.56	0.8
LiI	3	5.430	-13.01	12.71	0.7
$LiNO_3$	10	5.430	-9.563	14.39	0.4
NaCl	6.1	3.870	-2.164	6.930	0.1
NaBr	9	3.870	-4.208	4.816	0.5
NaI	12	3.870	-4.710	4.196	0.5
KCl	5	3.550	-0.5272	6.964	0.5
KBr	5.5	3.550	-1.860	7.272	0.5
KI	4.5	3.550	-5.820	6.921	0.5
$CaCl_2$	7.5	7.030	-24.14	18.11	0.5
$CaBr_2$	7.7	7.030	-24.58	16.86	0.5
CaI_2	9	7.030	-32.00	13.63	0.5

[a] Given in mol kg^{-1}. [b] In Å. [c] In Å mol^{-1} L. [d] In mol^{-1} L. [e] AARD is the average relative deviation for the calculated osmotic coefficients : $AARD(\%) = (100/N)\sum_k \left|\phi_{cal}^{(k)} - \phi_{\exp}^{(k)}\right| / \phi_{\exp}^{(k)}$. N is the number of points.

b) Association within the MSA model

In all these applications of the MSA model, ion association was not taken into account. The works of Bernard, Blum, Simonin and others [30-32] introduced the association within MSA. This version of the model is the so-called Bi-MSA, in which ion association is treated in the Wertheim formalism. This formalism has the main advantage of not requiring any explicit expression for the associated molecules activity coefficients. The strong ion association is here treated by adding a sticky potential between the particles, which depends on the association constant K. The result is analytical and describes properly the associated molecule, which looks like a dumbbell.

The main idea is that the association adds a term to the excess free Helmholtz energy per volume unit ΔF.

$$\Delta F^{MSA} = \Delta F^{el} + \Delta F^{HS} + \Delta F^{MAL} \qquad (3.44)$$

with ΔF^{el} and ΔF^{HS} defined in eqns.(3.21) and (3.28).

Let's consider the reaction

$$A_+ + B_- \xleftrightarrow{K_{asso}} AB \qquad (3.45)$$

The association constant K_{asso} is an adjusted parameter in the model.

The mass action law (MAL) reads [30]

$$\frac{\rho_{AB}}{\rho_A^0 \rho_B^0} = K_{asso} g_{AB}^{(c)} \tag{3. 46}$$

where ρ^0_k is the number densities of "free" (non -associated) *k* particles, and ρ_{AB} the number density of associated molecule *AB*. $g_{AB}^{(c)}$ is the contact value for the radial distribution function of particles A and B. In this case case, ΔF^{MAL} is expressed by

$$\beta \Delta F^{MAL} = \sum_{k=A}^{B} \rho_k \ln \alpha_k + \frac{1}{2} \rho_A^0 \rho_B^0 K_{asso} g_{AB}^{(c)} \tag{3. 47}$$

In this equation ρ_k is the total number density of species *k*, and α_k is the ratio $\alpha_k = \rho_k^0 / \rho_k$. K_{asso} is the equilibrium constant for the A-B pair.

The expressions for the thermodynamic coefficients are calculated with the help of eqns. (3.16) and (3.17).

$$\Delta \ln \gamma_i^{MAL} = \ln \alpha_i - \frac{1}{2} \rho_A^0 \rho_B^0 K_{asso} g_{AB}^{(c)} \frac{\partial \ln g_{AB}^{(c)}}{\partial \rho_i} \tag{3. 48}$$

$$\Delta \phi^{MAL} = -\frac{\rho_A^0 \rho_B^0}{\rho_t} \frac{K_{asso} g_{AB}^{(c)}}{2} \left(1 + \frac{\partial \ln g_{AB}^{(c)}}{\partial \rho_t} \right) \tag{3. 49}$$

The application of the BiMSA was successful for the description of aqueous solutions containing a single electrolyte [31] or mixtures of electrolytes [32]. Moreover, the values obtained for the adjusted association constant K_{asso} were of the same order of magnitude as literature values.

c) Other extensions of the MSA model

Other versions of the MSA model have been studied through the years. An exponential version was investigated [33, 34] in order to correct the unphysical behavior of g_{++} which takes negative values at small ion separation.

Another version of the model taking the solvent explicitly into account as a hard sphere with a dipole moment was studied by Blum [35]. The solution of the system is quite tedious and the resulting expressions are very complicated. Nevertheless, it constitutes a useful reference model.

REFERENCES

[1] H. L. Friedman, *J. Chem. Phys.*, 1982, **76**, 1092.

[2] S. A. Adelman, *J. Chem. Phys.*, 1976, **64**, 724.

[3] M. P. Allen and D. J. Tildesley, in *Computer Simulations of Liquids*, Oxford University Press, 1989.

[4] J. P. Hansen and I. R. McDonald, in *Theory of simple liquids*, Academic Press, 1986.

[5] D. A. McQuarrie, in *Statistical mechanics*, Harper Collins, 1976.

[6] W. Kunz, Etude de la structure et de la dynamique de solutions d'électrolytes simples dans différents solvants, Mémoire d'habilitation, 1992.

[7] M. Jardat, O. Bernard, P. Turq and G. R. Kneller, *J. Chem. Phys*, 1999, **110**, 7993.

[8] L. Belloni, Statique et dynamique dans les solutions de polyelectrolytes sphériques, Thèse d'etat, 1987.

[9] L. Belloni, *J. Chem. Phys.*, 1993, **98**, 8080.

[10] J. J. Salacuse and G. Stell, *J. Chem. Phys.*, 1982, **77**, 3714.

[11] G. Zerah and J. P. Hansen, *J. Chem. Phys.*, 1986, **84**, 2336.

[12] F. J. Rogers and D. A. Young, *Phys. Rev. A*, 1984, **30**, 999.

[13] E. Waisman and J. L. Lebowitz, *J. Chem. Phys.*, 1971, **56**, 3086.

[14] C. W. Outhwaite, and V. C. L. Hutson, *Mol. Phys.*, 1975, **29**, 1521.

[15] L. Blum, Primitive Electrolytes in the Mean Spherical Approximation, in *Theoritical Chemistry: Advances and Perspectives*, edited by H. Eyring and D. Henderson, volume 5, pp. 1-66, Academic Press, 1980.

[16] L. Blum, *Mol. Phys.*, 1975, **30**, 1529.

[17] L. Blum and J. S. Hoye, *J. Phys. Chem.*, 1977, **81**, 1311.

[18] L. Blum, *J. Phys. Chem.*, 1988, **92**, 2969.

[19] L. L. Lee, *J. Chem. Phys.*, 1983, **78**, 5270.

[20] R. Triolo, J. R. Grigera and L. Blum, *J. Phys. Chem.*, 1976, **80**, 1858.

[21] G. A. Mansoori, N. F. Carnahan, K. E. Starling and T. W. Leland Jr., *J. Chem. Physics*, 1971, **54**, 1523.

[22] W. Ebeling and K. Scherwinsky, *Z. Phys. Chemie, Leipzig*, 1983, **264**, 1.

[23] J. P. Simonin, *J. Chem. Soc., Faraday Trans.*, 1996, **92**, 3519.

[24] J. F. Hinton and E. S. Hamis, *Chem. Rev.*, 1971, **71**, 627.

[25] W. J. Hamer and Y. C. J. Wu, *J. Phys. Chem. Ref. Data*, 1972, **1**, 1047.

[26] T. Sun, J. L. Lénard and A. S. Teja, *J. Phys. Chem.*, 1994, **98**, 6870.

[27] J. P. Simonin, L. Blum and P. Turq, *J. Phys. Chem.*, 1996, **100**, 7704.

[28] J. P. Simonin, *J. Phys. Chem. B*, 1997, **101**, 4313.

[29] P. Novotny and O. Söhnel, *J. Chem. Eng. Data*, 1988, **33**, 49.

[30] O. Bernard and L. Blum, *J. Chem. Phys.*, 1996, **104**, 4746.

[31] J. P. Simonin, O. Bernard and L. Blum, *J. Phys. Chem. B*, 1998, **102**, 4411.

[32] J. P. Simonin, O. Bernard and L. Blum, *J. Phys. Chem. B*, 1999, **103**, 699.

[33] K. L. Gering and L. L. Lloyd, *Fluid Phase Equilibrium*, 1989, **48**, 111.

[34] D. Chandler and H. C. Anderson, *J. Chem. Phys.*, 1971b., **54**, 26.

[35] L. Blum and D. J. Wei, *J. Chem. Phys.* 1987, **87**, 555.

Chapter IV- Application of MSA at high temperatures

A. Theory

A further extension of the MSA model corresponds to the description of osmotic and activity coefficients at high temperatures, as introduced by Sun and Téja[1].

In the MSA model, the parameter $\beta=1/kT$ does not take into account all temperature effects occurring in a solution. Therefore, temperature dependences for the MSA parameters are required to describe accurately temperature effects on activity and osmotic coefficients. As for the concentration dependences, different expressions have been tried[1]. A simple linear dependence has been studied here,

$$\sigma_+(C,T) = \sigma_+^{(0)} + \sigma'^{(0)}_+ \ \Delta T + (\sigma_+^{(1)} + \sigma'^{(1)}_+ \Delta T)\ C \qquad (4.\ .1)$$

$$\varepsilon^{-1}(C,T) = \varepsilon_W^{-1}\ [1 + (\alpha + \alpha'\ \Delta T)\ C\ ] \qquad (4.\ .2)$$

with ΔT= T-298.15K . This assumption involves 3 new adjustable parameters: $\sigma'^{(0)}_+$, $\sigma'^{(1)}_+$ and α'.

These relations can be inserted directly into the expressions for the MSA thermodynamic coefficients without modification of the latter (the thermodynamic coefficients are calculated by derivation of F with respect to ρ). The expressions for the osmotic and activity coefficients are then the same as in eqns. (3.32) to (3.40). Eqns. (3.39) and (3.40) require the knowledge of the densities of solvent and solution at different temperatures. The following expressions, taken from the literature [2][2, 28], have been used

$$d_w = 0.99965 + 2.0438\times10^{-4}t - 6.174\times10^{-5}t^{3/2} \qquad (4.\ .3)$$

$$d = d_w + \left(A + Bt + Ct^2\right)c + \left(D + Et + Ft^2\right)c^{3/2} \qquad (4.\ .4)$$

with d_w and d the densities of pure water and solution, respectively, t the temperature in degrees Celsius and c the concentration in mol dm^{-3}.

---

[1] W. J. Hamer and Y. C. J. Wu, *J. Phys. Chem. Ref. Data*, 1972, **1**, 1047.
[2] P. Novotny and O. Söhnel, *J. Chem. Eng. Data*, 1988, **33**, 49.

B. Results

Data for thermodynamic coefficients at high temperature are scarce. Not all alkaline earth- salts could be fitted because of the lack of experimental data. Nevertheless, six salts have been studied: Five 1-1 salts and one 1-2 salt ($CaCl_2$).

Table 3.3 – Results and parameters obtained from fits of the osmotic coefficients of salts for different temperatures.

	$10^{-3}\ \sigma_+'^{(0)}$ [a]	$10^{-5}\ \sigma_+'^{(1)}$ [b]	$10^{-4}\ \alpha'$ [c]	AARD (%)	m_{max}	Temp. Range	Ref.
LiCl	-2.81	4.91	-3.84	0.44	19.2	298-373	1, 3, 4
LiBr	-3.10	-10.33	-6.37	1.09	21.6	298-483	1, 5, 6
$CaCl_2$	-3.50	-2.02	-7.70	0.82	7.9	298-373	1, 7
NaCl	6.00	-54.32	0.355	0.52	6.1	298-373	1, 8
NaBr	4.87	-38.28	-1.08	0.53	7.0	298-373	1, 4, 7
NaI	-6.00	-10.04	-12.18	1.00	10.0	298-373	1, 8

The results are collected in Table 3.3. Plots are shown in Figures 3.4 and 3.5. The range of temperature studied here was 298-373 K for all solutions, except for the LiBr solution which was studied between 298 and 483 K.

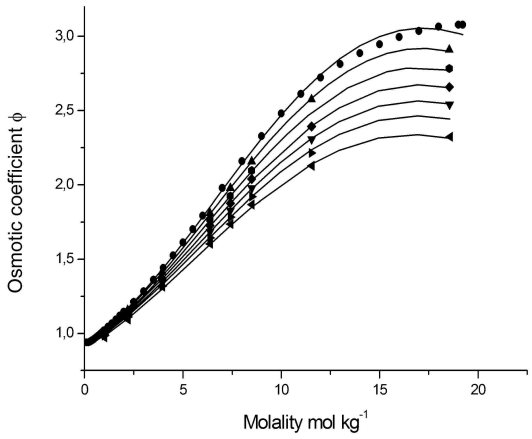

Figure 4.1- Plot of experimental and calculated osmotic coefficients for the equaous LiCl solutions between 298 and 373K. (—): Calculated values with the MSA model. (■): 298K, (▲): 316K, (●): 323K, (♦): 336K, (▼): 348K, (►): 366K, (◄): 373K

[3] H. F. Gibbard Jr. and G. Scatchard, *J. Chem. Eng. Data*, 1973, **18**, 293.
[4] A. Apelblat, *J. Chem. Therm.*, 1993, **25**, 63.
[5] J. L. Y. Lénard, S. M. Jeter and A. S. Teja, ASHRAE Trans., 1992, **98**, 167.
[6] R. J. Lee, R. M. DiGuilio, S. M. Jeter and A. S. Teja, ASHRAE Trans, 19XX, **YYY**, 709.
[7] G. Jakli and W. A. Van Hook, *J. Chem. Eng. Data*, 1972, **17**, 348.
[8] H. F. Gibbard Jr., G. Scatchard, R. A. Rousneau and J. Creek, *J. Chem. Eng. Data*, 1974, **19**, 281.

The expectations concerning the parameters values are the followings. $\sigma'^{(0)}$ is expected to be negative, describing the decrease of the hydration sphere with temperature. $\sigma'^{(1)}$ is ought to be positive, since the decrease of the hydration sphere due to the concentration is the smaller the higher the temperature is. Concerning α' , it is assumed to be of positive value, since the permittivity is known to decrease with temperature.

As it can be seen in Table 3.3, the parameters do not always follow our expectations. This is mainly due to the simple temperature dependence used in our model. More precisely, a plot of the osmotic coefficient for NaCl solutions between 25 and 100 degrees Celsius, as shown in figure 3.5 reveals that for concentrations below 4 mol kg^{-1}, ϕ increases between 25 and 50 degrees Celsius and decreases above 50 degrees. At higher concentrations, ϕ exhibits the same monotonous decrease as in the case of aqueous LiCl solution. The fitted curves have not been plotted in figure 3.5, but they decrease monotonously from 25 to 100 degrees C.

Nevertheless, the AARD is in all cases under 1 % for a wide temperature range of 298-373 K. These results are in all cases as good as if not better than the results from the

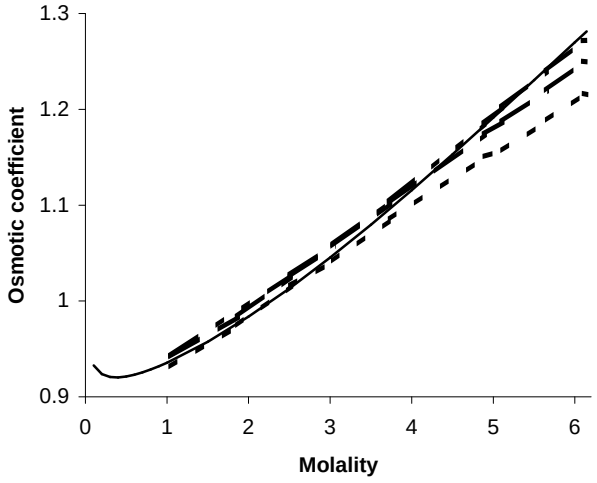

Figure 4.2- Plot of the experimental osmotic coefficients for aqueous solutions of NaCl at different temperatures. (—): 298K. (– -- –): 323K. (– –): 348K. (- -): 373K

Pitzer model. The number of parameters are also much reduced. However, the Pitzer parameters are adjusted by fitting activity coefficients and enthalpies, which has not been done until now with the MSA model.

Eqns. (4.1) and (4.2) will be used in our further works on applying MSA to complex chemical solutions at high temperatures.

C. The case of LiCl hydrates

Summary

As seen in the preceding section, the MSA model may be extended to the description of aqueous electrolyte solutions up to high concentrations and high temperatures. The following study is the first application of this extended MSA model to the calculation of thermodynamic properties of applied chemical systems.

In this study, the thermodynamic properties of saturated LiCl solutions have been calculated. At saturation, LiCl forms hydrates, in which the hydration number depends on the temperature of solution. At 423K for instance, LiCl is in an anhydrous form at the saturated concentration of 30 mol kg^{-1}, and at 198K, LiCl is in the pentahydrate form at 8 mol kg^{-1}.

These solubility properties make LiCl salt one of the most soluble alkaline earth salts. The thermodynamic properties of LiCl hydrates have been described with the help of the MSA model from the fits of osmotic coefficients for aqueous LiCl solutions up to saturation (i.e. above 20 mol kg^{-1}) in the temperature range 273-423K.
In this temperature range, the Pitzer model could not be used, due to its inability to accurately describe osmotic coefficients of aqueous solutions above 11 mol kg^{-1}.

The solubility products of the different LiCl hydrates have been calculated within the MSA model. The enthalpies, entropies and heat capacities of the hydrates have also been calculated. The resulting values obtained with MSA were found to be in agreement with the values given in the NBS tables.

Published in Journal of Chemical Engineering Data in 2002, vol. 46(7), p. 1331-1336

An example of application of MSA at high temperatures: The case of LiCl hydrates

Christophe MONNIN [(1)], Michel DUBOIS [(1,2)], Nicolas PAPAICONOMOU [(3)] and Jean-Pierre SIMONIN [(3)]

(1) CNRS/Université Paul Sabatier,
"Laboratoire Mécanismes de Transfert en Géologie", 38 rue des Trente-Six Ponts, 31400 Toulouse, FRANCE
monnin@lmtg.ups-tlse.fr

(2) Université des Sciences et Technologies de Lille
UMR "Processus et Bilans des Domaines Sédimentaires", 59655 Villeneuve d' Ascq CEDEX, FRANCE

(3) CNRS/Université Pierre et Marie Curie,
"Laboratoire des Liquides Ioniques et Interfaces Chargées", 4 Place Jussieu, 75005 Paris FRANCE

Abstract

We have compiled and critically evaluated literature data for the solubility of lithium chloride salts (anhydrous LiCl, $LiCl.H_2O$, $LiCl.2H_2O$, $LiCl.3H_2O$ and $LiCl.5H_2O$) in pure water. These data have been represented by empirical temperature-molality expressions from which we calculated the coordinates of the eutectic and of the peritectics.

We have then calculated the thermodynamic properties of the LiCl salts from their solubilities in pure water using two different models of aqueous LiCl solutions (Pitzer' s ion interaction model and the Mean Spherical Approximation model). This allows the calculation of the activity of water and of the LiCl(aq) activity coefficient to the very low temperatures (199K) and/or the very high concentrations (up to 30M) characteristic of the $LiCl-H_2O$ system. We have thus been able to calculate the water-ice equilibrium constant to 199K.

Results of the Pitzer-Holmes-Mesmer ion interaction model are reliable only for LiCl molalities below 11M. At higher molalities (corresponding to the solubilities of $LiCl.2H_2O(s)$, of $LiCl.H_2O(s)$, and of anhydrous LiCl for temperatures between 273 and 433K), we alternatively used the Mean Spherical Approximation model. We calculated entropies and standard enthalpies of formation of the various solids from fits of their solubility products with respect to temperature. Our values are in good agreement with the NBS values. There is a linear correlation between the entropies and standard enthalpies of formation and the number of water molecules in the LiCl hydrates, as already reported for $MgCl_2.nH_2O$, $MgSO_4.nH_2O$ and $Na_2CO_3.nH_2O$.

I – Introduction

Beside anhydrous LiCl, there exists four solid lithium chloride hydrates, with respectively 1, 2, 3 and 5 water molecules (Figure 4.3). These salts are extremely soluble in water. For example, the solubility of the monohydrate $LiCl.H_2O$ is about 20 mol/kg.H_2O in pure water at 273K. At the eutectic temperature of the $LiCl-H_2O$ system (199K), which is one of the lowest of all alkali- or alkaline earth-water systems, the stable solid is the pentahydrate $LiCl.5H_2O$. Despite this very low temperature, the concentration of the saturated solutions is very high, 7.86 mol/kg H_2O [1, 2] at the eutectic. The calculation of the thermodynamic properties of the lithium chloride salts from their solubilities is a challenge to aqueous solution modeling. In the present work, we have compiled and critically evaluated existing

solubility data of the LiCl salts in pure water. We use aqueous solution models based on Pitzer' s ion interaction formalism[3] and the Mean Spherical Approximation (MSA) [4] to calculate the properties of the saturated LiCl solutions (activity of water and activity coefficient of aqueous LiCl), and from there the solubility products of the lithium chloride salts. We then compare our standard enthalpies and entropies of solid lithium chloride salts, obtained from a regression of the solubility products versus temperature, to literature values which mainly come from calorimetry [5]. We also use empirical correlations between the thermodynamic properties of solid hydrates and their number of water molecules as a check of the consistency of our results.

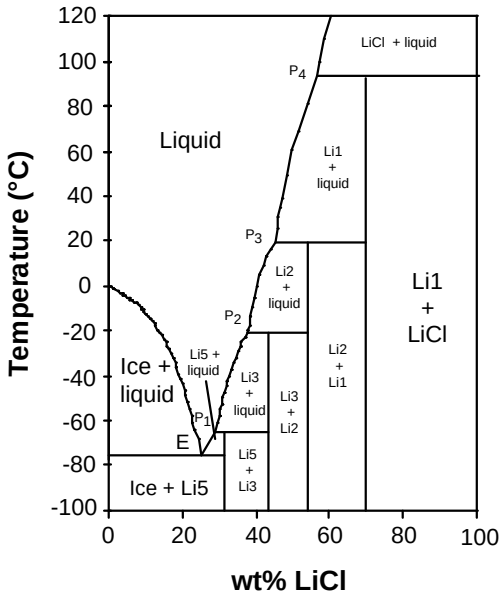

Figure 4.3 - A schematic phase diagram for the LiCl-H_2O system (modified from Rollet [31]). Li*n* refers to the hydrate including *n* water molecules.

II – A compilation of literature data

There exist numerous data (more than 450 experimental points) for the solubility of lithium chloride hydrates in pure water as a function of temperature. Most of these data have been compiled by Cohen-Adad [6]. We have found that the phase diagram of the H_2O-LiCl system can be completed by the data Gibbard and Fawaz [7] and Garrett and Woodruff [8] for the ice melting curve. We have been unable to find out what criteria Cohen-Adad [6] retained for the data selection. So we have carried out our own data evaluation, which turns out to be in accordance with that of Cohen-Adad for all salts but the pentahydrate. Our data evaluation is

based on plots of experimental points in composition-temperature diagrams, from which values outside the general trend were rejected.

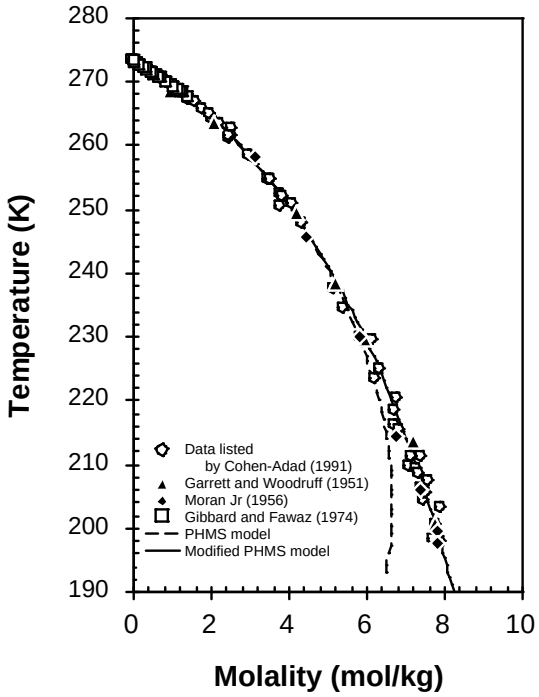

Figure 4.4 - The water-ice equilibrium curve for the LiCl-H_2O system. Data are those compiled by Cohen-Adad [6] with additional points from Gibbard and Fawaz [7], Garrett and Woodruff [8] and Moran Jr [1]. (PHMS = Pitzer-Holmes-Mesmer-Spencer model; modified PHMS: PHMS model with the water ice-equilibrium constant fitted to the data).

Literature data for the melting of ice and for the solubility of the various LiCl hydrates are represented in Figure 4 to Figure 4.8. The rejected data are indicated by a question mark in these figures. Data have been represented by empirical mathematical expressions given in Table 4.1. The data for LiCl.$5H_2O$ are very scattered. The relationship given in Table 4.1 is only meant to indicate the order of magnitude of the pentahydrate solubility in pure water.

Table 4.1 - Solubility-temperature relationships for ice and for the solid lithium chloride salts

Phase		*Temperature range of fit (K)*	N/N_t
Ice	$m = 8.44579210^4 + 76.87556\times(T/K)$ $-5.74046710^{-2}\times(T/K)^2 - \frac{1.2817481 0^6}{(T/K)}$ $-1.7197971 0^4\times\ln(T/K)$	197- 273	160/176
Pentahydrate	$m = 0.187668\times(T/K) - 29.1690$	197- 207	18/36
Trihydrate	$m = 0.001448828\times(T/K)^2$ $-0.572436\times(T/K) + 66.2148$	205- 255	47/56
Dihydrate	$m = 5.351751 0^{-5}\times(T/K)^3$ $-0.0416003\times(T/K)^2 + 10.8571\times(T/K)$ -936.36358	237- 293	52/68
Monohydrate	$m = 0.0011932\times(T/K)^2$ $-0.651544\times(T/K) + 108.036$	291- 371	102/112
Anhydrous LiCl	$m = 1.676761 0^{-4}\times(T/K)^2$ $-8.143541 0^{-2}\times(T/K) + 37.4487$	368- 573	28/37

m: LiCl molality (mol/kg H_2O); T: absolute temperature;. N: number of data retained in the fit; N_t; total number of experimental data points

The coordinates of the eutectic and of the various peritectics have been calculated from the expressions reported in Table 4.2. Our values are in good agreement with those determined experimentally by Vuillard and Kessis [2], Akopov [9], Kessis [10] and Moran Jr [1].

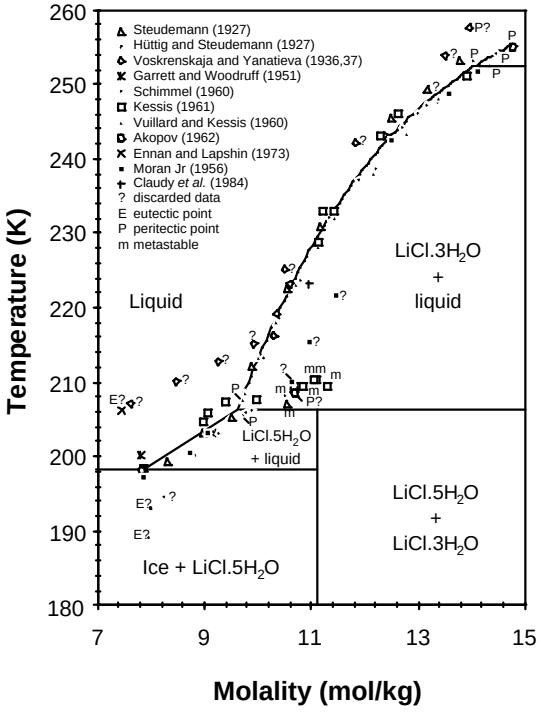

Figure 4.5 - The solubility of the LiCl penta- and trihydrates in pure water versus temperature. Because our data selection for the pentahydrate differs from that of Cohen-Adad [6], all retained points refer to the original papers.

III – Models of aqueous LiCl solutions

a) Pitzer's ion interaction approach

The thermodynamic properties of aqueous lithium chloride solutions have been extensively investigated by Holmes and Mesmer [11] who used Pitzer' s ion interaction model to correlate calorimetric (heat capacities, enthalpies of dilution, etc.) and free energy (emf, isopiestic, vapor pressure, freezing point depression, etc.) measurements. The data that Holmes and Mesmer used in the calculation of Pitzer model parameters cover LiCl concentrations up to 3.9 M for temperatures between 251 and 273K, and concentrations up to 9.4 M for temperatures to 523K. Holmes and Mesmer used values of the Debye-Hückel slope A_ϕ strictly valid for temperatures above 273K, but they have successfully treated data down to 252K [11].

Table 4.2 - LiCl molality and temperature of the eutectic and the peritectics of the LiCl-H_2O system.

	Experimental		Calculated[(11)]	
	m_{LiCl} mol/kg	T K	m_{LiCl} mol/kg	T K
Eutectic	7.86[(1)]	198.4[(1)] 198.15[(2)]	7.87	197,3
5-3 Peritectic	9.71[(1)] 9.78[(2)]	207.75[(1,2,3)] 207.55±0,1[(4)]	9.82	207.8
3-2 Peritectic	14.34[(1)] 14.46[(5)]	252.65[(1,2,3)]	14.60	255.89
2-1 Peritectic	19.42[(3)] 19.52[(6)]	292.55[(3)] 292.2±0.1[(4)] 292.2±0,25[(5)] 292.25±0.25[(7)] 292.22±0.2[(8)] 292.22±0.22[(9)]	19.57	293.94
1-anhydrous Peritectic	29.88[(10)]	366.65±0.5[(7,10)] 366.66±0.3[(8)]	30.26	369,74

(1) Vuillard and Kessis [2] ; (2) Akopov [9] ; (3) Kessis [10] ; (4) Moran Jr [1] ; (5) Schimmel [27] ; (6) Benrath [39] ; (7) Applebey et al. [40] ; (8) Applebey and Cook [41] ; (9) Azizov et al. [42] ; (10) Benrath [43]; (11) This work.

Alternatively, in their low–temperature model of the Na–K–Ca–Mg–Cl–SO_4–H_2O system, Spencer *et al.*[12] have treated A_ϕ as an adjustable parameter and determined the following expression that allows its calculation down to 218K:

$$A_\phi = a_1 + a_2(T/K) + a_3(T/K)^2 + a_4(T/K)^3 + \frac{a_5}{(T/K)} + a_6\, ln(T/K) \tag{4.5}$$

The values of the a_i parameters are given in Table 4.3. In our work on the CsCl-H_2O system [13], we have checked that the discrepancy in the calculated CsCl osmotic coefficient using the two sets of values for A_ϕ does not exceed 0.002. In the present work, we have retained the A_ϕ expression given by Spencer *et al.* [12] and used it throughout the whole temperature range considered in this study.

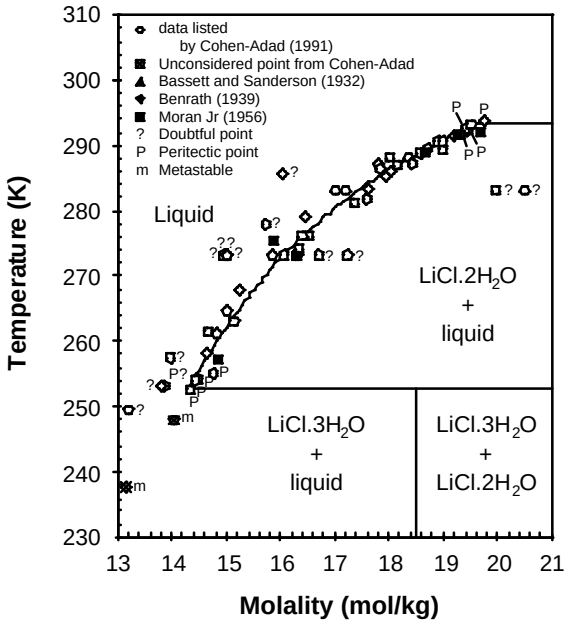

Figure 4.6 - The solubility of the LiCl dihydrate in pure water versus temperature. We retained data selected by Cohen-Adad [6], with the exception of two points from Schimmel [27] and Steudemann [32] that we considered metastable. Additional data from Bassett and Sanderson [33], Benrath [34] and Moran Jr [1] are taken into account.

Table 4.3 - Parameters of the expression (Eqn. 5) giving the variation of the Debye-Hückel slope for the osmotic coefficient [12].

	A_ϕ
a_1	86.6836498
a_2	0.0848795942
a_3	$-8.888785150\ 10^{-5}$
a_4	$4.88096393\ 10^{-8}$
a_5	-1327.31477
a_6	-17.6460172

b) The Mean Spherical Approximation

The mean spherical approximation was first introduced [14, 15] to account for the effect of volume exclusion in the thermodynamic description of molecular fluids. This theory has been subsequently applied to ionic solutions [16, 17]. For aqueous electrolytes, the MSA is equivalent to the Debye-Hückel (DH) theory at very low salt concentration. It yields good results at high concentration because it takes into account the finite size of the ions [4]. Unlike Pitzer's model, parameters of the MSA model (ion size, solvent permittivity) have a simple physical meaning. In the present work, we have used a version of the MSA model that has been recently applied to the description of the thermodynamic properties of aqueous ionic solutions [18-21]. An electrolyte solution is described as being composed of charged hard spheres (ions) distributed in a continuum (the solvent) characterized by its sole dielectric permittivity ε. At 298K, an accurate representation of the thermodynamic properties can be obtained to very high concentrations by allowing some parameters to vary with the solute concentration. We assumed that, for a binary solution, the size of the cation, σ_+, and the inverse of the solvent dielectric permittivity ε^{-1} vary linearly with the concentration:

$$\sigma_+ = \sigma_+^{(0)} + \sigma_+^{(1)} C$$

$$\varepsilon^{-1} = \varepsilon_W^{-1} (1 + \alpha C) \qquad (4.6)$$

where C is the salt concentration, ε_W^{-1} the permittivity of pure water, and $\sigma_+^{(0)}$ the ion size at infinite dilution. $\sigma_+^{(1)}$ and α are adjustable parameters. Notice that $\sigma_+^{(0)}$ is a constant characteristic of a given cation [19]. The size of anions (in the present case aqueous chloride) is taken as a constant (crystallographic, or "optimum", size). In all cases, the fitted parameter $\sigma_+^{(0)}$ was found to be greater or equal to the corresponding crystallographic value, which may be interpreted as a consequence of hydration.

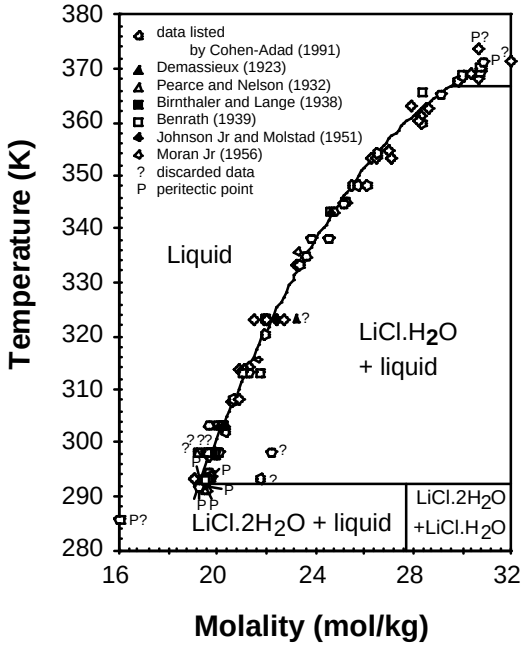

Figure 4.7 - The solubility of the LiCl monohydrate in pure water versus temperature. Data from Demassieux [35], Pearce and Nelson [36], Birnthaler and Lange [37], Benrath [34], Johnson Jr and Molstad [38] and Moran [1] are added to those retained by Cohen-Adad [6].

In the present work, this MSA model has been extended to temperatures ranging from 273 to 433K, by assuming that the parameters appearing in Eqn. 6 have the following simple linear temperature dependence:

$$\sigma_+(C,T) = \sigma_+^{(0)} + \sigma'^{(0)}_+ \ \Delta T + (\sigma_+^{(1)} + \sigma'^{(1)}_+ \Delta T)\ C$$

$$\varepsilon^{-1}(C,T) = \varepsilon_W^{-1}\ [1 + (\alpha + \alpha'\ \Delta T)\ C\ ] \qquad (4.7)$$

with ΔT= T-298.15K . This assumption involves 3 new adjustable parameters : $\sigma'^{(0)}_+$, $\sigma'^{(1)}_+$ and α'.

These parameters have been determined by a least-square fit of the osmotic coefficients for LiCl solutions using empirical formulae for ε_W between 0 and 100°C [22] and between 100°C and 200°C [23], to molalities of about 19 mol/kg below 100°C. The relative deviation of the fit was 0.6 %. The values for $\sigma_+^{(0)}$, $\sigma_+^{(1)}$ and α have been taken from previous work [19], *i.e.* $\sigma_+^{(0)} = 5.430$ Å, $\sigma_+^{(1)} = -9.147\ 10^{-2}$ Å.mol^{-1}.L, $\alpha = 0.1545$ mol^{-1}.L. The optimum values found for the parameters are: $\sigma'^{(0)}_+ = -2.191\ 10^{-3}$ Å.K^{-1}, $\sigma'^{(1)}_+ = 3.369\ 10^{-5}$ Å.mol^{-1}.L.K^{-1} and $\alpha' = -2.855\ 10^{-4}$ mol^{-1}.L.K^{-1}. Note that the effective size of Li^+ decreases with temperature at constant concentration, as indicated by the negative value of $\sigma'^{(0)}_+$. For

this adjustment, the parameters of the model have been fitted to osmotic coefficient data for LiCl solutions [24, 25] to a typical molality of 19 mol/kg below 100°C. The resulting global average relative deviation was 0.6 %.

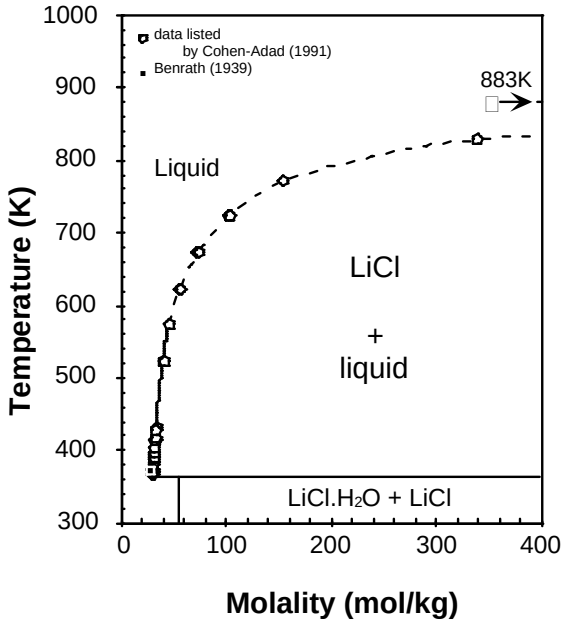

Figure 4.8 - The solubility of anhydrous LiCl in pure water versus temperature. Data are those compiled by Cohen-Adad, along with that from Benrath [34]. The plain curve represents the data fitted in this work (up to 573K). The dashed curve is for visual support of the high temperature data.

In Figure 4.9 we have plotted osmotic coefficients of LiCl solutions at 25°C. It is not possible to fit the data over the whole concentration range with Pitzer' s model within experimental accuracy. It can only be used to reproduce the osmotic coefficient data to about 11 mol/kg.H_2O, the molality at which the variation of the osmotic coefficient of LiCl solutions with concentration starts leveling off. On the contrary, the MSA model can reproduce the data over the full concentration range with the same number of adjustable parameters (three) as Pitzer' s model. We have been able to fit the data between 273 and 473K with the MSA model.

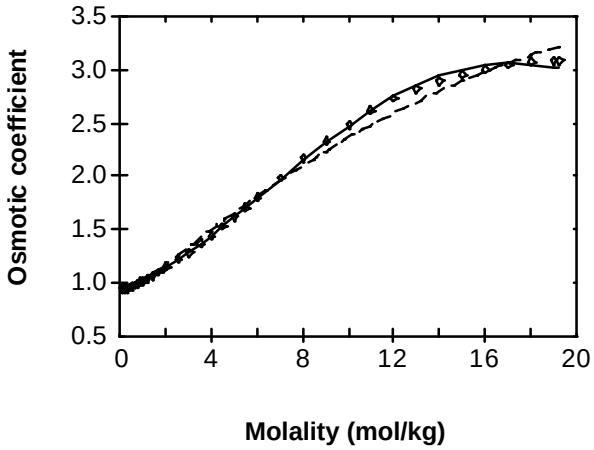

Figure 4.9 - Osmotic coefficient of LiCl aqueous solutions at 298K (symbols: experimental data[11, 24]; dashed curve: Pitzer-Holmes-Mesmer model; plain curve: MSA).

III – The ice melting curve of the LiCl-H_2O system

The equilibrium constant of the liquid water–ice reaction have been determined by Spencer *et al.* [12] as a function of temperature (Eqn. 1). Figure 4.4 compares the freezing point depression calculated using the Pitzer-Holmes-Mesmer model [11] for the aqueous phase and the water-ice equilibrium constant of Spencer *et al.*, to the literature experimental data. In Figure 4.4, we have retained 140 points also selected by Cohen-Adad, to which we have added the data of Garrett and Woodruff [8], Moran Jr [1], and Gibbard and Fawaz [7]. Contrarily to Cohen-Adad, data for the eutectic given by Hüttig and Steudemann [26] and Schimmel [27] were not included in the data set.

Table 4.4 - Parameters of Eqn. 4 for ice and the LiCl salts.

	A	*B*	*C*	*T range of fit (K)*	*Nb points*
Ice	-21.04085	268.5233	3.575348	199-273	160
LiCl anhydrous	252.0552	-7442.90	-37.39279	368-429	25
$LiCl.H_2O$	410.8374	-16068.61	-60.5503	293-368	63
$LiCl.2H_2O$	8.482008	436.1729	0	273-291	24
$LiCl.3H_2O$	11.58593	-720.9875	0	205-233	25
$LiCl.5H_2O$	13.9346	-1684.852	0	198-208	2

One can see that the model results deviate from the experimental data for temperatures below about 230K. The discrepancy can be corrected by a slight adjustment of the C^{Φ}_{LiCl} parameter in the Pitzer-Holmes-Mesmer model, but such a correction induces a marked change at 230K in the variation of C^{Φ}_{LiCl} with temperature. Such a modification would not be in accordance with the results of Holmes and Mesmer [11] who found that Pitzer' s parameters

$\beta^{(0)}_{LiCl}$, $\beta^{(1)}_{LiCl}$ and C^{Φ}_{LiCl} vary (almost) linearly with temperature. So there is no reason why C^{Φ}_{LiCl} would suddenly change at 230K. On another hand, the water-ice equilibrium constant given by Spencer *et al.* [12] has been determined to temperatures of about 227K. Adjusting this equilibrium constant to the data is enough for the model to agree with the experimental data (Figure 4.4). The following expression can describe the variation of the water-ice equilibrium constant down to 198K:

$$\ln K_{sp} = A + \frac{B}{(T/K)} + C\ln(T/K) \tag{4.8}$$

From the parameters of the above expression (Table 4.4), we calculate a value of 5.887 J/mol for the ice heat of fusion at 273K, in good agreement with the accepted value of 5.998 J/mol [22].

IV – Calculation of the LiCl.nH$_2$O solubility products from solubility data

The solubility products of the five LiCl salts have been calculated for each temperature, from the aqueous LiCl molality and from the aqueous LiCl activity coefficient and the activity of water given either by the Pitzer-Holmes-Mesmer model or by the MSA model.

The chemical equilibrium for LiCl hydrates is written as follows

$$LiCl-(H_2O)_n \xleftrightarrow{K_{sp}} LiCl + nH_2O \tag{4.9}$$

With LiCL-$(H_2O)_n$(s) the solid LiCl hydrate, and n the number of water molecules. The solubility product of this reaction is:

$$K_{sp} = a_{LiCl}a_w^n \tag{4.10}$$

with a_w the activity of water and a_{LiCl} the activity of salt. The activities of water and LiCL are calculated as following:

$$\phi = -\frac{1}{\nu m M_w}\ln a_w \tag{4. 11}$$

$$a_{LiCl} = m_{LiCl}\gamma_{\pm}^2 \tag{4. 12}$$

with ϕ the osmotic coefficient of solution, m_{LiCl} the molality of LiCl salt, M_w the molar weight of solvent, and $\gamma_{\pm}$ the mean ionic activity coefficient. The osmotic coefficients and the activity

coefficients are calculated either with the MSA model or with the Pitzer model by extrapolating.the results of fits to the saturation concentration.

As shown above, only the MSA is able to accurately calculate the thermodynamic properties of LiCl solutions above molalities of about 11M. We have thus used the MSA to calculate the solubility products of the most soluble LiCl salts, i.e. LiCl(s), LiCl.H_2O(s) and LiCl.2H_2O(s) for temperatures above 273K. Unlike MSA, Pitzer' s model can be used for temperatures below 273K, but because of the concentration limit to which it is valid, solubility data for LiCl.2H_2O(s) between 255 and 273K (which extends from about 13 to about 15M) could not be taken into account. Similarly, solubility data for LiCl.3H_2O(s) between 235 and 250K (corresponding to molalities between 12 and 14M) have not been considered in the present calculations. Because of the scatter in the solubility data for the pentahydrate, its solubility product has been calculated from the coordinates of the eutectic and of the peritectic assuming a linear change of ln K_{sp} versus the inverse of temperature (corresponding to a zero heat capacity of reaction).

Eqn. 8 has been fitted to the calculated solubility products. The parameters A, B and C are reported in Table 4.4. A curvature in the Arrhenius plots was found only for anhydrous LiCl and for the monohydrate.

Table 4.5 - Standard thermodynamic properties of compounds in the LiCl-H_2O system.

	$\Delta_f H^0$ (kJ / mol)	S^0 (J / mol / K)	C_p^0 (J / mol / K)
LiCl(aq)	-445.64 (a)	69.9 (a)	-67.8 (a)
H_2O(l)	-285.83 (a)	69.91 (a)	75.291 (a)
LiCl(s)	-414.83 (b)	56.49 (b)	243.0 (b)
	-408.61 (a)	59.33 (a)	
LiCl.H_2O(s)	-714.55 (b)	97.18 (b)	494.1 (b)
	-712.58 (a)	102.84 (a)	
LiCl.2H_2O(s)	-1013.68 (b)	139.20 (b)	-
	-1012.65 (a)		
LiCl.3H_2O(s)	-1309.12 (b)	188.30 (b)	-
	-1311.30 (a)		
LiCl.5H_2O(s)	-1889.11 (b)	302.24 (b)	-

(a) NBS; (b) this work

V – Thermodynamic properties of the solid LiCl hydrates

The standard entropy, the standard enthalpy, and the standard heat capacity (298K, 1 bar) of the dissolution reactions of the lithium chloride hydrates can be calculated from the A, B and C parameters of eqn. 8. Holmes and Mesmer [11] give the heat capacity of LiCl

aqueous solutions, but we have not found any heat capacity data for the lithium chloride hydrates. So we have supposed that the heat capacities of the dissolution reactions do not vary with temperature.

We then have used the standard thermodynamic data for LiCl(aq) and H_2O(l) from the NBS Tables [5] to calculate the absolute entropy, the standard enthalpy of formation and the heat capacity of the LiCl salts, that we report in Table 4.5. The magnitude of the discrepancy between our values of the standard enthalpies and entropies of dissolution of the LiCl salts and those calculated from the NBS tables [5] is similar to what has been found for example, for sodium carbonates [28] and magnesium chlorides and sulfates [29].

Finally, it has already been observed for $Na_2CO_3.nH_2O$ [28], $MgCl_2.nH_2O$ and $MgSO_4.nH_2O$ [29], that the contribution of each water molecule to the absolute entropy or the standard enthalpy of formation of a hydrated solid is approximately constant. This result may be interpreted in terms of group contribution, which states that the thermodynamic properties of a hydrated solid phase are the sum of the contributions of the corresponding quantities for the cation in aqueous solution, and of those for the anion and for the water molecules in the crystalline structure (see [30]) for the example of hydrated borates, and references therein). This leads to a linear trend when the standard enthalpy or entropy is plotted versus the number of hydration waters, which we here observe for $LiCl.nH_2O$ (Figure 4.10).

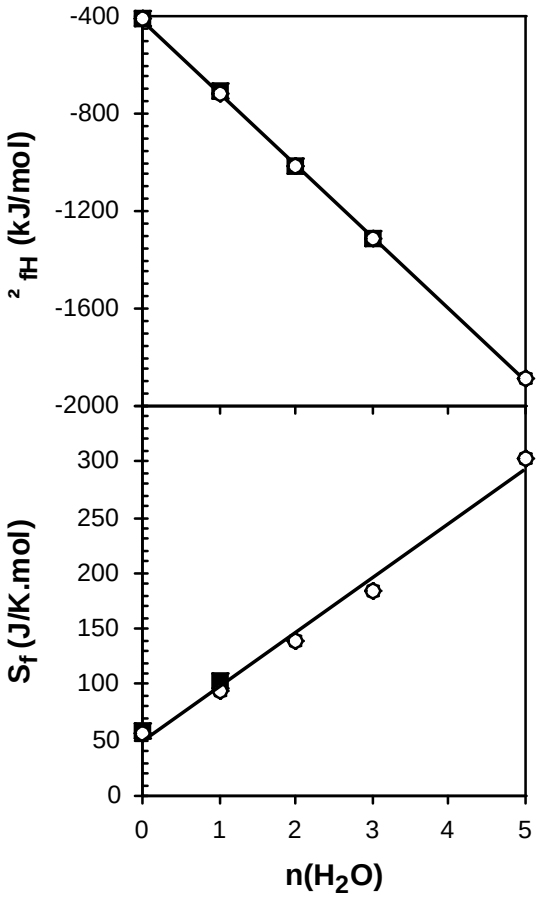

Figure 4.10 - Absolute entropies and standard enthalpies of formation of the solid lithium chloride hydrates versus the number of water molecules in the crystalline structure. (circles: this work; squares: NBS[5]; the two sets of values for the enthalpy cannot be distinguished on the plot).

References:

(1) H. E. Moran Jr, *J. Phys. Chem.*, 1956, **60**, 1666-1667.

(2) G. Vuillard and J. J. Kessis, *Mém. Soc. Chim.*, 1960, **5ème série**, 2063-2067.

(3) K. S. Pitzer, *J. Phys. Chem.*, 1973, **77**, 268-277.

(4) L. Blum, in 'Theoretical chemistry: Advances and perspectives', ed. H. Eyring and H. Henderson, New York, 1980.

(5) D. D. Wagman, W. H. Evans, V. B. Parker, R. H. Schumm, I. Halow, S. M. Bailey, K. L. Churney, and R. L. Nuttall, *J. Phys. Chem. Ref. Data*, 1982, **Suppl. N°2**.

(6) R. Cohen-Adad, in 'Solubility of LiCl in water', ed. R. Cohen-Adad and J. W. Lorimer, 1991.

(7) H. F. Gibbard and A. Fawaz, *J. Sol. Chem.*, 1974, **3**, 745-755.

(8) A. B. Garrett and S. A. Woodruff, *J. Phys. Colloi. Chem.*, 1951, **55**, 477-490.

(9) E. K. Akopov, *Zh. Neorg. Khim.*, 1962, **7**, 385-389.

(10) J. J. Kessis, *Bull. Soc. Chim. Fr.*, 1961, 1503-1504.

(11) H. F. Holmes and R. E. Mesmer, *J. Phys. Chem.*, 1983, **87**, 1242-1255.

(12) R. J. Spencer, N. Møller, and J. H. Weare, *Geochim. Cosmochim. Acta*, 1990, **54**, 575-590.

(13) C. Monnin and M. Dubois, *Eur. J. Mineral.*, 1999, **11**, 477-482.

(14) J. K. Percus and G. J. Yevick, *Phys. Rev.*, 1964, **136**, B290-296.

(15) J. L. Lebowitz and J. K. Percus, *Phys. Rev.*, 1966, **144**, 251-258.

(16) E. Waisman and J. L. Lebowitz, *J. Phys. Chem.*, 19__, **52**, 4307-4309.

(17) L. Blum and J. S. Høye, *J. Phys. Chem.*, 1977, **81**, 1311-1316.

(18) J. P. Simonin, L. Blum, and P. Turq, *J. Phys. Chem.*, 1996, **100**, 7704-7709.

(19) J. P. Simonin, *J. Phys. Chem. B*, 1997, **101**, 4313-4320.

(20) J. P. Simonin, O. Bernard, and L. Blum, *J. Phys. Chem. B*, 1998, **102**, 4411-4417.

(21) J. P. Simonin, O. Bernard, and L. Blum, *J. Phys. Chem. B*, 1999, **103**, 699-704.

(22) CRC, 'Handbook of Physics and Chemistry', CRC Press, 1995-96.

(23) M. Uemastsu and E. U. Franck, *J. Phys. Chem. Ref. Data*, 1980, **9**, 1291-1306.

(24) H. F. Gibbard and G. Scatchard, *J. Chem. Eng. Data*, 1973, **18**, 293-298.

(25) H. F. Holmes and R. E. Mesmer, *J. Chem. Thermodynamics*, 1981, **13**, 1035-1046.

(26) G. F. Hüttig and W. Steudemann, *Z. anorg. Chem.*, 1927, **126**, 105-117.

(27) F. A. Schimmel, *J. Chem. Eng. Data*, 1960, **5**, 510-?

(28) C. Monnin, *Geochim. Cosmochim. Acta*, 2001, **65**, 181-182.

(29) R. T. Pabalan and K. S. Pitzer, *Geochim. Cosmochim. Acta*, 1987, **51**, 2429-2443.

(30) J. Li, B. Li, and S. Gao, *Phys. Chem. Minerals*, 2000, **27**, 342-346.

(31) A. P. Rollet, in 'Lithium', ed. P. Pascal, 1966.

(32) W. Steudemann, 'Die Thermische Analyse des Systeme des Wassers mit den Lithiumhalogeniden', Ph-D thesis Jena (Germany), 1927.

(33) H. Bassett and I. Sanderson, *J. Chem. Soc.*, 1932, 1855-1864.

(34) H. Benrath, *Z. anorg. Chem.*, 1939, **240**.

(35) N. Demassieux, *Ann. Chim.*, 1923, **20**, 233-296.

(36) J. N. Pearce and A. F. Nelson, *J. Amer. Chem. Soc.*, 1932, **54**, 3544-3555.

(37) W. Birnthaler and E. Lange, *Z. Elektrochem.*, 1938, **44**, 679-693.

(38) E. F. Johnson Jr and M. C. Molstad, *J. Phys. Colloi. Chem.*, 1951, **55**, 257-281.

(39) H. Benrath, *Z. anorg. allgem. Chem.*, 1932, **205**, 417-424.

(40) M. P. Applebey, F. H. Crawford, and K. Gordon, *J. Chem. Soc.*, 1934, 1665-1671.

(41) M. P. Applebey and R. P. Cook, *J. Chem. Soc.*, 1938, 547.

(42) E. O. Azizov, S. V. Grechischenko, and V. G. Shevchuk, *Russ. J. Phys. Chem.*, 1975, **53**, 1765

(43) H. Benrath, *Z. anorg. Chem.*, 1934, **220**, 145-153.

Chapter V-
Application of MSA to complex solutions

Summary

In this chapter, complex chemical solutions have been studied and described with the MSA model.

Complex solutions are solutions in which various chemical equilibrium exist, and in which many species coexist, such as ions and neutral species. Furthermore, such solutions are in equilibrium with a phase containing the neutral species. Such solutions are interesting in this work since it is the first application of the version of the MSA model with concentration dependencies.

CO_2/salt/water systems have been studied by many groups, and especially Maurer's [1-4]. In their work, the solubility pressure of CO_2 in various electrolyte aqueous solutions have been measured. These solutions are examples of the complex solutions we intend to study. Ions and neutral species exist in the solution (CO_2 and H_2O). Carbon dioxide dissociates in water via two chemical equilibrium to form hydrocarbonate and carbonate ions. In this case, the water hydrolysis is also taken into account. Furthermore, carbon dioxide is a very volatile species, yielding some vapor liquid equilibrium for this species. Moreover, the water (less but still volatile) is also in equilibrium in the liquid and vapor phases. CO_2/Salt/water systems are then interesting solutions for our work.

Another main advantage of these systems lies in the fact that they have been described with the Pitzer model in the papers of Maurer's group. This allows us to compare the Pitzer and MSA models.

The Pitzer model can describe accurately such systems with the help of cross parameters (CO_2/salt), which implies that the model is not predictive for these systems. The objective of the MSA model is to obtain similar accuracy, but with fewer and more physical parameters than those used in the Pitzer model.

Three systems have been chosen in this study : NaCl/CO_2/water, NaOH/CO2/water and HAc/CO2/water systems. HAc stands for acetic acid. These three systems correspond to three types of solutions which are: two weak acid aqueous mixtures (CO_2 and HAc), aqueous mixtures of strong base and weak acid (NaOH and CO_2, respectively) and aqueous mixtures of salt and weak acid (NaCl and CO_2, respectively).

As it will be detailed below, the dissociation of carbon dioxide and water is negligible for the NaCl/CO_2 and HAc/CO_2 aqueous solutions, a fact which has the big advantage of simplifying a lot the calculations.

The MSA model has been found to be a good model for such systems. It was more predictive than the Pitzer model, with the use of fewer cross parameters. Furthermore, the MSA diameters adjusted in this work for the carbon dioxide and acetic acid have been found to be coherent with literature values.

In press , admitted in Journal of Physical Chemistry B.

Description of vapor-liquid equilibrium for CO_2 in electrolyte solutions using the mean spherical approximation.

N. Papaiconomou[*,a,b], *J.-P. Simonin*[b], *O. Bernard*[b] *and W. Kunz*[a]

[a] Institute of Physical and Theoretical Chemistry, University of Regensburg, D-93040 Regensburg, Germany. Fax: 49 941 943 4532; Tel: 49 941 943 4045. E-mail: werner.kunz@chemie.uni-regensburg.de

[b] Laboratoire LI2C, Université Pierre et Marie Curie, Boîte n° 51, 4 place Jussieu, 75252 Paris Cedex 05, France. Fax 33 (0)1 44 27 38 34. E–mail: sim@ccr.jussieu.fr

* To whom correspondence should be addressed.

The Mean Spherical Approximation (MSA) is used to describe the vapor pressure over aqueous solutions containing an electrolyte and carbon dioxide. Three electrolytes have been studied: NaOH, NaCl, and acetic acid (HAc). A good representation is obtained with a reduced number of parameters as compared to previous models. These parameters account for the concentration and temperature dependence of the solute sizes, and the relative permittivity of solution. The numerical values of these physically interpretable parameters are in a reasonable range.

I) Introduction

Aqueous solutions of carbon dioxide are of considerable interest in industry, e.g. for the production of fertilizers or for the design of separation process equipments. Carbon dioxide has also become of environmental concern since the discovery of the greenhouse effect. Ways to reduce and control the amount of carbon dioxide in the atmosphere, the prediction of sea water ability to regulate atmospheric carbon dioxide (CO_2), or the introduction of pressurized carbon dioxide in geological layers require a good understanding of complex chemical solutions and reliable thermodynamic models.

These models have to describe complex systems, in which several phases and species are in equilibrium and where various components interact with each other. Electrolytes have a major influence on the equilibrium, resulting in salting-in and salting-out effects on the gas solubility. In the case of salting-in effect, the vapor pressure decreases because of the extra solubilization of gas and vice-versa for salting-out.

Vapor pressure data of carbon dioxide solutions have been reported in the literature[1-4]. These authors measured the vapor pressure of several carbon-dioxide-containing aqueous electrolyte solutions over wide temperature ranges. The experimental data were fitted by solving the vapor liquid equilibrium (VLE) equations with the help of electrolyte models such as the Pitzer model[1-4] or the Chen and Evans model[1]. When the Pitzer model was used, up to 5 additional ternary salt-carbon dioxide parameters were introduced.

The Mean Spherical Approximation model (MSA) is an analytical electrolyte model that was introduced some decades ago[5-8]. The Ornstein-Zernike integral equation is solved with a linearized closure relation. The first version of the MSA was at the primitive level, where the solvent is taken as a continuum of relative permittivity ε. The ions in solution are described as charged hard spheres of equal diameter σ, which defines the so-called "restricted level" of description. Later, the model was extended to the unrestricted level where the ions have different diameters. Applications to highly-concentrated solutions at 298 K and also for higher temperatures, as well as multi-electrolyte solutions, have been given in several papers[9-12]. Associating solutes have recently been taken into account in the MSA model, with the so-called Binding-MSA (BIMSA)[13, 14]. A version of the MSA model with discrete solvent, the ion-dipole model, has also been studied [15].

The present work is the first application of the unrestricted primitive MSA model to complex solutions including phase equilibrium of more than one component. Three different types of solutions are investigated here: aqueous solutions of carbon dioxide with acetic acid (HAc), NaOH and NaCl, in which the dissolved carbon dioxide is considered as a weak acid. These systems represent three types of mixtures: two weak acids, a weak acid and a strong base, and finally a weak acid and a salt, respectively. For these systems, the liquid phase is in equilibrium with a vapor phase containing carbon dioxide, water, and possibly acetic acid.

The first section of this paper is devoted to the description of the liquid phase and the vapor liquid equilibrium (VLE). First, the chemical equilibrium occurring in the carbon dioxide solutions are described. Then a description of the MSA model for the activity coefficients is given. Finally, the

VLE equations are detailed. In the second section, the three different systems studied are presented. The last section is devoted to the results and discussions and also to the fitting procedure used.

II) Theory

1) Modeling of the liquid phase

a) Modeling of the chemical equilibrium involving carbon dioxide.

In aqueous solutions, carbon dioxide undergoes the following reactions

$$CO_2 + H_2O \underset{}{\overset{K_1}{\rightleftharpoons}} HCO_3^- + H^+ \quad (1)$$

$$HCO_3^- \overset{K_2}{\rightleftharpoons} CO_3^{2-} + H^+ \quad (2)$$

where K_1 and K_2 are the equilibrium constants of the reactions (1) and (2), respectively. The dissociation of water may be written as

$$H_2O \overset{K_3}{\rightleftharpoons} H^+ + OH^- \quad (3)$$

where K_3 is the equilibrium constant of water dissociation. The general equilibrium constant expression is given by:

$$K_j = \frac{\prod a_i^P}{\prod a_i^R} \quad (4)$$

where a_i^P is the activity of the product *i*, a_i^R the activity of the reactant *i* and K_j is the equilibrium constant of reaction *j*. The activity is given by the relation $a_i = m_i \gamma_i$ with m_i and γ_i being the molality and the activity coefficient of solute *i*, respectively. The molality of each species at equilibrium may be calculated by solving the chemical equilibrium equations. The activity coefficients and the activity of solvent are calculated using the MSA model, as detailed below. The K_i values of the equilibrium (1) to (3), taken from the literature[1, 2] are given in Table 1. Values for K_1, K_2 and K_3 at 313 K are 4.53×10^{-7}, 1.02×10^{-10} mol kg^{-1} and 2.89×10^{-14} mol^2 kg^{-2}, respectively.

Table1. Temperature dependent equilibrium constants for chemical reactions (1)-(3) and for the dimerisation of the acetic acid. The values are taken from refs 2, 24. $\ln K_R / K_{R,U} = A_R/(T/K) + B_R \ln(T/K) + C_R(T/K) + D_R$

Reaction	A_R	B_R	$10^2 C_R$	D_R
Eqn. 1 [a]	-7742.6	-14.506	-2.8104	102.28
Eqn. 2 [b]	-8982.0	-18.112	-2.249	116.73
Eqn. 3 [c]	-13445.9	-22.4773	0	140.932
$2\,HAc \overset{K^V_{dim}}{\rightleftharpoons} (HAc)_2$ [d]	7928.7	0	0	-19.1001

[a] $K_{R,U}$=1. [b] $K_{R,U}$=1 mol kg^{-1}. [c] $K_{R,U}$=1 (mol kg^{-1})^2. [d] $K_{R,U}$=1 kg mol^{-1}.

b) Description of activity coefficients.

In the MSA model, a solute is regarded as a charged hard-sphere of diameter σ immersed in a continuum characterized solely by its relative permittivity ε. The description of solution is made at the so-called McMillan-Mayer (MM) level[16], involving solvent-averaged ion-ion interactions (effective potential of mean force). The resulting potential is composed of a short-range potential, arising from excluded volume effects, described by the hard sphere potential (HS), and a long-range potential arising from electrostatic forces (hereafter denoted by *el*).

As the long-range potential is electrostatic, the MSA reduces to the Debye-Hückel limiting law at very low ionic concentration. The MSA model also has a screening parameter Γ equivalent to κ, the Debye screening parameter. These two parameters are related by the simple expression at infinite dilution: $2\Gamma \sim \kappa$.

In the MSA formalism, the thermodynamic properties may be derived from the excess Helmholtz energy per volume unit, ΔF. This energy can be split into two terms arising from the electrostatic and hard sphere interactions. If the solute associates and the corresponding chemical equilibrium is treated in the Wertheim formalism[17-19], a supplementary mass action law (MAL) term further adds to the excess Helmholtz energy. An advantage of the Wertheim formalism is that no supplementary parameter and no individual activity coefficient are needed to describe the associated molecules.

The total excess MSA Helmholtz energy (to be added to the ideal part) may then be decomposed into 3 contributions as[10, 11, 14]

$$\Delta F^{MSA} = \Delta F^{el} + \Delta F^{HS} + \Delta F^{MAL} \tag{5}$$

in which Δ means an excess quantity.

Each contribution results into an excess activity coefficient

$$ln\,\gamma_i^X = \frac{\partial \beta \Delta F^X}{\partial \rho_i} \tag{6}$$

with X= *el*, *HS*, *MAL* and ρ_i being the number density of species *i* (number of particles per volume unit), and into a contribution to the osmotic coefficient

$$\Delta \phi^X = \rho_t \frac{\partial}{\partial \rho_t}\left[\frac{\beta \Delta F^X}{\rho_t}\right] \tag{7}$$

with $\rho_t = \sum_i \rho_i$ (the summation being made over all solutes) and where the derivation is performed at constant mole fraction of each solute (ρ_i / ρ_t =constant).

Then the activity and osmotic coefficients are given by

$$ln\,\gamma_i = \Delta\, ln\,\gamma_i^{el} + \Delta\, ln\,\gamma_i^{HS} + \Delta\, ln\,\gamma_i^{MAL} \tag{8}$$

$$\phi = 1 + \Delta\phi^{el} + \Delta\phi^{HS} + \Delta\phi^{MAL} \quad (9)$$

by virtue of the relations $\phi^{ideal} = 1$ and $ln\ \gamma^{ideal} = 0$.

Experimental data for the thermodynamic coefficients are measured at the Lewis-Randall (LR) level, on the molality scale. In principle, the calculated values of the coefficients have to be converted from the MM level to the LR level, which requires the knowledge of the solution density [11]. Due to the lack of information on this data, and since this correction is generally small in the concentration range studied, it will be neglected here.

The number density, ρ_i, of a species *i* was calculated using the relation (in the SI unit system)

$$\rho_i = N_{Avo} c_i$$

with

$$c_i = m_i d(T)$$

where N_{Avo} is the Avogadro constant, c_i is the molar concentration of species *i* (in units of mol m^{-3}), *m* is its molality (in mol kg^{-1}) and *d(T)* is the temperature-dependent density of CO2-free solution (in kg m^{-3}), estimated using a formula proposed in the literature [20].

In the following, a detailed summary of each contribution to the thermodynamic coefficients is given.

In the following, a detailed summary of each contribution to the thermodynamic coefficients is given.

Electrostatic contribution. Expressions for the contribution ΔF^{el} have been given in several papers in the case of the restricted (where all ions have the same diameter)[5-7] and unrestricted (where each ion has a specific diameter)[8-10] primitive model. The general unrestricted primitive model equation for the excess Helmholtz energy (per volume unit) is[10]:

$$\beta\Delta F^{el} = -\lambda \sum_i \left(\rho_i z_i \frac{\Gamma z_i + \eta\sigma_i}{1 + \Gamma\sigma_i} \right) + \frac{\Gamma^3}{3\pi} \quad (10)$$

$$\lambda = \frac{\beta e^2}{4\pi\varepsilon_0\varepsilon}$$

$$\eta = \frac{1}{\Omega}\frac{\pi}{2\Delta}\sum_i \frac{\rho_i\sigma_i z_i}{1 + \Gamma\sigma_i}$$

$$\Omega = 1 + \frac{\pi}{2\Delta}\sum_i \frac{\rho_i\sigma_i^3}{1 + \Gamma\sigma_i}$$

$$\Delta = 1 - \frac{\pi}{6}\sum_i \rho_i\sigma_i^3$$

where $\beta=1/k_BT$ (with k_B the Boltzmann constant and T the temperature), e is the proton charge , ε_0 is the permittivity of a vacuum and ε the "effective" dielectric constant of solution. z_i and σ_i are the charge and the diameter of ion i, respectively. Γ is the above mentioned MSA screening parameter, given by the following equation:

$$\Gamma^2 = \pi\lambda\sum_i \rho_i \left[\frac{z_i - \eta\sigma_i^2}{1+\Gamma\sigma_i}\right]^2 \tag{11}$$

This equation is easily solved by iteration taking for Γ the initial value of $\Gamma_0 = \kappa/2$, with κ the Debye screening parameter

$$\kappa = \left(4\pi\lambda\sum_i \rho_i z_i^2\right)^{1/2} \tag{12}$$

Extension of the model to highly concentrated electrolyte solutions can be made by assuming a linear concentration dependence for the cation diameter and for the inverse of the permittivity[10]

$$\sigma_+ = \sigma_+^{(0)} + \sigma_+^{(1)} c_s \tag{13}$$

$$\varepsilon^{-1} = \varepsilon_w^{-1}\left(1+\alpha c_s\right) \tag{14}$$

where c_s is the concentration of salt. The anion diameter is assumed to be constant and equal to its crystallographic value for simple ions[10].

Since eqns. (6) and (7) are the derivatives of the excess Helmholtz energy with respect to the number density, the concentration dependence of both MSA parameters, σ_+ and ε, has to be taken into account. This leads to the following results[10]

$$ln\,\gamma_i^{MSA} = -\lambda\left[\frac{\Gamma z_i^2}{1+\Gamma\sigma_i} + \eta\sigma_i\left(\frac{2z_i - \eta\sigma_i^2}{1+\Gamma\sigma_i} + \frac{\eta\sigma_i^2}{3}\right)\right] + \sum_j \rho_j q_j \frac{\partial\sigma_j}{\partial\rho_i} + \beta\Delta E^{MSA}\varepsilon\frac{\partial\varepsilon^{-1}}{\partial\rho_i} \tag{15}$$

$$\Delta\phi^{MSA} = -\frac{\Gamma^3}{3\pi\rho_t} - \lambda\frac{2\eta^2}{\pi\rho_t} + \frac{1}{\rho_t}\sum_i \rho_i q_i D(\sigma_i) + \frac{\beta\Delta E^{MSA}}{\rho_t}\varepsilon D(\varepsilon^{-1}) \tag{16}$$

where

$$q_i = \lambda\left[\frac{\Gamma^2 z_i^2}{\left(1+\Gamma\sigma_i\right)^2} + \eta\frac{\eta\sigma_i^2\left(2-\Gamma^2\sigma_i^2\right) - 2z_i}{\left(1+\Gamma\sigma_i\right)^2}\right] \tag{17}$$

and $D(A) = \sum_k \rho_k \frac{\partial A}{\partial\rho_k}$ which yields using eqns. (13), (14)

$$D(\sigma_+) = \sigma_+ - \sigma_+^{(0)} \tag{18}$$

$$\varepsilon D(\varepsilon^{-1}) = 1 - \varepsilon/\varepsilon_w \tag{19}$$

Hard-Sphere contribution. The Boublik-Mansoori-Carnahan-Starling equation was used for the HS excess Helmholtz energy (per volume unit)[10]:

$$\frac{\pi}{6}\beta\Delta F^{HS} = \left(\frac{X_2^3}{X_3^2} - X_0\right) ln(1-X_3) + \frac{3X_1X_2}{1-X_3} + \frac{X_2^3}{X_3(1-X_3)^2} \tag{20}$$

where

$$X_n = \frac{\pi}{6}\sum_i \rho_i \sigma_i^n \tag{21}$$

Proper use of eqns. (6) and (7), taking care again for the diameter concentration dependence, leads to[10]

$$ln\,\gamma_i^{HS} = -ln(1-X_3) + \sigma_i F_1 + \sigma_i^2 F_2 + \sigma_i^3 F_3 + \sum_j Q_j \rho_j \frac{\partial \sigma_j}{\partial \rho_i} \tag{22}$$

$$\Delta\phi^{HS} = \frac{X_3}{1-X_3} + \frac{3X_1X_2}{X_0(1-X_3)^2} + \frac{X_3^2(3-X_3)}{X_0(1-X_3)^3} + \frac{1}{\rho_t}\sum_j Q_j \rho_j D(\sigma_j) \tag{23}$$

with

$$Q_i = F_1 + 2\sigma_i F_2 + 3\sigma_i^2 F_3$$

$$F_1 = \frac{3X_2}{1-X_3}$$

$$F_2 = \frac{3X_1}{1-X_3} + \frac{3X_2^2}{X_3(1-X_3)^2} + \frac{3X_2^2}{X_3^2} ln(1-X_3)$$

$$F_3 = \left(X_0 - \frac{X_2^3}{X_3^2}\right)\frac{1}{1-X_3} + \frac{3X_1X_2 - X_2^3/X_3^2}{(1-X_3)^2} + \frac{2X_2^3}{X_3(1-X_3)^3} - \frac{2X_2^3}{X_3^3} ln(1-X_3)$$

Mass Action Law. Let A and B be two species leading to the following reactions: A dimerizes to yield AA, and B associates with A to form AB.

$$A + A \rightleftharpoons AA \quad (K_{dim}) \tag{24}$$

$$A + B \rightleftharpoons AB \quad (K_{asso}) \tag{25}$$

with K_{dim} and K_{asso} the equilibrium constants of these two reactions. These two reactions will be used below for the HAc /CO_2 system.

The mass action law (MAL) reads[13, 17-19]

$$\frac{\rho_{AA}}{\rho_A^0 \rho_A^0} = K_{dim} g_{AA}^{(c)} \tag{26}$$

$$\frac{\rho_{AB}}{\rho_A^0 \rho_B^0} = K_{asso} g_{AB}^{(c)} \tag{27}$$

where ρ^0_k, ρ_{AA} and ρ_{AB} are the number density of "free" (non -associated) *k* particles, the number density of the dimer particle *AA*, and the number density of the associated molecule *AB*, respectively. $g_{XY}^{(c)}$ is the contact value for the radial distribution function of particles X and Y.

The general expression of the excess Helmholtz energy considering one or more associations between molecules *k* and *l* is, according to Bernard and Blum[13]

$$\beta\Delta F^{MAL} = \sum_k \rho_k \ln\alpha_k + \sum_{k,l} \rho_k^0 \rho_l^0 K_{kl} \tag{28}$$

In this equation ρ_k is the total number density of species *k*, and α_k is the ratio $\alpha_k = \rho_k^0 / \rho_k$. K_{kl} is the equilibrium constant for the k-l pair. For convenience, in eqns. (26) and (27), we define K_{AA} and K_{AB} through the relations

$$K_{AA} = K_{dim} g_{AA}^{(c)}$$
$$K_{AB} = K_{asso} g_{AB}^{(c)} / 2$$

Assuming that *A* and *B* are neutral hard spheres, $g_{AA}^{(c)}$ and $g_{AB}^{(c)}$ are given by their value for contacting hard spheres as

$$g_{AA}^{(c)} = g_{AA}^{HS(c)}$$
$$g_{AB}^{(c)} = g_{AB}^{HS(c)}$$

The expressions for the thermodynamic coefficients are calculated with the help of eqns. (6) and (7).

$$\Delta \ln\gamma_i^{MAL} = \ln\alpha_i - \sum_{k,l} \rho_k^0 \rho_l^0 K_{kl} \frac{\partial \ln g_{kl}^{HS}}{\partial \rho_i} \tag{29}$$

$$\Delta\phi^{MAL} = -\frac{1}{\rho_t} \sum_{k,l} \rho_k^0 \rho_l^0 K_{kl} \left(1 + \frac{\partial \ln g_{kl}^{HS}}{\partial \rho_t} \right) \tag{30}$$

The contact distribution function is given by[14]

$$g_{ij}^{HS(c)} = \frac{1}{1-X_3} + 3\frac{X_2}{(1-X_3)^2}\frac{\sigma_i\sigma_j}{\sigma_i+\sigma_j} + 2\frac{X_2^2}{(1-X_3)^3}\left(\frac{\sigma_i\sigma_j}{\sigma_i+\sigma_j}\right)^2 \tag{31}$$

with X_2 and X_3 defined in eqn. (21).

The conservation of A and B gives

$$2\rho_{AA} + \rho_{AB} + \rho_A^0 = \rho_A \tag{32}$$

$$\rho_{AB} + \rho_B^0 = \rho_B \tag{33}$$

Inserting these relations into eqns. (26) and (27) leads to

$$\alpha_A = \frac{1}{1 + 2\rho_B\alpha_B K_{AB} + 2\rho_A\alpha_A K_{AA}} \tag{34}$$

$$\alpha_B = \frac{1}{1 + 2\rho_A\alpha_A K_{AB}} \tag{35}$$

2) Description of the vapor phase

Vapor liquid equilibrium arise from the thermodynamic equilibrium of species between the liquid and vapor phases. The basic relation representing this equilibrium is

$$\mu_i^V = \mu_i^L \tag{36}$$

in which μ_i^L is the chemical potential of species *i* at temperature *T* and pressure *P* in the liquid phase and μ_i^V is its chemical potential at temperature *T* and pressure *P* in the vapor phase.

a) VLE for the solvent.

For solvent *w* in equilibrium between the liquid and vapor phases, the chemical potentials read

$$\mu_w^L = \mu_w^{*,L}(T,P) + RT\,ln\,a_w \tag{37}$$

$$\mu_w^V = \mu_w^{*,V}(T,P_w^*) + RT\,ln\left(P_w\varphi_w / P_w^*\varphi_w^*\right) \tag{38}$$

where a_w is the activity of *w*, μ_w^X denotes the chemical potential of *w* in phase X, P_w is the partial pressure of solvent *w*, and φ_w the fugacity coefficient of solvent *w* in the vapor phase. The symbol * used as a superscript denotes the pure solvent reference state. The partial pressure P_i is defined by the relation $P_i = P\,y_i$, where *P* is the total pressure and y_i is the mole fraction of species *i* in the vapor phase.

The VLE condition, eqn. (36), and eqns. (37), (38) yield

$$\mu_w^{*,V}(T,P_w^*) - \mu_w^{*,L}(T,P) = RT\,ln\,a_w - RT\,ln\left(P_w\varphi_w / P_w^*\varphi_w^*\right) \tag{39}$$

The standard chemical potential $\mu_w^{*,V}(T,P_w^*)$ is independent of the pressure. For pure liquid, one has[21]

$$\left.\frac{\partial\mu_w^{*,L}}{\partial P}\right|_T = v_w^* \tag{40}$$

where v_w^* is the partial molar volume of solvent *w* in pure solvent reference state.

The derivated equation arising from the VLE is:

$$-v_w^{*,L}\,dP = RTd\left(ln\,a_w P_w^*\varphi_w^* / P_w\varphi_w\right) \tag{41}$$

The integration of this equation, yielding the VLE equation is

$$\int_{P_w^*}^{P} v_w^{*,L}\,dP = RT\int_1^x d\left(ln\,a_w P_w^*\varphi_w^* / P_w\varphi_w\right) \tag{42}$$

since at $P=P^*$, $x_i=1$ (pure solvent).

Recalling that $v_i^{*,L}$ is uncompressible between P_w^* and P, and the f_w is f_w^* when $x_w=1$, one obtains

$$-\frac{v_w^{*,L}}{RT}\left(P - P_w^*\right) = \ln a_w P_w^* \varphi_w^* / P_w \varphi_w \qquad (43)$$

which is similar to the following expression for the equilibrium of solvent,

$$P\, y_w \varphi_w = P_w^* a_w \varphi_w^* exp\left(\frac{v_w^*(P - P_w^*)}{RT}\right) \qquad (44)$$

In this equation, P_w^* may be calculated with the help of the Saul and Wagner equation[23].

The fugacity coefficients are calculated with the help of the truncated second virial equation[22]

$$\ln \varphi_i = \frac{P}{RT}\left[2\sum_{j=1}^{N} y_i B_{ij}(T) - \sum_{k=1}^{N}\sum_{l=1}^{N} y_k y_l B_{kl}(T)\right] \qquad (45)$$

where B_{ii} is the second virial coefficient and B_{ij} ($j \bullet i$) is the second cross virial coefficient. The sums in eqn. (41) run over all species in the vapor phase.

Table 2. Cross second virial coefficients and partial molar volume for CO_2 at infinite dilution in water taken from ref 2.

T (K)	$10^{-3} B_{co_2,w}$ ($dm^3\ mol^{-1}$)	$10^{-3} v_{co_2,w}^{\infty}$ ($dm^3\ mol^{-1}$)
313.15	-163.1	33.4
333.15	-144.6	34.7
373.15	-115.7	38.3
393.15	-104.3	40.8
413.15	-94.3	43.8
433.15	-85.5	47.5

b) VLE for the solute.

For the solute, the reference state is the infinitely diluted solution, denoted by the symbol •. In this case

$$\mu_i^L = \mu_i^{\infty,L} + RT \ln a_i \qquad (46)$$

with i the solute. One obtains, as in eqn.():

$$\mu_i^{*,V}\left(T, P_w^*\right) - \mu_i^{*,L}\left(T, P\right) = RT \ln a_i - RT \ln\left(P_i \varphi_i \,/\, P_w^* \varphi_w^*\right) \qquad (47)$$

As in eqn. (5), one has

$$\left.\frac{\partial \mu_i^{\infty,L}}{\partial P}\right|_T = v_{i,w}^{\infty} \qquad (48)$$

where $v_{i,w}^{\infty}$ is the partial molar volume of species i infinitely diluted in solvent w.

Eqn. (7) becomes for the solute:

$$\int_{P_i^w}^{P} v_i^{\infty,L} dP = RT \int_{x_i=0}^{x} d\left(\ln a_i P_w^* \varphi_w^* / P_i \varphi_i\right) \qquad (49)$$

Now, let $H^{P}_{i,w}$ be the Henry's constant of species i in solvent w at the solvent saturated vapor pressure. It is defined by

$$H^{P}_{i,w} = \lim_{m_i \to 0} \frac{P\, y_i \varphi_i}{m_i} \tag{50}$$

Eqn. (14) and (15) lead to the relation

$$-\frac{v_w^{\infty,L}}{RT}\left(P - P_w^*\right) = ln\frac{a_i}{P y_i \varphi_i} + ln\, H^{P}_{i,w} \tag{51}$$

since $a_i = x_i$ at infinite dilution. The well-known Henry's law is then:

$$P\, y_i \varphi_i = H^{P}_{i,w}\, exp\left(\frac{v^{\infty}_{i,w}(P\text{-}P^*_w)}{RT}\right) a_i \tag{52}$$

The pressure P and the mole fractions y_i of species i in the vapor phase are obtained by solving simultaneously eqns. (44) and (52).

Table 3. Second virial coefficients for water and carbon dioxide taken from ref 2.

$$10^{-3} B_{i,i} / (dm^3 mol^{-1}) = a_i + b_i (c_i / T)^{d_i}$$

i	a_i	b_i	c_i / K	d_i
CO_2	65.703	-184.854	304.16	1.4
H_2O	-53.53	-39.29	647.3	4.3

Table 4. Henry's constant for the solubilities of acetic acid and carbon dioxide in pure water. Values taken from ref 2.
$ln\, H^{P}_{i,w}(T, p^{s}_{w}) / (MPa\ kg\ mol^{-1}) = A_{i,w} + B_{i,w}/T + C_{i,w}T + D_{i,w}\, ln(T)$

i	$A_{i,w}$	$B_{i,w} / K$	$C_{i,w} / K^{-1}$	$D_{i,w}$
CO_2	192.876	-9624.4	0.01441	-28.749
HAc	52.9967	-8094.25	0	-6.41203

III) Systems studied

1) The NaCl/CO_2/water system

a) Liquid phase.

The NaCl/CO_2 system is composed of a salt and a weak acid in water. NaCl is assumed to be fully dissociated. The chemical equilibrium in the liquid phase are given by eqns. (1) to (3).

Considering the values of the equilibrium constants K_1, K_2, and K_3 between 313 K and 433 K, the molalities of the HCO_3^- and CO_3^{2-} ions are always smaller than 10^{-3} mol kg^{-1} for CO_2 concentration

below 1 mol kg^{-1}. Therefore, these concentrations may be neglected as compared to that of CO_2. It will be assumed that the liquid phase is composed of three species: the carbon dioxide and the ions Na^+ and Cl^-.

b) VLE.

This system is composed of two volatile species, carbon dioxide and water, and one non-volatile species, NaCl. The VLE for water is given by eqn. (44). For the carbon dioxide, the VLE is given by eqn. (52), where the subscript *i* is replaced by CO_2. The relation for mole fractions in the vapor phase is:

$$y_w + y_{CO_2} = 1 \tag{53}$$

The set of equations (44), (52) and (53) may be solved using an iteration procedure yielding the three variables P, y_w and y_{CO_2}.

2) The NaOH/ CO_2/ water system

a) Liquid phase.

This system is composed of a strong base, NaOH, and a weak electrolyte, CO_2. The NaOH is assumed to be totally dissociated. Here, eqns. (1) to (3) are taken into account. The hydroxide anions are produced by eqn. (3) and by the total dissociation of NaOH in water.

The molalities of each species are calculated with the help of eqns. (1) to (4), the mass conservation equation

$$m_{CO_2}^{init} = m_{HCO_3^-} + m_{CO_3^{2-}} + m_{CO_2} \tag{54}$$

where $m_{CO_2}^{init}$ is the molality of carbon dioxide introduced initially in the liquid phase, and the electroneutrality relation

$$m_{Na^+} + m_{H^+} = m_{HCO_3^-} + 2m_{CO_3^{2-}} + m_{OH^-} \tag{55}$$

b) VLE.

The vapor phase for this system has the same composition as for the NaCl/CO2 system. The same iteration procedure was used for solving the equations in P, y_w and y_{CO_2}.

3) The HAc/ CO2/ water system

a) Liquid phase.

This system involves two weak acids in water. The dissociation of the acetic acid is

$$HAc \underset{}{\overset{K_{HAc}}{\rightleftharpoons}} H^+ + Ac$$

where K_{HAc} is the equilibrium constant. Its value is 1.75 10^{-5} mol kg^{-1} at 313 K.

Since the molality of the acetic acid is below 4 mol kg^{-1} in the available data, the concentrations of HCO_3^-, CO_3^{2-} and acetate ions may be neglected. Thus, the solution was assumed to contain only non-ionic species: carbon dioxide and undissociated acetic acid.

Two further assumptions were made. Firstly, the dimerization of acetic acid was considered. It is well known[24, 25] that this process is appreciable in concentrated acetic acid solutions. The dimerization reaction was written as follows

$$2\ HAc \underset{}{\overset{K_{dim}}{\rightleftharpoons}} (HAc)_2 \qquad (56)$$

where K_{dim} is the dimerization constant of acetic acid and is defined as in eqns. (4) and (24). Its value, found in the literature, is discussed in the next subsection.

Unlike the NaCl/CO_2 and NaOH/CO_2 systems, the aqueous HAc/CO_2 solutions exhibit a salting-in effect for the carbon dioxide. This reveals that specific interactions exist between acetic acid and carbon dioxide. Earlier modeling of this system with the Pitzer model[2] also assumed CO_2-HAc interactions, taken into account through the introduction of 4 CO_2-HAc interaction parameters.

In our model we assume that these interactions may be described with an association equilibrium between CO_2 and HAc

$$CO_2 + HAc \underset{}{\overset{K_{dim}}{\rightleftharpoons}} (CO_2\text{-}HAc) \qquad (57)$$

where K_{asso} is the association constant between carbon dioxide and acetic acid, defined as in eqn. (4). It is an adjustable parameter.

The two equilibrium corresponding to eqns. (56) and (57) have been treated within the Wertheim formalism as detailed in eqns. (24)-(35).

b) VLE.

There are four species in the vapor phase: water, carbon dioxide, acetic acid and its dimer. Association between HAc and CO_2 is not assumed in the vapor phase because this is a dilute phase. The VLE equations for water and carbon dioxide remain the same as before, except for the fugacity coefficients that now take into account the mole fraction of acetic acid and its dimer. Eqn. (52) is used to describe the VLE of acetic acid.

The equilibrium constant for the dimerization of the acetic acid in the vapor phase is known[2]

$$K_{dim}^V = \frac{P_0 y_{dim} \varphi_{dim}}{P y_{HAc}^2 \varphi_{HAc}^2}$$

with $\bullet_{HAc}$ and $\bullet_{dim}$ the fugacity coefficients for the acetic acid and its dimer in the vapor phase, respectively. P_0 is 1 atmosphere.

The values of the cross virial coefficients for acetic acid, $B_{HAc,CO2}$ and $B_{dim,CO2}$, as well as the molar volume of HAc in pure water have been set to zero, due to the lack of experimental data. Note that this implies that $\bullet_{HAc}=\bullet_{dim}$. The value of the dimerization constant K^{V}_{dim} of acetic acid in the vapor phase is given in Table 1. The values of Henry's constants, of the cross virial coefficients and of the molar volumes in pure water are collected in Tables 2, 3 and 4. Together with the relation

$$y_w + y_{CO_2} + y_{HAc} + y_{dim} = 1 \qquad (58)$$

the system can be solved for P and for the y_i's, the different mole fractions in the vapor phase. For this purpose, a Newton-Raphson procedure was used.

IV) Results

The model parameters are: the diameter of the sodium cation, σ_{Na+}, for the solutions containing NaCl or NaOH; the diameter of the HAc molecule for those containing acetic acid; the diameter of the CO_2 molecule; and the permittivity of solution, ε. Following earlier work in which the MSA model was applied to the thermodynamics of ionic aqueous solutions[11, 12], the following concentration and temperature dependencies were introduced

$$\sigma_i = \sigma_i^{(0)} + \sigma_i^{(0,T)}\Delta T + \sum_j \left(\sigma_{i-j}^{(1)} + \sigma_{i-j}^{(1,T)}\Delta T\right) c_j \qquad (59)$$

$$\varepsilon^{-1} = \varepsilon_w^{-1}\left[1 + \sum_j \left(\alpha_j + \alpha_j^{(T)}\Delta T\right) c_j\right] \qquad (60)$$

where j stands for all species in solution, including the anion and species i itself.

In the case of the HAc solutions, they were determined in a global fit of data for ternary solutions, together with the other parameters. The cross parameters $\sigma_{i-j}^{(1)}$ and $\sigma_{i-j}^{(1,T)}$ account for the influence of species j on the size of species i; they may be calculated by fitting the pressures of the ternary systems.

It must be noticed that the CO_2 parameters $\sigma_{CO_2}^{(0)}$, $\sigma_{CO_2}^{(0,T)}$, $\sigma_{CO_2-CO_2}^{(1)}$ and $\sigma_{CO_2-CO_2}^{(1,T)}$ are specific to this species. Their values are common to the 3 systems studied in this work.

The vapor pressure data for the three systems studied were taken from the work of Rumpf et al.[1, 2]. Pressures were measured in the range of temperature 313-433 K for different concentrations of both electrolyte and carbon dioxide.

1) Adjustment of parameters concerning the CO2-free electrolyte systems

This procedure was carried out for NaCl and NaOH for which experimental values of the osmotic coefficient up to saturation and at different temperatures are available, in contrast to the HAc solutions. Two types of parameters were adjusted: the cation diameter and the relative permittivity. Following eqns. (59) and (60), these parameters are written as

$$\sigma_{Na^+}^{(\phi)} = \sigma_{Na^+}^{(0)} + \sigma_{Na^+}^{(0,T)}\Delta T + \left(\sigma_s^{(1)} + \sigma_s^{(1,T)}\Delta T\right)c_S \quad (61)$$

$$\varepsilon^{(\phi)-1} = \varepsilon_w^{-1}\left[1 + \left(\alpha_S + \alpha_S^{(T)}\Delta T\right)c_S\right] \quad (62)$$

and

$$\Delta T = T - 298.15$$

where the superscript (ϕ) stands for the binary salt/water system, s stands for the salt NaX (X = Cl or OH), $\sigma_s^{(1)} = \sigma_{Na^+-Na^+}^{(1)} + \sigma_{Na^+-X^-}^{(1)}$ and the similar relation for $\sigma_s^{(1,T)}$. In the same way, $\alpha_s = \alpha_{Na^+} + \alpha_{X^-}$ and similarly for $\alpha_s^{(T)}$. In these relations the $\sigma_i^{(0)}$, $\sigma_i^{(0,T)}$, $\sigma_s^{(1)}$ and $\sigma_s^{(1,T)}$ parameters may be determined by a fit of data for binary solutions. They were obtained by a fit of the osmotic coefficients for the electrolyte solutions.

The fits were done using a Marquardt least square procedure. First, $\sigma_{Na^+}^{(0)}$, $\sigma_s^{(1)}$ and α_s were adjusted by using data at 298 K. Then the remaining parameters $\sigma_{Na^+}^{(0,T)}$, $\sigma_s^{(1,T)}$ and $\alpha_s^{(T)}$ were adjusted by using the data at higher temperatures. The results are gathered in Table 5.

Table 5. Values of MSA parameters from the fits of the osmotic coefficients for pure CO_2-free electrolyte solutions (see eqns. (53) and (54)).

Salt	*max. m*[a]	*Temp. range*	$\sigma^{(0)}$[b]	$10^4\sigma^{(0,T)}$[c]	$10^2\sigma^{(1)}$[d]	$10^5\sigma^{(1,T)}$[e]	$10^2\alpha$[f]	$10^4\alpha^{(T)}$[g]	*AARD*[h] *(%)*
NaCl	6	298-573 K	3.689	-6.229	-4.139	-4.720	7.154	-1.216	1.77
NaOH	10	298-473 K	3.803	0	-3.972	0	5.508	1.451	1.28

[a]In units of mol kg^{-1}. [b]In units of 10^{-10} m. [c]In units of 10^{-10} m K^{-1}. [d]In units of 10^{-10} m dm^3 mol^{-1}. [e]In units of 10^{-10} m dm^3 mol^{-1} K^{-1}. [f]In units of dm^3 mol^{-1}. [g]In units of dm^3 mol^{-1} K^{-1}. [h] $AARD = 1/n\sum_i \left|\phi_{cal}^{(i)} - \phi_{\exp}^{(i)}\right| / \phi_{\exp}^{(i)}$, with n= number of points.

2) Adjustment of parameters concerning the CO_2-containing electrolyte systems

a) NaCl/CO_2 system.

In this system, the following parametrization was applied to the sodium ion diameter, the permittivity of solution and the carbon dioxide diameter

$$\sigma_{Na^+} = \sigma_{Na^+}^{(\phi)} + \left(\sigma_{Na^+-CO_2}^{(1)} + \sigma_{Na^+-CO_2}^{(1,T)}\Delta T\right)c_{CO_2} \quad (63)$$

$$\varepsilon = \varepsilon^{(\phi)} \quad (64)$$

$$\sigma_{CO_2} = \sigma_{CO_2}^{(0)} + \sigma_{CO_2}^{(0,T)}\Delta T + \sigma_{CO_2-NaCl}^{(1)}\, c_{NaCl} \quad (65)$$

with $\sigma_{Na^+}^{(\phi)}$ and $\varepsilon^{(\phi)}$ defined in eqns. (61) and (62), respectively. Notice that in eqn. (65) $\sigma_{CO_2-NaCl} = \sigma_{CO_2-Na^+} + \sigma_{CO_2-Cl^-}$.

Although carbon dioxide certainly influences the permittivity of solution (at least through the reduction of the concentration of water molecules), no dependence of the permittivity on the CO_2 concentration needed be considered. Since the concentration of carbon dioxide is always low, a concentration dependence for the carbon dioxide diameter was not needed. No temperature dependent cross parameter ($\sigma_{i-j}^{(1,T)}$ in eqn. (59)) was necessary for the CO_2 diameter.

This introduces 5 new parameters, as seen in eqns. (63) and (65): $\sigma_{Na^+-CO_2}^{(1)}$, $\sigma_{Na^+-CO_2}^{(1,T)}$, $\sigma_{CO_2}^{(0)}$, $\sigma_{CO_2}^{(0,T)}$ and $\sigma_{CO_2-NaCl}^{(1)}$. They were adjusted by least-square fit of experimental VLE data. The parameters $\sigma_{CO_2}^{(0)}$ and $\sigma_{CO_2}^{(0,T)}$ are specific carbon dioxide parameters. They are common to three carbon dioxide systems. Values for $\sigma_{CO_2}^{(0)}$ and $\sigma_{CO_2}^{(0,T)}$ are given in Table 6. The 3 cross parameters $\sigma_{NaCl-CO_2}^{(1)}$, $\sigma_{NaCl-CO_2}^{(1,T)}$ and $\sigma_{CO_2-NaCl}^{(1)}$ are specific for the ternary system. They are specified in Table 7. The crystallographic value was taken for the diameter of Cl^-. One finds in the literature[26] the value of σ_{Cl^-} =3.62×10^{-10} m.

b) NaOH/CO$_2$ system.

For this system, the MSA parameters were taken as

$$\sigma_{Na^+} = \sigma_{Na^+}^{(\phi)} \tag{66}$$

$$\varepsilon = \varepsilon^{(\phi)} \tag{67}$$

$$\sigma_{CO_2} = \sigma_{CO_2}^{(0)} + \sigma_{CO_2}^{(0,T)}\Delta T \tag{68}$$

Contrary to eqns. (63) and (65), no cross parameter was necessary for σ_{Na^+} and for σ_{CO_2}. As stated previously, the two CO_2 parameters, $\sigma_{CO_2}^{(0)}$ and $\sigma_{CO_2}^{(0,T)}$, are the same as for the NaCl/CO_2 system.

The sizes of OH^-, HCO_3^-, CO_3^{2-} and H^+ were kept constant (concentration independent). While the OH^- and H^+ diameters were taken from previous work[11], the two parameters $\sigma_{HCO_3^-}$ and $\sigma_{CO_3^{2-}}$ have been fitted to the NaOH/CO_2 system, but are not specific to this system. These parameter values may be used in further modelings of carbon dioxide solutions where the dissociation of carbon dioxide has to be taken into account. Values of the anions and the hydronium diameters are collected in Table 8.

c) HAc/CO_2 system.

As mentioned above, the interaction between the two particles was taken into account through the association constant K_{asso} (see eqn. (57)). Nevertheless, one cross parameter was introduced in the acetic acid diameter in order to improve the accuracy of fit:

$$\sigma_{HAc} = \sigma_{HAc}^{(0)} + \sigma_{HAc}^{(0,T)} \Delta T + \sigma_{HAc-CO_2}^{(1)} \, c_{CO_2} \tag{69}$$

$$\sigma_{CO_2} = \sigma_{CO_2}^{(0)} + \sigma_{CO_2}^{(0,T)} \Delta T \tag{70}$$

No further parameter was introduced for the permittivity, that is $\varepsilon = \varepsilon_w$.

The two CO_2 parameters in eqn. (70), $\sigma_{CO_2}^{(0)}$ and $\sigma_{CO_2}^{(0,T)}$, are common to the other systems studied. As in eqn. (68), no cross parameter was necessary for σ_{CO_2}. No temperature dependent cross parameter ($\sigma_{i-j}^{(1,T)}$ in eqn. (59)) was necessary for the acetic acid diameter.

For this system, 4 new parameters were adjusted: $\sigma_{HAc}^{(0)}$, $\sigma_{HAc}^{(0,T)}$, $\sigma_{HAc-CO_2}^{(1)}$ and K_{asso}. They were obtained by fitting the solubility pressures of carbon dioxide in the ternary aqueous solution. The values are collected in Tables 6 and 7. The maximum proportion of associated CO_2 is found to be 69% of the overall amount of carbon dioxide at 313K.

The value for K_{dim} (see eqn. (56)), was found in the literature. The value of 0.146 kg mol^{-1}, given in ref 25, gave better results than that of 0.0517 kg mol^{-1} from ref 24. The value of K_{dim} was therefore fixed to 0.146 kg mol^{-1}.

Table 6. Values of MSA parameters from the fit of carbon dioxide solubility pressures.

Species	*Temp. range*	$\sigma^{(0)a}$	$10^3\sigma^{(0,T)b}$
CO_2	313-433 K	3.408	-3.973
HAc	313-433 K	6.526	-10.992

[a]In units of 10^{-10} m. [b]In units of 10^{-10} m K^{-1}.

3) Fitting procedure of the carbon dioxide solutions:

The adjustment procedure for the carbon dioxide, acetic acid and cross parameters, schematized in Fig. 1 is now explained.

1) For the NaCl/CO_2 system, one calculates the γ_i's and a_w with eqns. (15), (16), (22) and (23).
   For the HAc/CO_2 system, the γ_i's and a_w are calculated using eqns. (15), (16), (22), (23), (29), (30), (34) and (35). For these systems, the next step is step 5 below (because eqns. (1) to (3) are not taken into account).

For the $NaOH/CO_2$ system, the solution is initially assumed to be ideal: $\gamma_i = 1$.

2) The liquid equilibrium are solved with the association constants taken from the literature and eqns. (4), (54) and (55), yielding the concentrations of the different species.

3) The values of the γ_i's are computed for the concentrations of species obtained in step 2 for a set of MSA parameters.

4) The steps 2 and 3 are repeated until the calculated stork concentrations of each species *i* fulfils the criterion: $\frac{\left|m_i^{(n)} - m_i^{(n-1)}\right|}{m_i^{(n)}} < 10^{-5}$ where $m_i^{(n)}$ is the *n*th calculated molality of species *i*.

5) The pressure and the mole fractions of species in the vapor phase are calculated by solving the VLE equations (44) and (52) by using either an iteration or a Newton-Raphson procedure.

6) Unless the criterion: $\frac{\left|P^{calc} - P^{exp}\right|}{P^{exp}} < 10^{-5}$ on the pressure is fulfilled (where P^{exp} is the experimental pressure and P^{calc} is the calculated one) the Marquardt least-square procedure is repeated (steps 1-6 with another set of MSA parameters).

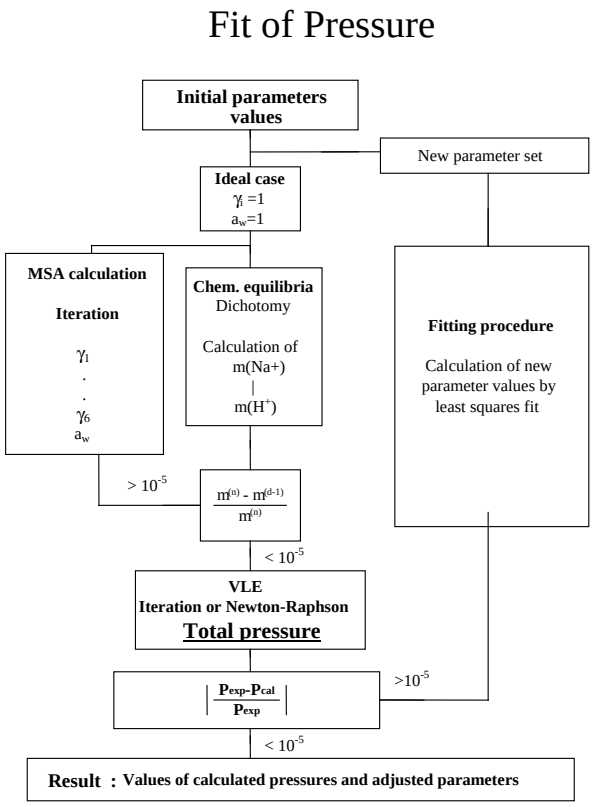

Fig. 1. Diagram of the fitting procedure used for the description of CO_2 solubility pressures in aqueous electrolyte solutions.

V) Discussion

1) Aqueous electrolyte solutions

The calculations for the binary NaCl aqueous solutions were carried out up to 6 mol kg^{-1} of NaCl in the temperature range 298-573 K. In the case of NaOH aqueous solutions, the data description was done up to 10 mol kg^{-1} and in the temperature range 298-473 K. The experimental data for the osmotic coefficients were taken from refs 27, 28 and 29 for the NaCl solutions and from refs 27, 30 and 31 for the NaOH solutions. Following the recommendations of ref 32, points above 473 K from ref 31 were not used.

For each salt, 6 parameters were fitted, as detailed in the preceding section. The results are given in Table 5 and a typical plot for NaOH osmotic coefficients is shown in Figure 2. The overall Average Absolute Relative Deviation (AARD) for the two salts is satisfactory, considering the simple concentration and temperature dependence relations for the diameter and the solution permittivity. The $\sigma^{(0)}$, $\sigma^{(1)}$ and α parameters are similar in magnitude to those obtained by Simonin et al.[10, 11]. The slight deviations from their values are due to the absence of the McMillan Mayer to Lewis-Randall (MM-LR) conversion in our calculations.

Table 7. Cross parameters and results of fits.

System A+B	*max. m_{co2}* [a]	*max. m_{salt}* [a]	*Temp. range*	*$10^2\sigma^{(1)}_{A-B}$* [b]	*$\sigma^{(1)}_{B-A}$* [b]	*$10^4\sigma^{(1,T)}_{B-A}$* [c]	*K_{asso}* [d]	*AARD* [e] *(%)*
CO_2 + NaOH	1.73	1	313-433 K	0	0	0	-	6.82
CO_2 + NaCl	0.46	6	313-433 K	-0.1571	-0.01382	1.2983	-	3.47
CO_2 + HAc	1.28	4	313-433 K	0	-0.21527	0	0.263	4.47

[a] In units of mol kg^{-1}. [b] In units of 10^{-10} m dm^3 mol^{-1}. [c] In units of 10^{-10} m dm^3 mol^{-1} K^{-1}. [d] In units of dm^3 mol^{-1}. [e] $AARD = 1/n \sum_i \left| P_{cal}^{(i)} - P_{\exp}^{(i)} \right| / P_{\exp}^{(i)}$, with n= number of points.

The negative value of $\sigma^{(1)}$ is consistent with the expectation that the effective diameter of the cation (plus hydration shell) decreases with salt concentration. The positive value of the α parameter is coherent with the experimental observation that the solution permittivity decreases with salt concentration. The negative value of $\sigma^{(0,T)}$ means a decrease of the effective diameter of the cation with temperature, as expected from thermal effects on hydration.

In the case of NaOH, the adjustment of $\sigma^{(1,T)}_{Na^+}$, $\sigma^{(1,T)}_{NaOH}$ and $\alpha^{(T)}_{NaOH}$ yielded a relative deviation quite comparable to the one obtained with the $\alpha^{(T)}_{NaOH}$ parameter alone. Thus, it was decided to set $\sigma^{(1,T)}_{Na^+}$ and $\sigma^{(1,T)}_{NaOH}$ to zero and adjust only $\alpha^{(T)}_{NaOH}$.

Table 8. Values for the ion diameters (in units of 10^{-10}m) fitted with the MSA model.

σ_{H^+} [a]	σ_{Cl^-} [a]	σ_{OH^-} [a]	$\sigma_{HCO_3^-}$ [b]	$\sigma_{CO_3^{2-}}$ [b]
5.04	3.62	3.55	4.30	5.23

[a]Taken in ref 11. [b]Fitted in this work.

2) Carbon dioxide solutions

The experimental pressure values were taken from the papers of Rumpf et al.[1, 2] in the temperature range 313-433 K for each solution. For the NaCl/CO_2 system, pressures were given for two different salt concentrations, namely 4 and 6 mol kg^{-1}, and up to 0.5 mol kg^{-1} of carbon dioxide. For the NaOH/CO_2 system, pressures were given at 1 mol kg^{-1} of salt and up to 2 mol kg^{-1} of carbon dioxide. Finally, for the HAc/CO_2 system, the experimental data ranged up to 1.7 mol kg^{-1} of carbon dioxide at one acetic acid concentration of 4 mol kg^{-1}. The results of our description are given in Tables 6 and 7 and typical plots of the pressures in the three systems are shown in Figures 3 to 5.

The AARD value of 3.5% for the NaCl/CO_2 system is larger than the value of 1.9% obtained with the Pitzer model. However, the present MSA model introduces 11 adjustable parameters as compared to the 16 parameters for the Pitzer model. The Pitzer model needs 5 ternary parameters, as

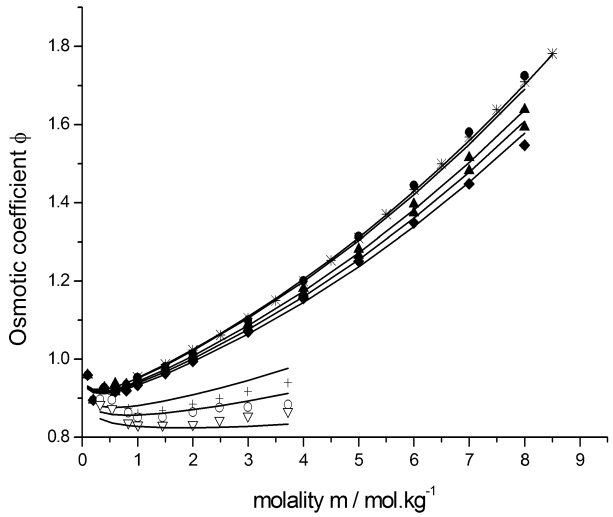

Figure 2. Plot of the osmotic coefficients for aqueous NaOH solutions, up to 8 mol kg^{-1} and for different temperatures. Experimental values taken from refs 27-30. (*): 298.15 K. (●): 308.15 K. (▲): 323.15 K. (▼): 333.15 K. (♦): 348.15 K. (+): 423.15 K. (○): 448.15 K. (▽): 473.15 K.

compared to 3 in the MSA model. Moreover, setting $\sigma^{(1)}_{CO_2-NaCl}$ to zero, one still obtains a satisfactory AARD value of 3.7%.

Concerning the NaOH/CO_2 system, the Pitzer model described the system with an AARD value of 9%. No cross parameter was introduced, meaning that the vapor pressures of the ternary system

could be predicted using the results for binary systems. However, as many as 46 parameters were needed, corresponding to the three binary subsystems NaOH/H_2O, $NaHCO_3$/H_2O and Na_2CO_3/H_2O. In this work, with the use of 8 adjusted parameters (4 parameters for the binary system CO_2/H_2O, 4 parameters for the binary system NaOH/H_2O and no cross parameter), the MSA model gives an accuracy of 6.8%.

For the HAc/CO_2 system, the precision was 2% with the Pitzer model, using 8 parameters (including 4 cross parameters). The result of this work is 4.5% with 7 parameters (including 2 cross-parameters).

VI) Conclusion

The overall quality of fits is satisfactory compared to the Pitzer model. Moreover, the parameters have a more direct physical meaning and the number of parameters is reduced.

It appears that the chemical equilibrium associated with the carbon dioxide reactions (eqns. (1) and (2)) play only a little role for the solubility of carbon dioxide, unless the supporting solution contains a base. In all other cases, it seems reasonable to neglect these equilibrium, which makes the calculations much simpler.

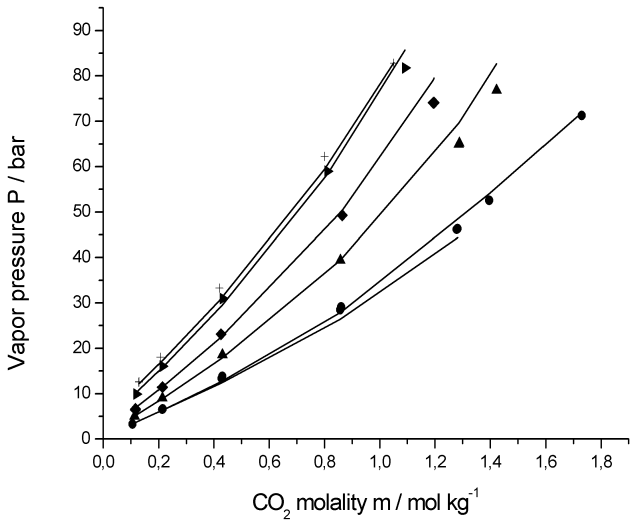

Figure 3. Plot of the pressure over HAc/CO_2 aqueous solutions at the HAc concentration of 0.9 mol kg^{-1} up to 413 K. Experimental values taken from ref 2. (•): 313.15 K.(▲):333.15K(♦):353.15K(►):393.15K(+):413.15K

It can be shown from the present study that the vapor phase is composed in each case of more than 98 % of carbon dioxide. This is due to the very high value of the Henry's coefficient of carbon dioxide. Consequently, the activity coefficient that influences most the VLE is the carbon dioxide activity coefficient, γ_{CO_2} . It is observed that this quantity does not vary much with concentration

and temperature. So, it is found with our treatment that in the range 313-433 K, γ_{CO_2} varies from 1.6 to 2 for the system NaCl/CO_2 at 4 mol kg^{-1} of NaCl, from 2.2 to 2.6 for the same system at 6 mol kg^{-1} of NaCl, from 1.2 to 1.3 for the system NaOH/CO_2, and from 0.5 to 0.7 for the system HAc/CO_2.

The only system exhibiting a salting-in effect is the solution of carbon dioxide and acetic acid, with a CO_2 activity coefficient γ_{CO_2} smaller than 1. In our modeling, this system is assumed to be a mixture of uncharged hard spheres, leading to a repulsive effect, with activity coefficients γ_{CO_2} larger than unity. In contrast, the association between carbon dioxide and acetic acid introduced in our model is an attractive effect that causes the γ_{CO_2} to be decreased below 1. So, at 1.3 mol kg^{-1} of carbon dioxide and 4 mol kg^{-1} of acetic acid, and with a value of 0.3 for the association constant K_{asso}, the values for the activity coefficients are as follows: $\gamma_{CO_2}^{HS} = 1.98$, $\gamma_{CO_2}^{MAL} = 0.33$, yielding $\gamma_{CO_2} = \gamma_{CO_2}^{HS}\gamma_{CO_2}^{MAL} = 0.66$. Again, since the major component in the vapor phase is the carbon dioxide, the dimerization of acetic acid in the liquid phase has a negligible influence on the calculated pressures.

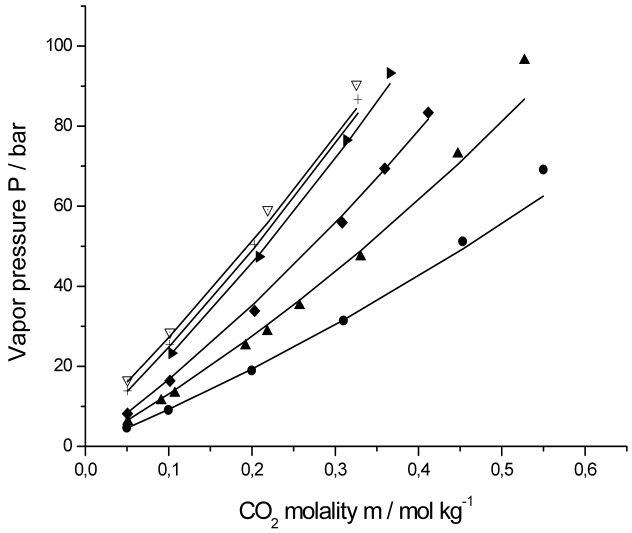

Figure 4. Plot of the pressure over aqueous NaCl/CO_2 solutions at 4 mol kg^{-1} of the salt and up to 433 K. Experimental values taken from ref 1. (•): 313.15 K.(▲): 333.15 K. (♦): 353.15 K. (►): 393.15 K. (+): 413.15 K. (▽): 433.15 K.

The two parameters $\sigma_{CO_2}^{(0)}$ and $\sigma_{CO_2}^{(0,T)}$ obtained for the carbon dioxide parameters are common to the three systems. The value of the carbon dioxide diameter at infinite dilution and 298 K, $\sigma_{CO_2}^{(0)}$, is 3.41×10^{-10} m which is reasonable considering the value of 1.22×10^{-10} m for a C=O bond. The interpretation of the parameter $\sigma_{CO_2}^{(0,T)}$ is the same as for the Na^+ cation.

These parameter values were found to provide also a good description of the binary CO_2/H_2O mixture. In the temperature range 373-433 K, and for concentrations of carbon dioxide up to 0.5 mol kg^{-1} [33], the model describes the pressures with a precision of 3.15 % if one uses $\sigma_{CO_2}^{(0)}$ and $\sigma_{CO_2}^{(0,T)}$ given in Table 5. A plot is given in Figure 6. In this case, the activity coefficient of the carbon dioxide is slightly above 1 and decreases slowly with temperature.

The values of the anion diameters $\sigma_{HCO_3^-}$ and $\sigma_{CO_3^{2-}}$ are consistent with the values generally found in the literature[34]. The carbonate anion is somewhat large, which can be explained by the solvation shell surrounding this doubly charged anion.

The HCO_3^- and CO_3^{2-} diameter values adjusted in the $NaOH/CO_2$ system, may be expected to give satisfactory representation of other aqueous electrolyte systems containing carbon dioxide.

For the acetic acid, the value of the adjusted infinite dilution diameter $\sigma^{(0)}$ of 6.53×10^{-10} m seems plausible. Considering the geometrical form of the acetic acid and the size of the different bonds of the molecule, one obtains with the program MOPAC™ (Molecular Package) a distance of 5.1×10^{-10} m between the hydrogen atom of the carboxylic acid group and the hydrogen atom of the methyl group. The value of 6.53×10^{-10} m is close to the value of 6.22×10^{-10} m found by Cartailler et al.[25]. The concentration and temperature dependent parameters are also coherent, as explained before.

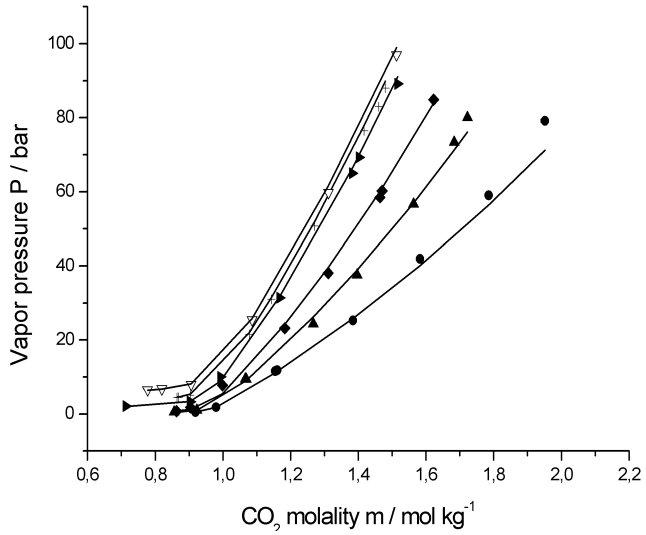

Figure 5. Plot of the pressure over aqueous $NaOH/CO_2$ solutions at 0.96 mol kg^{-1} of NaOH up to 433 K. Experimental values taken from ref 2. (•): 313.15 K. (▲): 333.15 K. (♦): 353.15 K. (►): 393.15 K. (+): 413.15 K. (▽): 433.15 K.

Finally, it may be noted that the influence of salts on the CO_2 solubility pressure follows the Hofmeister series[35] much as the surface tension of electrolyte solutions[36]. This is not surprising since in both cases there is a balance between ionic hydration and the direct interaction between ions and

gas molecules. Probably, both dispersion and hydration forces are responsible for this effect. In the present paper, these effects are buried in the parameters that are adjusted to the macroscopically measured pressures. In a forthcoming paper these effects will be quantified by taking explicitly into account the influence of dispersion and hydration forces.

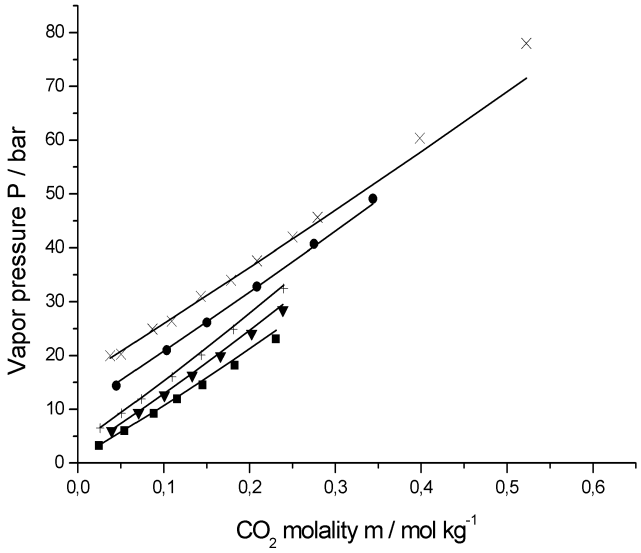

Figure 6. Plot of the pressure over aqueous CO_2 solutions up to 433 K. Experimental values taken from ref 33. (•): 373.15 K. (▼): 393.15 K. (+): 413.15 K. (■): 453.15 K. (×): 473.15 K.

Acknowledgment. This work is part of a project (AiF-FV-Nr. 12 137/N/1) sponsored by the German Ministery of Economy and Employment (BMWA) via the Arbeitsgemeinschaft industrieller Forschungsvereinigungen "Otto von Guericke" e.V. (AIF).

References

1 Rumpf, B.; Nicolaisen, H.; Öcal, C.; Maurer, G. *J. Solution Chem.* **1994**, *23*, 431.

2 Rumpf, B.; Xia, J.; Maurer, G. *Ind. Eng. Chem. Res.* **1998**, *37*, 2012.

3 Rumpf, B.; Xia, J.; Maurer, G. *J. Chem. Thermodynamics* **1997**, *29*, 1101.

4 Bieling, V.; Kurz, F.; Rumpf, B.; Maurer, G. *Ind. Eng. Chem. Res.* **1995**, *34*, 1449.

5 Waisman, E.; Lebowitz, J. L. *J. Chem. Phys.* **1970**, *52*, 4307; *ibid.* **1972**, *56*, 3086.

6 Blum, L. *Mol. Phys.* **1975**, *30*, 1529.

7 Blum, L. *Theoretical Chemistry: Advances and Perspectives*, ed. H. Eyring and D. Henderson, Academic Press, New York, 1980, vol. 5, p. 1.

8 Blum, L.; Høye, J. S. *J. Phys. Chem.* **1977**, *81*, 1311.

9 Sun, T.; Lénard, J. L.; Teja, A. S. *J. Phys. Chem.* **1994**, *98***,** 6870.

10 Simonin, J. P.; Blum, L.; Turq, P. *J. Phys. Chem.* **1996**, *100*, 7704.

11 Simonin, J. P. *J. Phys. Chem. B* **1997**, *101*, 4313.

12 Monnin, C.; Dubois, M.; Papaiconomou, N.; Simonin, J.-P. *J. Chem. Eng. Data* **2002**, *47*, 1331.

13 Bernard, O.; Blum, L. *J. Chem. Phys.* **1996**, *104*, 4746.

14 Simonin, J. P.; Bernard, O.; Blum, L. *J. Phys. Chem. B*, **1998**, *102*,4411; Simonin, J. P.; Bernard, O.; Blum, L. *J. Phys. Chem. B* **1999**, *103*, 699

15 Blum, L.; Wei, D. J. *J. Chem. Phys.* **1987**, *87*, 555.

16 McMillan, W. G.; Mayer, J. E. *J. Chem. Phys.* **1945**, *13*, 276.

17 Wertheim, M.S. *J. Stat. Phys.* **1983**, *35*, 19.

18 Wertheim, M.S. *J. Chem. Phys.* **1986**, *85*, 2929; Wertheim, M.S. *J. Chem. Phys.* **1987**, *87*, 7323; Wertheim, M.S. *J. Chem. Phys.* **1988**, *88*, 1214.

19 Olausen, K.; Stell, G. *J. Stat. Phys.* **1991**, *62*, 221.

20 Novotny, P.; Söhnel, O. *J. Chem. Eng. Data* **1988**, *3*, 49

21 Prausnitz, J. M.; Lichtenthaler, R. N.; Gomes de Azevedo, E. *Molecular Thermodynamics of Fluid-Phase Equilibrium*, Prentice Hall, Upper Saddle River, New Jersey, 1999.

22 Hayden, G. J.; O'Connell, J. P. *Ind. Eng. Chem. Process Des. Dev.* **1975**, *14*, 209.

23 Saul, A.; Wagner, W. *J. Phys. Chem. Ref. Data* **1987**, *16*, 893.

24 Harris, A. L.; Thompson, P. T.; Wood, R. H. *J. Soution Chem.* **1980**, *9*, 305.

25 Cartailler, T.; Turq, P.; Blum, L.; Condamine, N. *J. Phys. Chem.* **1992**, *96*, 6766.

26 Marcus, Y. *J. Solution Chem.* **1983**, *12*, 271.

27 Hamer, W. J.; Wu, Y.-C. *J. Phys. Chem. Ref. Data* **1972**, *1*, 1047.

28 Gibbard Jr., H. F.; Scatchard, G.; Rousseau, R. A.; Creek, J. L. *J. Chem. Eng. Data* **1974**, *19*, 281.

29 Liu, C.; Lindsay Jr., W. T. *J. Phys. Chem.* **1970**, *74*, 341.

30 Akerlöf, G.; Kegeles, G. *J. Am. Chem. Soc.* **1937**, *59*, 1855.

31 Campbell, A. N.; Bhatnagar, O. N. *J. Chem. Eng. Data* **1984**, *29*, 166.

32 Pabalan, R. T.; Pitzer, K. *Geochim. Cosmochim. Acta* **1987**, *51*, 829.

33 Müller, G.; Bender, E.; Maurer, G. *Ber. Bunsenges. Phys. Chem.* **1988**, *92*, 142.

34 Barthel, J. M. G.; Krienke, H.; Kunz W. *Physical Chemistry of Electrolyte Solutions*, Springer, New-York, 1998.

35 Hofmeister, F. *Arch. Exp. Pathol. Pharm.* **1888**, *XXVI*, 247.

36 Collins, K. D.; Washabaugh, M. W. *Quarterly Rev. Biophys.* **1985**, *18*, 323.

Chapter VI-
Development of a new electrolyte model: the MSA-NRTL model

A. Introduction

As pointed out in the first chapter, many empirical models have been built for describing the properties of solutions of neutral solutes. These equations, can predict the effect of a neutral solute on a solution, but are unable to describe the effect of a charged solute on the properties of a neutral solution. This is due to the fact that ionic forces are of a completely different nature from the short-range forces existing between neutral solutes.

Two ways of investigation have then been explored for developing reliable electrolyte models.

Firstly, some physically well-based theoretical models have been studied, such as the MSA or the HNC model for example. These models provided expressions for the free energy and the activity coefficients in the MM framework, where the solvent is regarded as a continuum. Nevertheless, since the solvent is not explicitly accounted for, application of such models to the description of solutions on the whole mole fraction range is not easy. Moreover, the complexity of the theoretical equations make it often difficult to apply then to complex chemical solutions.

A second more applied way of research, was the development of already existing empirical models, and their extension to electrolytes. In this investigation, many considerations have been made on how to integrate the electrostatic effect into the Gibbs energy.

The main idea used until now, is that the excess Gibbs energy is the combination of two terms: a short-range term corresponding to the previous empirical models (see chapter II),

and a new long-range term corresponding to the electrostatic contribution due to the introduction of an electrolyte in the neutral solution.

$$G^{ex}=G^{ex,SR} + G^{ex,LR} \tag{6.1}$$

The $G^{ex,SR}$ is given by models such as the NRTL, UNIQUAC, or Wilson models. The $G^{ex,\,LR}$ is the long-range term corresponding to coulombic interactions.

The problem is that most electrolyte theories (Debye-Hückel, MSA, etc.) are not calculated in the LR framework, where *G* is the energy function, but at the MM level of description, in which the chemical potential of the solvent is kept constant. Moreover, the thermodynamic quantities calculated from these models are on a molality scale, whereas the excess Gibbs energy is to be expressed on the mole fraction scale.

These conceptual problems have been studied by Pitzer twenty years ago. He calculated an expression of the LR excess Gibbs energy for the Extended Debye Hückel theory by assuming that the electrostatic contribution obtained with the excess Gibbs energy had the same expression as in the MM framework, for which expressions have already been given [1].

This assumption generally can be used for calculating an electrostatic term of a model built in the LR framework, departing from expressions of an electrostatic model built in the MM framework.

We now give the demonstration yielding the expression of the so-called Pitzer-Debye-Hückel (PDH) electrostatic contribution to the excess Gibbs energy.

1. Calculation of an Pitzer-Debye-Hückel excess Gibbs energy.

Let us first write the relation between excess Gibbs energy and thermodynamic coefficients[2] as

$$\begin{aligned} \Phi - 1 &= -\frac{1}{\nu m_{MX} M_w RT}\frac{\partial G^{ex}}{\partial N_w} \\ \ln\gamma_{\pm} &= \frac{1}{\nu RT}\frac{\partial G^{ex}}{\partial N_{MX}} \end{aligned} \tag{6.2}$$

[1] K. S. Pitzer, J. Phys. Chem., 1973, 77, 268 and K. S. Pitzer, Acc. Chem. Res., 1977, 10, 371.
[2] J. M. Prausnitz, R. N. Lichtenthaler and E. Gomes de Azevedo, in *Molecular Thermodynamics of Fluid-Phase Equilibrium*, Prentice Hall, Upper Saddle River, New Jersey, 1999.

written on the mole fraction scale, (the letter γ for the activity coefficient is kept, because there is no possible confusion in this demonstration).

By virtue of eqn. (6.1), ϕ-*1* is

$$\phi - 1 = \Delta\phi^{LR} + \Delta\phi^{SR} \tag{6. 3}$$

Let us recall the Debye-Hückel expression for the electrostatic contribution to the osmotic coefficient in the continuous solvent model

$$\Delta\Phi^{DH} = -|z_+ z_-| A_\Phi \frac{\sqrt{I}}{1 + b\sqrt{I}} \tag{6. 4}$$

with *b* the adjustable "dosest approach" parameter.

The idea is now to consider that the expression for $\Delta\phi^{DH}$ obtained from the electrostatic contribution to the excess Gibbs energy $G^{ex,LR}$ is the same as $\Delta\phi^{DH}$ in eqn. (6.4), that is

$$\Delta\Phi^{DH} = -\frac{1}{\nu m_{MX} M_w RT} \frac{\partial G^{ex,LR}}{\partial N_w} \tag{6. 5}$$

Then, we obtain:

$$\frac{\partial G^{ex,LR}}{\partial N_w} = \nu m_{MX} M_w |z_+ z_-| A_\Phi \frac{\sqrt{I}}{1 + b\sqrt{I}} \tag{6. 6}$$

or

$$\frac{\partial G^{ex,LR}}{\partial N_w} = M_w \sum_i^{ion} m_i |z_+ z_-| A_\Phi \frac{\sqrt{I}}{1 + b\sqrt{I}} \tag{6. 7}$$

In this equation the product : $\sum_i^{ion} m_i |z_+ z_-|$ is two times the ionic strength.

$$I = \frac{1}{2} \sum_i^{ion} m_i z_i^2 = \frac{1}{2} \nu m_{MX} |z_+ z_-| \tag{6. 8}$$

Then:

$$\frac{\partial G^{ex,LR}}{\partial N_w} = 2 M_w A_\Phi \frac{I^{3/2}}{1 + b\sqrt{I}} \tag{6. 9}$$

Converting m_w with the formula: $m_i = \frac{1}{M_w}\frac{N_i}{N_w}$, leads to:

$$I = \frac{1}{2}\sum_i^{ion} m_i z_i^2 = \frac{1}{2M_w}\sum_i^{ion} \frac{N_i}{N_w} z_i^2 \qquad (6.\ 10)$$

We have then:

$$\frac{\partial G^{ex,LR}}{\partial N_w} = 2\sqrt{\frac{1}{M_w}} A_\Phi \frac{\left(\frac{1}{2}\sum_i^{ion} \frac{N_i}{N_w} z_i^2\right)^{3/2}}{1+\rho\sqrt{\frac{1}{2}\sum_i^{ion} \frac{N_i}{N_w} z_i^2}} \qquad (6.\ 11)$$

with $\rho = \sqrt{\frac{1}{M_w}} b$

a) Pitzer Debye Huckel equations:

The extended Debye Hückel term, known as the Pitzer-Debye-Hückel term, is used in semi-empirical models where the excess Gibbs energy is composed of an electrostatic and a short range terms. The electrostatic term is important at low concentrations.

Furthermore, as pointed out by Pitzer[3], this electrostatic term is added to the excess Gibbs energy to improve models that are inaccurate at low and very low concentration, in particular because the short range expressions did not satisfy the Debye-Huckel limiting law. The mole fraction x is normally written as

$$x_i = \frac{N_i}{N_w + \sum^{ion} N_i}$$

Since we deal only with low concentrations, the following assumption can be made

$$x_i \cong \frac{N_i}{N_w} \qquad (6.\ 12)$$

The ionic strength on the mole fraction scale is written as follows:

$$I_x = \frac{1}{2}\sum_i^{ion} x_i z_i^2 \qquad (6.\ 13)$$

[3] K. S. Pitzer, J. Am. Chem. Soc., 1980, 102, 2902.

The relation between I and I_x is

$$I = \frac{1}{2}\sum_{i}^{ion} m_i z_i^2 = \frac{1000}{M_w} I_x \qquad (6.\ 14)$$

Eqns. (6.11), (6.12) and (6.13) yield to:

$$\frac{\partial G^{ex,LR}}{\partial N_w} = 2\sqrt{\frac{1}{M_w}} A_\Phi \frac{I_x^{3/2}}{1+\rho\sqrt{I_x}} \qquad (6.\ 15)$$

The integration of $ln(\gamma_w)$ yields the following expression for the EDH excess Gibbs energy

$$G_{PDH}^{ex} = -N_{tot} 4\sqrt{\frac{1}{M_w}} A_\Phi \frac{I_x}{\rho} \ln\left(1+\rho\sqrt{I_x}\right) \qquad (6.\ 16)$$

which is exactly the corresponding excess Gibbs energy of the solution written by Pitzer[3].
The resulting activity coefficient for ion i is obtained with eqns. (6.2) and (6.16), which

$$\ln\gamma_i = -\sqrt{\frac{1}{M_w}} A_\Phi \left(\frac{2z_i^2}{\rho} \ln\left(1+\rho\sqrt{I_x}\right) + \frac{z_i^2 I_x^{1/2} - 2I_x^{3/2}}{1+\rho\sqrt{I_x}} \right) \qquad (6.\ 17)$$

b) Extended Debye-Hückel equations :

We now show that the formula, eqn. 6.17, derived by Pitzer may be extended to higher solute mole fraction. Let us now not make the assumption of Pitzer, eqn. (6.12).
Then

$$m_i = \frac{N_i}{N_w}\frac{1}{M_w} = \frac{x_i}{x_w}\frac{1}{M_w} \qquad (6.\ 18)$$

where x_i is the mole fraction of ion i.
So,

$$I_N = \frac{1}{2}\sum_{i}^{ion} \frac{N_i}{N_w} z_i^2 = \frac{1}{2}\sum_{i}^{ion} \frac{x_i}{x_w} z_i^2 \qquad (6.\ 19)$$

Then the solvent activity coefficient becomes:

$$\frac{\partial G^{ex,LR}}{\partial N_w} = 2\sqrt{\frac{1}{M_w}} A_\Phi \frac{I_N^{3/2}}{1+\rho\sqrt{I_N}} \qquad (6.\ 20)$$

The integration of the preceding equation gives us the excess Gibbs energy for long range interactions, expressed on a mole fraction scale:

$$G^{ex}_{EDH} = -N_{tot} x_w 4 \sqrt{\frac{1}{M_w}} A_\Phi \frac{I_N}{\rho} \ln\left(1 + \rho \sqrt{I_N}\right) \qquad (6.\ 21)$$

which is of the same form as G^{ex}_{PDH}. The only difference is that I_N is substituted by I_x (i.e: in mole written instead of mole fraction).

The resulting ionic activity coefficient for species *i* is in this case:

$$\ln \gamma_i = -\sqrt{\frac{1}{M_w}} A_\Phi \left(\frac{2 z_i^2}{\rho} \ln\left(1 + \rho \sqrt{I_N}\right) + \frac{z_i^2 I_N^{1/2}}{1 + \rho \sqrt{I_N}} \right) \qquad (6.\ 22)$$

This equation is similar to the first term of the Pitzer activity coefficient[1].

The demonstration has shown that the conversion of an expression of the activity coefficient defined in the MM framework can give an expression of the excess Gibbs energy. The PDH expression of the excess Gibbs energy is until today the reference equation for empirical *g*-models of electrolyte solutions. However, since the PDH expression is used in models describing electrolyte solution up to very high concentrations, the EDH expression may be preferred to the PDH expression, since it is corresponds to the correct electrostatic expression at high concentration.

The next subsection will now detail our work on developing a new g-model for electrolyte solutions, exploring a new expression for the electrostatic contribution to the excess Gibbs energy, as well as the short-range contribution to G^{ex}.

B. The MSA NRTL model

Summary

The aim of our work was to develop a model for electrolyte solutions fulfilling the following criteria.

First, to develop an electrolyte model with a physically well-based electrostatic contribution. Second, the model should be able to describe multi-solvent electrolyte solutions. Third, the model should be able to describe neutral solutions without any change in the model

equations. Lastly, the model should require only binary parameters and, if possible in the case of multi-solvent solutions, binary solvent-parameters that can be found in the literature.

Considering these criteria, an extension of the NRTL model with a MSA term was found to be the most interesting route.

The NRTL equation is a simple and accurate model for the description of mixtures of solvents, as shown in chapter 1. The binary solvent-solvent parameters required in the NRTL model are already available from previous fits of experimental data for solvent mixtures. Furthermore, with the MSA-NRTL, it is possible to describe non-electrolyte solutions. In this case, the MSA term reduces to zero, (no charge exist in the solution). In this case, the MSA-NRTL model strictly reduces to the well-known NRTL model. Finally, a previous version of NRTL, called the e-NRTL model, extended to electrolyte solutions with the help of a Debye-Hückel term had already been studied[4]. This ensures the NRTL may be applied to electrolyte solutions.

As pointed out before, the electrostatic term that has to be added to the NRTL model is important at low concentrations. At higher concentrations (above 2M), it reaches a low asymptotic value. In this case, the interactions between ions are short ranged. Thus, the substitution of the PDH term in the e-NRTL by a MSA term will not affect the precision of the e-NRTL for high concentrations. A modification of the NRTL term, dominant at high concentrations, is then required. In the original e-NRTL model, assumptions on ions interacting with their neighbourhood had been made in the NRTL model. Some of these have been relaxed in the new model.

Besides, following the work of Watanasiri et al.[5], a concentration dependence has been introduced in the NRTL parameters.

These modifications of NRTL combined with a MSA term resulted in the MSA-NRTL model. It has been succesfully applied to 20 aqueous electrolyte solutions. The parameters were found to be physical and of reasonable values. The modeling of ternary systems composed of one electrolyte and two solvent has also been possible. However, in this case, the "optimum" values of the parameters do not seem to be physically interpretable.

[4] J. L. Cruz and H. Renon, *AIChE J.*, 1978, **24**, 817, C. C. Chen and L. B. Evans, *AIChE J.*, 1982, **28**, 4.
[5] V. Abovsky, Y. Liu and S. Watanasiri., *Fluid Phase Equilibrium*, 1998, **150-151,** 277.

Published in Physical Chemistry Chemical Physics in 2002, vol. 4(18), p. 4435-4443.

MSA-NRTL model for the description of the thermodynamic properties of electrolyte solutions.

N. Papaiconomou[a, b], J.-P. Simonin[b], O. Bernard[b] and W. Kunz[*, a]

[a] *Institute of Physical and Theoretical Chemistry, University of Regensburg, D-93040 Regensburg, Germany. Fax: 49 941 9434532; Tel: 49 941 9434045. E-mail: werner.kunz@chemie.uni-regensburg.de*
[b] *Laboratoire LI2C, Université Pierre et Marie Curie, Boîte n° 51, 75252 Paris Cedex 05, France. Fax 33 (0)1 44 27 38 34. E–mail: sim@ccr.jussieu.fr*

The mean spherical approximation (MSA) approach for electrolyte solutions is combined with a modified non-random two-liquid (NRTL) approach. The resulting model is suitable for a description of the thermodynamic properties of electrolyte-multisolvent systems. The ability of this MSA-NRTL model is investigated by examining activity and osmotic coefficients of binary and ternary electrolyte solutions. Especially for non-aqueous solutions, the model is superior to standard semi-empirical calculations used in the chemical industry.

1. Introduction

The theory of electrolyte solutions has a long history. Promising starting points in the 19th century culminated in the famous theory of Debye and Hückel [1] in the 1920's. During the last decades, the statistical mechanics of electrolytes has been continuously developed both on the theoretical level [2-6] and on the simulation level [7, 8].

However, engineers in the industry have not assimilated these more and more sophisticated approaches which became nearly exclusively the domain of a few specialists. The industrial demand for relatively simple and universally applicable programs explains the noticeable success of Pitzer equations which are still standard for the description of industrial electrolyte systems. The Pitzer equations are composed of a Debye-Hückel term plus a virial correction to account for various effects in concentrated solutions.

Pitzer or Debye-Hückel terms are often integrated in industrial simulation packages of electrolytes in order to model the peculiarities of charged particles in phase equilibrium.

A prominent example is the so-called Electrolyte-NRTL (electrolyte-Non Random Two Liquid) approach [9, 10] based on the classical NRTL model by Renon and Prausnitz [11]. Other models are those of Fürst et al. [12] and of Gmehling and his group [13]. These approaches consist of an equation of state in which the electrolyte contribution is added through an *ad hoc* term to classical equations of state. On the other hand, in the last 30 years, advanced statistical mechanics have led to the emergence of new theories. One of them, the MSA (Mean Spherical Approximation), can yield analytic expressions in terms of parameters (e.g., ion size, permittivity) that have physical meaning. The MSA has been used for the development of both stand-alone programs [14-17] and in combination with equations of states [12, 18, 19]. However, these MSA approaches rarely found broader distribution in the industry.

The present paper is a first attempt at filling the gap between theoreticians and engineers by combining the MSA with the NRTL model. The latter is used to account for short-range interactions and the former describes the long-range electrostatic interactions. The combination of the expressions is made in a physically and thermodynamically consistent way, as explained below. The aim of this work is to develop a new model capable of taking profit of the interesting properties of both theories: the MSA is an accurate and physically

sound theory for ions; the NRTL is a powerful model for solvent mixtures and it is widely used in the industry.

In the following section we describe the classic Electrolyte-NRTL model (e-NRTL) as implemented in Aspen's data simulation package. We will take e-NRTL as the reference to test the ability of our model. In section 4.2, some modifications are proposed for the NRTL part. The basic principles of the MSA are presented and a procedure is proposed so as to match it with NRTL. Section 5 is devoted to the application of our model to the description of binary and ternary electrolyte systems.

2. General relations

We first give basic relations and definitions that will be used below.

Let us consider a salt, denoted by *s*, supposed to be a strong electrolyte in a solvent designated by *m*. In this solvent, one mole of this salt can give ν_c moles of cations *c* of valence z_c and ν_a moles of anions *a* of valence z_a.

The excess Gibbs energy of the system, composed of N_m solvent molecules and N_s salt molecules, may be defined with respect to the ideal case as

$$G^{exc} = G - G^{id}$$

where G^{id} is the ideal contribution to *G*.

The excess Gibbs energy may be decomposed into two contributions: one arising from long-range (LR) interactions and the other one from short-range (SR) interactions, which can be written as

$$G^{exc} = G^{LR} + G^{SR}$$

In an electrolyte solution, LR forces arise from electrostatic interactions; SR forces include volume exclusion interactions and electrostatic forces of shorter range than ion-ion Coulomb forces (e.g., ion-dipole forces).

Furthermore, one may define the deviation of Gibbs energy with respect to the reference state as

$$\Delta G = G - G^{ref} \qquad (1)$$

where G^{ref} is the Gibbs energy of the system in its reference state. Generally, the reference state for the solvent is pure solvent ($x_m=1$) while, for the ions, it is the infinite dilution limit (unsymmetric convention).

The thermodynamic quantities of interest in this work are the osmotic coefficient, Φ, and the mean ionic activity coefficient f_s, defined on a mole fraction basis. They are related to the Gibbs energy as follows.

For any species i, its activity coefficient is obtained according to

$$\ln f_i = \frac{\partial \beta \Delta G^{exc}}{\partial N_i} \tag{2}$$

where ΔG^{exc} is the excess part of ΔG. Thus, the mean ionic activity coefficient of salt, f_s, defined by [20]

$$\ln f_s = \frac{1}{\nu}(\nu_c \ln f_c + \nu_a \ln f_a) \tag{3}$$

is also given by

$$\ln f_s = \frac{1}{\nu}\frac{\partial \beta \Delta G^{exc}}{\partial N_s}$$

where N_s is the number of salt `` molecules'' introduced in the system, $\beta=1/kT$ (with k the Boltzmann constant and T the temperature) and $\nu=\nu_c+\nu_a$ (one mole of salt s releases ν moles of ions in solution).

When the activity coefficient of solute is obtained in the symmetric convention ($f_s=1$ when $x_s=1$), it may be easily transformed to the unsymmetric convention (denoted by the superscript *), by using the following transformation [21]

$$f_s^* = f_s / f_s^{(0)} \tag{4}$$

in which $f_s^{(0)}$ stands for the value of f_s (symmetric convention) taken at infinite dilution for s. Then, $f_s^* \to 1$ as $x_s \to 0$.

For a solution comprising only one solvent m and one salt s, one defines the osmotic coefficient as

$$\Phi = -\frac{x_m}{x_s}\ln a_m \tag{5}$$

where the activity of solvent is given by

$$a_m = f_m x_m \tag{6}$$

where x designates a mole fraction and f_m is given by eqn. (2). In eqn. (5), one also has

$$x_m / x_s = 1/(\nu m_s M_m)$$

with m_s the molality of salt and M_m the molar mass of solvent, because

$$x_m = 1/(1+\nu m_s M_m) \tag{7}$$

and $x_s = 1-x_m = \nu m_s M_m /(1+\nu m_s M_m)$.

The activity coefficient must be converted to the molality scale for comparison with experimental data. The conversion formula is [20]

$$\gamma_s^* = f_s^* /(1+\nu m_s M_m)$$

or, using eqn. (7),

$$\gamma_s^* = f_s^* x_m \tag{8}$$

where the symbol γ denotes an activity coefficient on the molal scale (the `` experimental''scale).

The quantities f_s and f_m satisfy the Gibbs-Duhem relation [21]

$$x_s d \ln f_s + x_m d \ln f_m = 0 \tag{9}$$

at constant temperature and pressure.

Then, eqn. (9) being fulfilled, it can be shown using eqns. (4) and (7) that the first-order thermodynamic quantities Φ and γ_s^*, defined by eqns. (5), (6) and (8), satisfy the Gibbs-Duhem relation in the form [20]

$$d[m_s(1-\Phi)] + m_s d \ln \gamma_s^* = 0 \tag{10}$$

3. Electrolyte-NRTL model

The classic e-NRTL model allows the calculation of activity coefficients of electrolyte solutions containing at least a trace amount of water [22]. e-NRTL is expressed at the Gibbs energy level. The total excess Gibbs energy, $G^{e\text{-}NRTL}$, is assumed to be the sum of three terms [9]

$$G^{e-NRTL} = G^{PDH} + G^{NRTL} + G^{Born} \tag{11}$$

in which the first term represents the Pitzer-Debye-Hückel (PDH) contribution for long-range electrostatic interactions, the second term is the NRTL contribution and the last term is introduced to account for solvation effects (Born term).

3.1. PDH term

Pitzer started [23] from an expression for the activity coefficient of the solvent; its form was inspired by a formula found in previous works [24, 25]. By integration, Pitzer found the excess Gibbs energy contribution to LR interactions as

$$\beta G^{PDH} = -N_t M_m^{-1/2} (4A_\Phi I_x / \rho) \ln\left(1 + \rho\sqrt{I_x}\right) \tag{12}$$

with N_t the total number of particles, $\rho = bM_m^{-1/2}$, b being related to the closest approach distance between ions, I_x the ionic strength on a mole fraction basis

$$I_x = \frac{1}{2}\sum_i z_i^2 x_i \tag{13}$$

and the Debye-Hückel parameter

$$A_\Phi = \frac{1}{3}\sqrt{2\pi N_{Av} d_m}\left(\frac{\beta e^2}{4\pi\varepsilon_0\varepsilon_m}\right)^{3/2}$$

where d_m is the solvent density, N_{Av} is the Avogadro number, e is the charge of the proton; ε_0 is the permittivity of a vacuum and ε_m is the relative permittivity of solvent. Usually, a value [23] of 14.9 for ρ seems to have been taken in the literature.

For the activity coefficient of any species i, one has

$$\ln f_i^{PDH} = -\frac{A_\Phi}{\sqrt{M_m}}\left[\frac{2z_i^2}{\rho}\ln\left(1 + \rho I_x^{1/2}\right) + \frac{z_i^2 I_x^{1/2} - 2I_x^{3/2}}{1 + \rho I_x^{1/2}}\right] \tag{14}$$

3.2. NRTL term

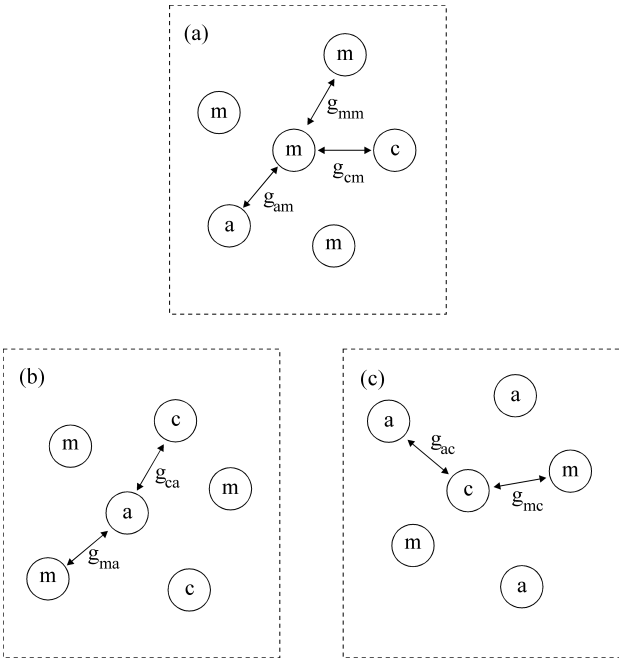

Fig.1 The 3 types of cells according to like-ion repulsion and local electroneutrality of the classical e-NRTL model. (a) cell with solvent central particle. (b) cell with anion central particle. (c) cell with cation central particle.

In e-NRTL, the effect of short-range interactions is described using the classic NRTL [11] for all species (ions and molecules) in solution.

So, three different types of arrangement may exist (see Figure 1) that correspond to central cation, anion or solvent. In this simplified picture, it is assumed that co-ions (i.e. ions of like charge) cannot be present in the same cell.

Denoting by g_{ji} ($=g_{ij}$) the interaction energy between two species *i* and *j*, the following quantities are generally introduced:

$$\tau_{ji} = \beta(g_{ji} - g_{ii}) \tag{15}$$

$$\tau_{ji,ki} = \beta(g_{ji} - g_{ki}) \tag{16}$$

for the differences between interaction energies.

The probability P_{ji} (the symbol P_{ji} is used here in place of G_{ji} [9, 10]) of finding a particle of species *j* in the immediate neighbourhood of a central particle of species *i* is assumed to obey a Boltzmann distribution as

$$P_{ji} = \exp(-\alpha\tau_{ji}) \tag{17}$$

One also defines

$$P_{ji,ki} = \exp(-\alpha\tau_{ji,ki}) \tag{18}$$

as the relative probability of finding a particle of species *j* near *i* compared to that of finding *k* near *i*. In these equations, α is the so-called non-randomness parameter (assumed to be identical for P_{ji} and P_{ki} in eqn. (17)). The inverse of the latter parameter represents the typical number of particles surrounding a central particle [11].

The last (closure) equation relates the local mole fractions of species *j* and *k*, X_{ji} and X_{ki}, around central species *i*, to the probabilities as

$$\frac{X_{ji}}{X_{ki}} = \frac{x_j}{x_k}\frac{P_{ji}}{P_{ki}} \tag{19}$$

where *j* and *i* are ions or solvent. This relation was first proposed by Chen and Evans [10]. Later, it was modified with the introduction of the valence z_i [26]. In this study we consider only the case of uni-univalent salts, in which the two different expressions are identical. We will elaborate on this point in a forthcoming paper, in which multivalent salts will be considered.

The relations between local mole fractions are

$$\sum_j X_{ji} = 1 \tag{20}$$

keeping in mind that, according to the above-mentioned assumption (exclusion of co-ions in the vicinity of an ion),

$$X_{cc} = X_{aa} = 0$$

and equivalently

$$P_{cc} = P_{aa} = 0$$

From eqns. (19) and (20), one gets

$$X_{ji} = x_j P_{ji} / \sum_k x_k P_{ki} \tag{21}$$

with x_j the mole fraction of species *j* in solution.

With these definitions, the NRTL contribution to the Gibbs energy per molecule of species *i*, $\overline{G_i}^{NRTL}$ (often denoted by $g^{(i)}$), averaged on the three possible configurations, can be calculated according to

$$\overline{G_i}^{NRTL} = \sum_j X_{ji} g_{ji}$$

which yields, using eqn. (21),

$$\overline{G_i}^{NRTL} = \sum_j x_j P_{ji} g_{ji} / \sum_j x_j P_{ji} \tag{22}$$

In order to calculate the excess Gibbs energy, the reference state values, $\overline{G_i}^{ref}$, must be specified. The reference state is pure solvent for the solvent and central ion only surrounded by counter-ions for the ions, as defined by Chen and Evans [10]. Then, one has

$$\overline{G_m}^{ref,NRTL} = g_{mm}$$

$$\overline{G_c}^{ref,NRTL} = \overline{G_a}^{ref,NRTL} = g_{ca}$$

and

$$\overline{G}^{ref,NRTL} = \sum_k x_k \overline{G}_k^{ref,NRTL} \tag{23}$$

Consequently, the NRTL deviation of the excess Gibbs energy of the solution (per molecule), averaged over all species, is given by

$$\Delta\overline{G}^{NRTL} = \sum_k x_k \Delta\overline{G}_k^{NRTL} \tag{24}$$

which yields the total deviation of excess Gibbs energy of the system

$$\Delta G^{NRTL} = N_t \Delta\overline{G}^{NRTL} \tag{25}$$

where $N_t = N_c + N_a + N_m$ is the total number of particles in solution.

In the case of a mixture of one salt and several solvents, that will be considered below, one gets, using eqns. (21) to (24),

$$\beta\Delta\overline{G}^{NRTL} = \sum_m \left[x_c X_{mc} \tau_{mc,ac} + x_a X_{ma} \tau_{ma,ca} + x_m \sum_j X_{jm} \tau_{jm} \right] \tag{26}$$

in which m in the summation represents a solvent and j represents any species (solvent or ion). The general relation for multi-salt multi-solvent systems has been given elsewhere [27].

One assumption is made in the classical e-NRTL: the number of cations surrounding a central solvent molecule is the same as the number of anions in the neighbourhood of the central solvent molecule (local electroneutrality assumption), meaning that $\tau_{cm} = \tau_{am}$ and $\tau_{mc,ac} = \tau_{ma,ca}$. With this simplification, the NRTL equations involve three adjustable

parameters: τ_{cs}, $\tau_{sc,ac}$ and α, for a binary electrolyte solution composed of one salt and one solvent.

3.3. Born term

The Born term in eqn. (11) represents the energy necessary to transfer an ion from infinite dilution in mixed solvent to the reference state of an infinitely diluted aqueous solution. In the e-NRTL model, it is taken as

$$\ln f_i^{BORN} = \frac{\beta e^2}{8\pi\varepsilon_0}\left(\frac{1}{\varepsilon_{m'}} - \frac{1}{\varepsilon_m}\right)\sum_i \frac{x_i z_i^2}{r_i} \tag{27}$$

where $\varepsilon_{m'}$ is the relative permittivity of the solvent mixture, and r_i is the Born ionic radius. For purely aqueous systems, $\ln f_i^{BORN}=0$.

4. MSA-NRTL model

4.1. MSA part

4.1.1. Restricted primitive model in its classical form

The starting point of the MSA theory dates back to the work of Percus and Yevick, Lebowitz and Percus, and Wertheim and Lebowitz [28-30]. It was developed particularly by Blum and co-authors for ionic solutions, at the primitive level (in which the solvent is modelled as a continuum) [17, 31, 32], see also [33, 34] and non-primitive level with the ion-dipole model [35] (in which the solvent is modelled as a hard sphere with embedded permanent point dipole).

The bases of the primitive MSA have been published in several review articles and monographs [14,31] so that only the results for thermodynamic properties are outlined here. The present discussion is focused on the so-called restricted primitive model (RPM) in which ions are taken as charged spheres of equal size in a continuous medium, characterised only by its dielectric permittivity. In this case, the RPM-MSA yields the following expression for the excess Helmholtz energy per unit volume, F_v^{MSA}, at the McMillan-Mayer (MM) level of solutions [36],

$$\beta F_v^{MSA} = -\lambda \frac{\Gamma}{1+\Gamma\sigma} \sum_i \rho_i z_i^2 + \frac{\Gamma^3}{3\pi} \tag{28}$$

in which the terms on the r.h.s. are the internal energy and entropic contributions, respectively. In this equation, Γ is the MSA screening parameter,

$$\Gamma = \frac{1}{2\sigma}(\sqrt{1+2\kappa\sigma} - 1) \tag{29}$$

κ is the Debye screening parameter,

$$\kappa = \sqrt{4\pi\lambda \sum \rho_i z_i^2} \tag{30}$$

so that $2\Gamma \approx \kappa$ at vanishing ionic concentration, and

$$\lambda = \frac{\beta e^2}{4\pi\varepsilon_0\varepsilon_m} \tag{31}$$

with σ the mean ionic size ($\sigma=(\sigma_+ + \sigma_-)/2$ where σ_+ and σ_- are the cation and anion diameters, respectively) and ρ_i the number density of ion *i* (i.e. the number of particles *i* per unit volume). The parameter λ is twice the Bjerrum distance [20]; its value is *ca.* 7×10^{-10} m at 25°C. In this work, the RPM-MSA model is used. This procedure is known to be relatively inaccurate for high anion-cation size asymmetry, at the primitive level of solutions. However, the RPM-MSA offers the advantage of leading to an explicit expression for Γ; moreover, in Procedure (II) below (see section 5.2), consistent sets of individual cation and anion sizes, σ_+ and σ_-, are determined. The use of a fully unrestricted MSA is left for future work.

Activity coefficients can be calculated by using the relation

$$\ln y_i^{*,MSA} = \frac{\partial \beta F_v^{MSA}}{\partial \rho_i} \tag{32}$$

where y^* denotes an activity coefficient on the molar scale (in the unsymmetric convention). One gets [31] from eqns. (3), (28) and (32)

$$\ln y_s^{*,MSA} = -\lambda \frac{\Gamma}{1+\Gamma\sigma} \left(\sum \frac{\nu_i}{\nu} z_i^2\right) \tag{33}$$

4.1.2. Adaptation of RPM-MSA for its combination with NRTL

The way in which the MSA may be used in place of the PDH equation is examined now.

The MSA model is known to account for electrostatic interactions between ions in a better way than the Debye-Hückel model [31]. Here, we propose to make the approximation [21]

$$G^{MSA} = F_v^{MSA} V \tag{34}$$

i.e. we identify the excess electrostatic Gibbs energy of the system, G^{MSA}, with the excess Helmholtz energy, $F_v^{MSA} V$.

It has been shown [15] that

$$\frac{\partial F_v^{MSA}}{\partial \Gamma} = 0$$

This relation yields the equation giving Γ (eqn. (29)) and it means that Γ is the `` optimum''screening parameter minimising the energy of the system [37].Therefore,

$$\frac{\partial \beta G^{MSA}}{\partial N_i} = V \left. \frac{\partial \beta F_v^{MSA}}{\partial N_i} \right|_{\Gamma} + \beta F_v^{MSA} \frac{\partial V}{\partial N_i} \tag{35}$$

in which the derivative in the first term of the r.h.s. is performed at constant Γ.

Using eqns. (28) and (35) and the relation $\rho_i = N_i / V$, we find after simplification

$$\ln f_i^{*,MSA} = \frac{\partial \beta G^{MSA}}{\partial N_i} = -\lambda z_i^2 \frac{\Gamma}{1+\Gamma\sigma} + \frac{\Gamma^3}{3\pi} \frac{\partial V}{\partial N_i} \tag{36}$$

yielding the MSA contribution to the activity coefficient in the unsymmetric convention, since Γ=0 when no ion is present (see eqns. (29) and (30)).

Then, from eqn. (3), one obtains the mean MSA activity coefficient of a salt *s*

$$\ln f_s^{*,MSA} = -\lambda \frac{\Gamma}{1+\Gamma\sigma} \left(\sum \frac{\nu_i}{\nu} z_i^2 \right) + \frac{\Gamma^3}{3\pi} \frac{1}{\nu} \frac{\partial V}{\partial N_s} \tag{37}$$

Moreover, for the solvent, one gets from eqn. (36)

$$\ln f_m^{*,MSA} = \frac{\Gamma^3}{3\pi} \frac{\partial V}{\partial N_m} \tag{38}$$

which may be inserted into eqn. (6) to yield the MSA contribution to the osmotic coefficient, eqn. (5).

It was found that the second term in eqn. (37) is much smaller than the first term, with a typical value between 0.01 and 0.05 for the ratio of the 2 terms; this result was found by

computing the quantity $\partial V/\partial N_s$ from density data [38] for alkali halides in water and in methanol at 25 and 100°C. Therefore, in the present work, we made the simplification

$$\frac{\partial V}{\partial N_c} = \frac{\partial V}{\partial N_a} = 0$$

and the quantity $\partial V/\partial N_m$ was calculated from the relation $V_m^{(0)} = N_m M_m/(N_{Av}\, d_m)$ for pure solvent. Therefore, we used the approximate relation

$$\frac{\partial V}{\partial N_m} = \frac{M_m}{N_{Av} d_m}$$

This simplification clearly presents the advantage of not requiring information on the density of solutions.

In the case of multi-solvent solutions, eqns. (37) and (38) may be used, assuming suitable mixing rules for the permittivity and the mean ionic diameter. Here, the following linear expressions were taken for the solvent mixtures

$$\varepsilon = \sum_m w_m \varepsilon_m \tag{39}$$

$$\sigma = \sum_m x_m \sigma_m \Big/ \sum_{m'} x_{m'} \tag{40}$$

where σ_m is the ionic diameter in solvent m, w_m is the mass fraction of solvent m in the solvent mixture (*i.e.* $\Sigma w_m = 1$) and ε_m is the permittivity of pure solvent m in the case of methanol/water and ethanol/water mixtures. In the case of dioxane/water mixtures, the value of ε was interpolated between that for pure water and the value of ε= 17.69 for the 70 Wt% dioxane mixture. This parametrisation describes experimental values for the mixtures with a precision better than 2.5 %.

It should be mentioned that other versions of the MSA could be used. So, one may think of taking ions of different sizes, which would be more realistic; in this case, the MSA still yields analytical, though larger, expressions. Besides, one may introduce concentration-dependent ion diameters and permittivity as shown in previous work [15], respecting the Gibbs-Duhem equation. Lastly, ion pairing could be introduced in the model. However, these modifications were found not to improve significantly the quality of fits. Therefore, the simple RPM version of the MSA was used in this work.

4.2. NRTL Contribution

The expression for the NRTL contribution is taken as in e-NRTL except for two modifications.

Firstly, the local electroneutrality condition around a solvent molecule is relaxed. This means that τ_{cm} is no more equal to τ_{am}. So, there are now 3 independent parameters: τ_{cm}, τ_{am} and $\tau_{mc,ac}$. By using eqns. (15) and (16), it is easy to show that $\tau_{ma,ca}$ is related to these parameters according to

$$\tau_{ma,ca} = \tau_{mc,ac} + \tau_{am} - \tau_{cm} \tag{41}$$

Secondly, in this first work, we suppose that the parameter $\tau_{mc,ac}$ is allowed to vary with solution composition, as suggested previously [39]. We adopt the same expression for the variation of this parameter, that is

$$\tau_{mc,ac} = \tau^{(1)}_{mc,ac} + \tau^{(2)}_{mc,ac} x_m \tag{42}$$

This formula may be interpreted by the fact that the mean interaction energies g_{mc} and g_{ac} are modified by solution composition. The parameters τ_{cm}, τ_{am}, $\tau_{mc,ac}^{(1)}$ and $\tau_{mc,ac}^{(2)}$ are adjustable parameters.

In the case of one salt in a solvent mixture, eqns. (2), (25) and (26) yield the activity coefficients

$$\ln f_m^{NRTL} = \beta\Delta\overline{G}_m^{NRTL} + \sum_{m'} \frac{x_{m'} P_{mm'}}{H_{m'}} \left(\tau_{mm'} - \beta\Delta\overline{G}_{m'}^{NRTL} \right) + \frac{x_c P_{mc,ac}}{H_{ac}} \left(\tau_{mc,ac} - \beta\Delta\overline{G}_c^{NRTL} \right) + \frac{x_a P_{ma,ca}}{H_{ca}} \left(\tau_{ma,ca} - \beta\Delta\overline{G}_a^{NRTL} \right) + \tau^{(2)}_{mc,ac} \frac{\partial \beta\Delta G^{-NRTL}}{\partial \tau_{mc,ac}} - \sum_{m'} x_{m'} \tau^{(2)}_{m'c,ac} \frac{\partial \beta\Delta G^{-NRTL}}{\partial \tau_{m'c,ac}} \tag{43}$$

for a solvent m (m' in the summations representing a solvent), and

$$\ln f_c^{NRTL} = \beta\Delta\overline{G}_c^{NRTL} + \sum_{m} \frac{x_m P_{cm}}{H_m} \left(\tau_{cm} - \beta\Delta\overline{G}_m^{NRTL} \right) - \frac{x_a}{H_{ca}} \beta\Delta\overline{G}_a^{NRTL} - \sum_{m} x_m \tau^{(2)}_{mc,ac} \frac{\partial \beta\Delta G^{-NRTL}}{\partial \tau_{mc,ac}} \tag{44}$$

for the cation c (the relation for $\ln f_a$ is obtained by inverting c and a subscripts and using eqns. (41) and (42)), and with the definitions

$$H_m = \sum_k x_k P_{km} \tag{45}$$

$$H_{ji} = \sum_k x_k P_{ki,ji} \tag{46}$$

Using eqns. (26) and (42), one gets

$$\frac{\partial \beta \Delta \overline{G}^{NRTL}}{\partial \tau_{mc,ac}} = x_c X_{mc}\left(1-\alpha\tau_{mc,ac}\right)+\alpha x_c X_{mc}\sum_{m'}\tau_{m'c,ac}X_{m'c}+$$
$$x_a X_{ma}\left(1-\alpha\tau_{ma,ca}\right)+\alpha x_a X_{ma}\sum_{m'}\tau_{m'a,ca}X_{m'a}$$

The activity coefficients for the ions in the unsymmetric convention are obtained using eqn. (4); the activity coefficients $f_i^{(0)}$ of ions (i=c or a) are obtained by taking the limit $x_s \to 0$ in eqn. (44).

4.3. Born term

An additional modification was brought to the classical e-NRTL. It concerns the reference state in the case of solvent mixtures. In e-NRTL [22], the reference state for the ions is purely aqueous solution (even when no water is present in the system). In the present model, the mixture of pure solvents and the infinite dilution of ions in the solvent mixture is taken as the reference state.

This convention offers two advantages: *(i)* it is the reference state used by experimentalists [40], with respect to which activity coefficients are commonly defined; *(ii)* there is no direct need for including a Born term in the Gibbs energy of the system. (However, a Born contribution could be inserted to account for the modification of ion hydration when the salt concentration is varied [9].) Let us recall that, in the case of anhydrous systems, the Aspen [22] simulation software requires the introduction of trace amount of water in the system for the program to run. This drawback is avoided with the solvent mixture reference state.

4.4. Final result

For the present MSA-NRTL model, we thus write

$$\ln f_i^{*} = \ln f_i^{*,NRTL} + \ln f_i^{*,MSA} \tag{47}$$

for each species *i*, in which $\ln f_i^{*,NRTL}$ is given by eqns. (4), (43), (44), and $\ln f_i^{*,MSA}$ is obtained from eqns. (37) and (38).

Then, these activity coefficients are inserted into eqns. (5), (6) and (8) to obtain thermodynamic quantities that may be compared with experimental data.

5. Results and discussion

Table 1 Procedure (I): Results for adjusted parameters from fit of osmotic coefficients[a] for aqueous electrolyte solutions (α=0.2).

Salt	m_{max}	$\tau^{(1)}_{mc,ac,}$	$\tau^{(2)}_{mc,ac}$	τ_{cm}	τ_{am}	σ [b]	*AARD (%)*[c]
HCl	16	26.89	-18.08	-7.691	-2.230	5.26	0.2
HBr	11	31.33	-21.64	-7.992	-2.851	3.86	0.1
HI	10	34.64	-25.46	-8.193	-2.232	4.19	0.08
HNO_3	28	12.46	-2.644	-4.946	-4.872	6.06	0.5
LiCl	19	26.99	-17.27	-7.594	-3.279	2.15	0.2
LiBr	20	41.01	-33.69	-8.257	-0.092	5.90	1.3
LiI	3	29.62	-18.73	-7.692	-4.140	4.69	0.03
LiOH	5	7.745	-2.738	-5.522	-1.320	1.13	0.06
$LiNO_3$	20	15.18	-4.791	-5.469	-5.057	4.45	0.2
NaCl	6	17.60	-8.484	-6.510	-3.380	4.50	0.01
NaBr	9	16.51	-6.209	-5.909	-4.690	4.61	0.01
NaI	12	22.66	-13.69	-7.230	-2.775	4.21	0.09
NaOH	20	28.58	-20.49	-7.641	-1.633	2.00	0.2
$NaNO_3$	10	9.641	-3.002	-5.185	-2.197	3.96	0.08
KCl	4	17.11	-9.851	-6.550	-1.664	3.93	0.001
KBr	5.5	13.22	-5.018	-5.869	-3.103	4.19	0.02
KI	4.5	12.54	-3.524	-5.247	-4.147	4.21	0.02
KOH	20	29.50	-21.75	-7.780	-1.112	3.57	0.4
KNO_3	3.5	13.72	-6.194	-5.533	-2.318	2.84	0.01

[a] Experimental values taken from ref [43]. [b]in units of 10^{-10} m. [c]$AARD = 1/n\ \Sigma|\Phi_{cal} - \Phi_{exp}|/\Phi_{exp}$, with n= number of points.

5.1. Gibbs-Duhem consistency

The activity coefficients automatically satisfy the Gibbs-Duhem (GD) equation (eqn. (9)) provided they are properly calculated using eqn. (2), from an expression for the Gibbs energy that is extensive [41]. The NRTL and MSA contributions to the Gibbs energy, eqns. (25) and (34), are indeed extensive quantities because each one turns out to be the product of an extensive variable (N_t in eqn. (25) and V in eqn. (34)) by an intensive function ($\overline{\Delta G}^{NRTL}(\{x_i\})$ and $F_v^{MSA}(\{\rho_i\})$, repectively).

At the beginning of this paper, it is mentioned that the quantities Φ and γ_s^* (the osmotic and mean solute activity coefficients at the experimental level) satisfy the GD equation in the form of eqn. (10). It was checked numerically that the MSA-NRTL expressions obtained at this level fulfil eqn. (10). The fulfilment of this condition is quite powerful because it ensures that the analytic expressions for Φ and γ_s have been calculated correctly and that no error is present in the software program.

5.2. Binary aqueous electrolyte solutions

The case of uni-univalent salts in water was first considered. The calculations have been carried out up to the highest concentration for which data are available, at 25°C. The parameters of the model, one MSA parameter and four NRTL parameters, were fitted to experimental data using a Marquardt-type least-square algorithm.

Two types of fits were performed. In procedure (I), eqn. (47) written for $i=s$ was fitted to experimental data by adjusting the parameters $\tau^{(1)}_{mc,ac}$, $\tau^{(2)}_{mc,ac}$ (of eqn. (42)), τ_{cm}, τ_{am} and σ (the MSA mean salt diameter), with the recommended value [9, 10] α=0.2. In procedure (II), it was tried to obtain values for τ_{cm} and τ_{am} that are characteristic of the cation and of the anion considered, respectively. Moreover, the parameter α was allowed to depend on the nature of the salt: α_s. The parameters $\tau^{(1)}_{mc,ac}$ and $\tau^{(2)}_{mc,ac}$ were adjusted as in the first type of fit. The values for salt diameter σ were deduced from previous work [32,34], in which values for individual ionic diameters had been adjusted using a MSA model. The relation $\sigma = (\sigma_c + \sigma_a) / 2$ was used here.

Table 2 Procedure (II): Results for adjusted parameters from fit of osmotic coefficients[a] for aqueous electrolyte solutions.

Salt	m_{max}	$\tau^{(1)}_{mc,ac,}$	$\tau^{(2)}_{mc,ac}$	$\alpha_{mc,ac}$	*AARD*[b] *(%)*
HCl	16	29.57	-20.43	0.180	0.5
HBr	11	34.40	-24.92	0.190	0.4
Hi	10	41.20	-25.48	0.191	0.1
HNO_3	28	19.80	-4.351	0.133	0.9
LiCl	19	33.48	-19.51	0.208	0.8
LiBr	20	38.73	-24.78	0.217	3.4
LiOH	5	17.09	-3.511	0.147	0.9
$LiNO_3$	20	20.16	-6.402	0.153	0.5
NaCl	6	21.80	-13.90	0.204	0.1
NaBr	9	25.35	-12.39	0.203	0.4
NaI	12	27.26	-14.28	0.210	0.09
NaOH	20	32.46	-19.42	0.219	0.5
$NaNO_3$	10	15.94	-2.734	0.135	0.09
KCl	4	23.42	-10.79	0.195	0.06
KBr	5.5	21.59	-9.014	0.188	0.09
KOH	20	32.05	-19.46	0.233	0.9
KNO_3	3.5	15.24	-1.894	0.125	0.4

[a] Experimental values taken from ref [43]. [b] $AARD = 1/n\ \Sigma\ |\Phi_{cal} - \Phi_{exp}\ |/\Phi_{exp}$, with n= number of points.

The results are summarised in Table 1 for procedure (I), and Tables 2 to 4 for procedure (II). The values for the individual ion diameters are collected in Table 5 (notice that, for the alkali cations, the variation of ion size is correlated with expected ionic hydration).

Table 3 Values of τ_{cm} obtained using procedure (II).

Ion	H^+	Li^+	Na^+	K^+
τ_{cm}	-8.5	-7.5	-7.0	-6.8

Table 4 Values of τ_{am} obtained using procedure (II).

Ion	*Cl*	*Br*	*I*	*OH*	NO_3
τ_{am}	-1.9	-2.2	-2.4	-1.4	-4.3

Table 5 Values of ionic diameters for procedure (II).

Ion	H^+	Li^+	Na^+	K^+	Cl^-	Br^-	I^-	OH^-	NO_3^-
σ_{Ion} [a]	5.04	5.43	3.87	3.45	3.62	3.90	4.32	3.55	3.40

[a] in units of 10^{-10} m.

The main comments concerning the results of Table 1, obtained following procedure (I), are basically identical to those given in ref. [10]. The τ_{cm} and τ_{am} values are all negative; because of eqn. (15), this result is consistent with the fact that the ion-solvent interaction dominates the solvent-solvent interaction, remembering that all the *g*'s are expected to be negative because they correspond to attractive forces. The quantity $\tau_{mc,ac}$ (see eqn. (42)) is positive for any composition because the cation-anion attraction is stronger than the cation-solvent attraction. Moreover, $\tau_{mc,ac}$ is found to increase with the salt concentration; since τ_{cm} is constant, this entails that g_{ac} decreases with this parameter, which may be interpreted by increased screening of anion-cation attraction when the salt concentration is increased. The overall quality of the fits, shown in the last column of Table 1, is good. The average absolute relative deviation (AARD) is highest in the case of LiBr; the same result has been obtained before in other studies [39]. Some typical plots are shown in Figures 2 to 4 for the case of LiCl, LiBr, and HNO_3 up to very high salt concentration.

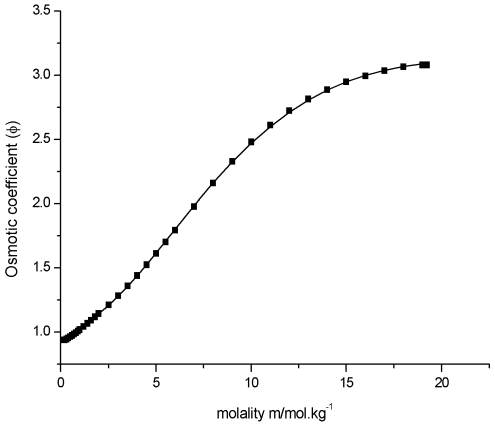

Fig. 2 Osmotic coefficients of LiCl in water at 298.15K according to procedure (I) (parameter values taken from Table 1).(●) : Experimental values taken from ref. [43]. (—) : Calculated curve.

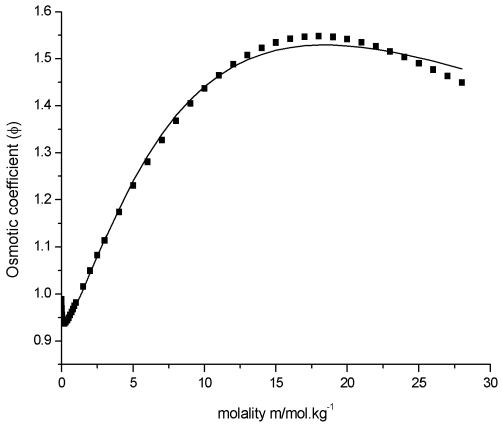

Fig. 3 Osmotic coefficients at 298.15 K of HNO_3 in water according to procedure (I) (parameter values taken from Table 1). (●) : Experimental values taken from ref. [43]. (—) : Calculated curve.

Concerning procedure (II), the results may be interpreted as follows. The adjusted values of $\tau^{(1)}_{mc,ac}$and $\tau^{(2)}_{mc,ac}$ in Table 2 have the same order of magnitude as those of Table 1. The values for α_s are close to 0.2, except in the case of nitrates for which they are somewhat smaller. Those for τ_{cm} in Table 3 are found to increase with the crystallographic size of the cation; this is a satisfactory result since the cation-water interaction (hydration) is expected to decrease when going from Li^+ to K^+. The variation of τ_{am} (Table 4) in the series Cl^-, Br^-, I^- can be explained as follows: for a given cation and a given salt concentration, experiment shows that the activity coefficient of salt increases in the order I>Br>Cl (this may be interpreted as the effect of the increasing size of anion [42, 32]); it is observed using eqn. (44) that the salt activity coefficient increases when τ_{am} (or τ_{cm}) decreases (becomes more negative). An equivalent discussion can be made for the alkali cations, for which the salt activity coefficients are in the order Li>Na>K for a given anion, and the sizes of hydrated cations are in the same order; the variation of τ_{cm} with respect to the ion size is similar to that of τ_{am}. The absolute τ_{am} values are always smaller than the absolute τ_{cm} values because anions of comparable size are usually less hydrated than cation in water.

Table 6 Procedure (I): Results from fit of mean activity coefficients for mixed-solvent solutions (Water-salt parameters taken from to Table 1 and solvent-solvent parameters taken from Table 8).

Ref.	*Solvents*	*Salt*	m_{max}	$\tau^{(1)}_{mc.ac.}$	$\tau^{(2)}_{mc.ac}$	τ_{cm}	τ_{am}	σ [a]	*AARD* [b] *(%)*
[44]	Methanol/Water	LiCl	0.20	10.65	0.667	-0.66	-6.40	6.00	1.5
[45]	Methanol/Water	NaBr	3.05	19.93	-1.008	-0.50	-11.2	5.70	2.8
[46]	Methanol/Water	KCl	3.87	7.342	2.266	-2.71	-4.45	4.90	2.9
[45]	Ethanol/Water	NaBr	4.87	9.890	0.131	-0.56	-3.40	6.30	5.5
[47]	Ethanol/Water	NaCl	2.00	12.34	1.109	-1.50	-6.56	4.10	3.3
[48-50]	Dioxane/Water	HCl	2.00	8.981	-2.146	5.40	2.48	6.70	3.1

[a] in units of 10^{-10} m. [b] $AARD = 1/n\ \Sigma\ |\gamma_{cal} - \gamma_{exp}\ |/\gamma_{exp}$, with n= number of points.

Results for the e-NRTL model are given elsewhere [39] for aqueous electrolyte solutions. Four parameters including two concentration dependent parameters are necessary in this treatment. It is found that in all cases the accuracy of MSA-NRTL description is slightly better than e-NRTL, mostly because of the changes brought to the NRTL part. For multi-

solvent electrolyte solutions, to our knowledge, no studies have been reported in the framework of the e-NRTL model with which our present results could be compared.

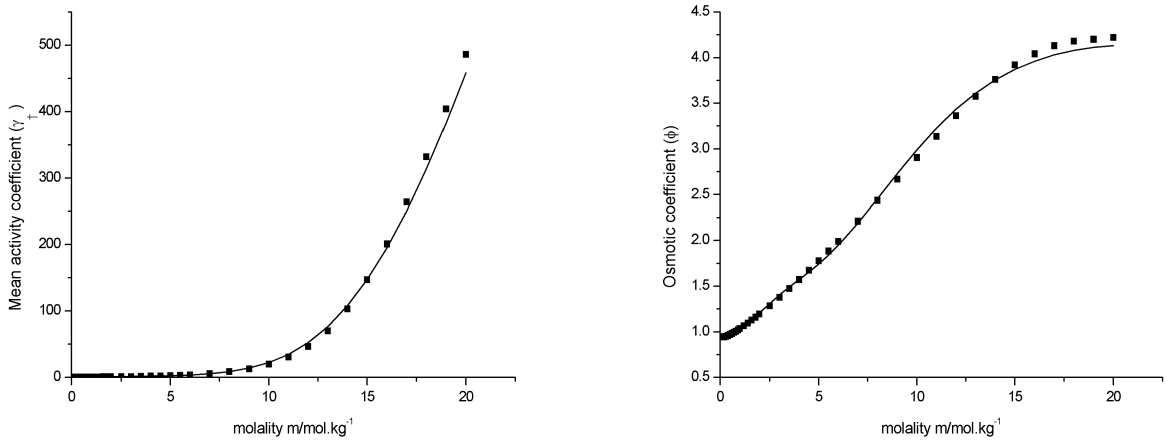

Fig. 4 Osmotic and activity coefficients for LiBr in water at 298.15 K according to procedure (I) (parameters taken from Table 1). Activity coefficients are calculated by using the parameter values obtained from the fit of osmotic coefficients. (●): Experimental values from [43]; (—): Calculated values.

5.3. Ternary systems: one salt in a binary solvent mixture.

The MSA-NRTL model was also used for describing ternary systems composed of one electrolyte and two solvents, one of which being water. As the e-NRTL model, the MSA-NRTL approach is able to describe ternary systems with the use of binary systems parameters only [11, 27]. In the present case, three types of binary parameters are necessary: the water/salt parameters corresponding to the binary electrolyte aqueous solution, the water(=solvent(1))/solvent(2) parameters corresponding to the binary water/solvent(2) mixture, and the salt/solvent(2) parameters corresponding to the binary non-aqueous electrolyte solution. The first two types of parameters have already been calculated. Water/salt parameters are given in the preceding section (see Tables 1-5) and water/solvent(2) parameters were taken from literature [27]. These values are reproduced in Table 8.

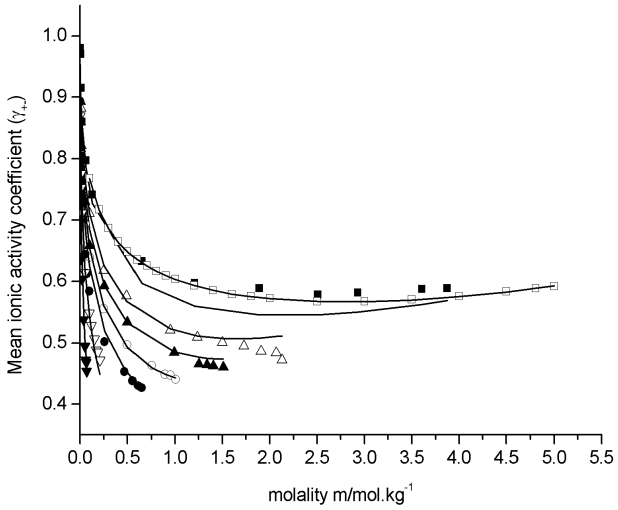

Fig. 5 Activity Coefficients of KCl in methanol/water mixtures (parameters taken from Tables 2-5, 7, 8.) Experimental values taken from ref. [46]: (□) pure aqueous solution [43], (■) 90 wt% water, (△) 80 wt% water, (▲) 60 wt% water, (○) 40 wt% water, (●) 20 wt% water, (▽) 10 wt% water, (▼) 0 wt% water. (—) Calculated curves.

Consequently, the only missing parameters are the five adjustable salt/solvent(2) parameters: the mean ionic MSA diameter σ in this solvent and the four τ NRTL parameters τ_{cm}, τ_{am}, $\tau^{(1)}_{mc,ac}$ and $\tau^{(2)}_{mc,ac}$ (see eqns. (41) and (42) in which *m* designates the non-aqueous solvent. In principle they could be obtained by fitting them to the thermodynamic data of the binary salt/solvent(2) systems. Nevertheless, in order to obtain the best fit for the ternary salt/water/solvent(2) system, we carried out a simultaneous fit of all the available data for the ternary systems.

Table 7 Procedure (II): Results from fit of mean activity coefficients for mixed-solvent solutions (Water-salt parameters taken from Tables 2-5; solvent-solvent parameters taken from Table 8).

Ref.	*Solvent*	*Salt*	m_{max}	$\tau^{(1)}_{mc,ac}$	$\tau^{(2)}_{mc,ac}$	τ_{cm}	τ_{am}	σ	*AARD*[a] *(%)*
[44]	Methanol/Water	LiCl	0.20	9.060	5.466	-4.64	-7.80	6.70	1.0
[45]	Methanol/Water	NaBr	3.05	12.19	-3.528	-4.32	2.12	6.70	5.1
[46]	Methanol/Water	KCl	3.87	8.285	1.792	-2.44	-4.96	4.60	2.9
[45]	Ethanol/Water	NaBr	4.87	12.30	-2.771	3.12	-2.96	6.60	3.3
[47]	Ethanol/Water	NaCl	2.00	4.594	5.584	-1.96	-0.84	4.10	2.9
[48-50]	Dioxane/Water	HCl	2.00	9.234	-2.977	6.52	3.40	6.90	3.4

[a] in units of 10^{-10} m. [b] $AARD = 1/n \, \Sigma \, |\gamma_{cal} - \gamma_{exp}| / \gamma_{exp}$, with *n*= number of points.

The experimental data taken for the adjustments were the mean activity coefficients, γ_s, of the salt at 25°C, obtained by electromotive force measurements. Six systems were studied. They were composed of various simple salts in water/methanol or water/ethanol mixtures; one system was HCl in water/dioxane mixtures.

Table 8 Solvent-solvent NRTL parameters (Values taken from ref. [27]).

Solvents (1/2)	$\tau_{1,2}$	$\tau_{2,1}$	α
Methanol/Water	-0.2249	0.8621	0.3
Ethanol/Water	0.4472	1.4623	0.3
Dioxane/Water	1.1607	0.8177	0.3

For five systems, the γ_s values were adjusted over the whole possible solvent composition from the pure water to the pure organic solvent electrolyte solution. Depending on the set of salt/water parameters chosen (Table 1 or Tables 2 to 5), corresponding to procedures (I) and (II), two sets of salt/solvent(2) parameters were calculated. The different results are summarised in Table 6 and 7, respectively. The average AARD on γ_s is of the order of 3 %. Typical plots are shown in Figures 5 to 7 for the case of KCl in water/methanol mixtures, NaCl in water/ethanol mixtures and HCl in water/dioxane mixtures.

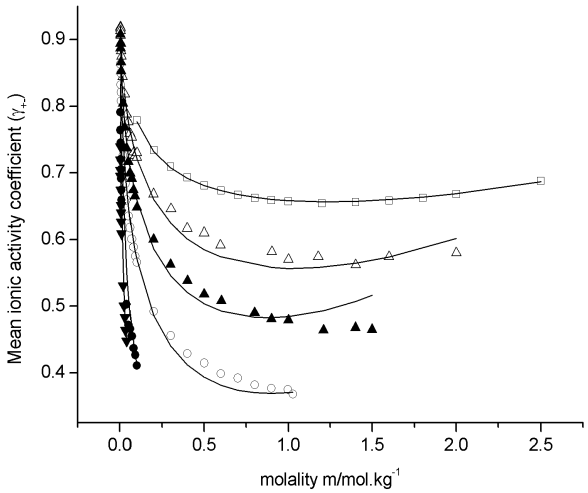

Fig. 6 Activity Coefficients of NaCl in ethanol/water mixtures (parameters taken from Tables 2-5, 7 and 8). Experimental values taken from ref. [47]: (□) pure aqueous solution [43], (△) 80 wt% water, (▲) 60 wt% water, (○) 40 wt% water, (●) 20 wt% water, (▼) 0 wt% water. (—) Calculated values.

Concerning the salt/solvent(2) parameters, the values of σ, $\tau_{mc,ac}^{(1)}$, and τ_{am} and τ_{cm} parameters exhibit a pattern similar to those for the salt/water systems. The positive values observed for τ_{am} and τ_{cm} in the case of dioxane mixtures may be due to the non-polar character of this solvent. However, a few unphysical results may be noticed. So, many values for $\tau_{mc,ac}^{(2)}$ and a few values for τ_{cm} and τ_{am} do not have the same behaviour as the corresponding parameters for aqueous solution. The values for $\tau_{mc,ac}^{(2)}$ are positive in several cases; those for the τ_{am} parameters are generally smaller than the τ_{cm} values. A possible reason for these features is that effects such as association, specific ion-dipole interactions, specific steric effects or preferential solvation occur but are not explicitly taken into account in this type of approach. Another explanation is that the introduction of the sole eqn. (42) might not be sufficient to fully account for the influence of salt on departures from ideality.

Other types of dependencies are currently examined that may yield better representations of these effects in electrolyte solutions. They will be reported in subsequent work.

Acknowledgements

This work is part of a cooperation with the german DECHEMA Institute in Frankfurt. We especially thank Dr. R. Sass and Dr. U. Westhaus from DECHEMA for their constant collaboration and help. We also thank our colleagues from the industry, especially Dr. D. Kleiber (Axiva) and Dr. J. Krissmann (Degussa) for helpful discussions. Financial support from the German Arbeitsgemeinschaft industrieller Forschungvereinigungen "Otto von Guericke" e.V. (AiF) is gratefully acknowledged.

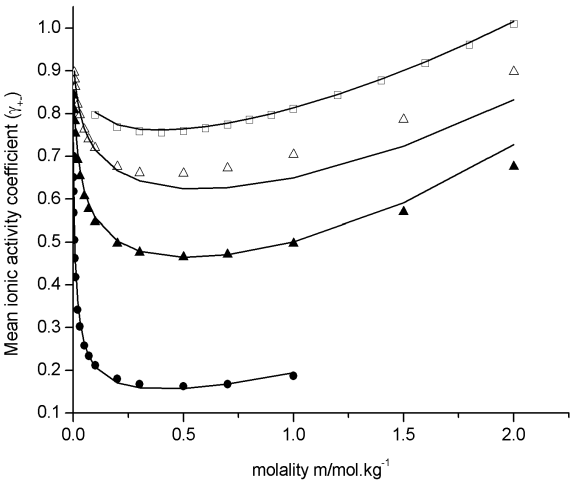

Fig. 7 Activity Coefficients of HCl in dioxane/water mixtures (parameters taken from Tables 1, 6, 8). Experimental values taken from refs. [48-50]: (□) pure aqueous solution [43], (△) 80 wt% water, (▲) 55 wt% water, (●) 30 wt% water. (—) calculated.

References

* To whom correspondence should be addressed.

1 P. Debye and E. Hückel, *Physik Z.*, 1923, **24**, 185.

2 J. C. Rasaiah and H. L. Friedman, *J. Chem. Phys.*, 1968, **48**, 2742.

3 P. S. Ramanathan and H. L. Friedman, *J. Chem. Phys.*, 1971, **54**, 186.

4 P. G. Kusalik and G. N. Patey, *J. Chem. Phys.*, 1988, **88**, 7715.

5 P. H. Fries and G. N. Patey, *J. Chem. Phys*., 1985, **82**, 429.

6 W. Ebeling and K. Scherwinski, *Z. Phys. Chem.*, 1983, **264**, 1.

7 P. Turq, F. Lantelme and H. L. Friedman, *J. Chem. Phys.*, 1977, **66**, 3039.

8 Ph. Bopp, in *The Physics and Chemistry of Aqueous Ionic Solutions*, NATO ASI Series C, ed. M.-C. Bellissent-Funel and G. W. Neilson, Reidel, Dordrecht, Netherlands, 1987, **205**, 217.

9 J. L. Cruz and H. Renon, *AIChE J.*, 1978, **24**, 817.

10 C. C. Chen and L. B. Evans, *AIChE J.*, 1982, **28**, 4.

11 H. Renon and J. M. Prausnitz, *AIChE J.*, 1968, **14**, 135.

12 W. Fürst and H. Renon, *AIChE J.*, 1993, **39**, 335.

13 J. Li, H. M. Polka and J. Gmehling, *Fluide Phase Equilibrium*, 1994, **94**, 89.

14 L. Blum, *Mol. Phys.*, 1975, **30**, 1529.

15 J. P. Simonin, L. Blum and P. Turq, *J. Phys. Chem.*, 1996, **100**, 7704.

16 K. L. Gering and L. L. Lloyd, *Fluid Phase Equilibrium*, 1989, **48**, 111.

17 L. Blum and J. S. Hoye, *J.Phys.Chem.*, 1977, **81**, 1311.

18 J. Schwarzentrüber, H. Renon and S. Watanasiri, *Fluid Phase Equilibrium*, 1989, **52**, 127.

19 Y. X. Zuo, D. Hang and W. Fürst, *Fluide Phase Equilibrium*, 1998, **150-151**, 267.

20 R. A. Robinson and R. H. Stokes, *Electrolyte Solutions, 2nd ed.*, ed. Butterworths: London, 1959.

21 J. M. Prausnitz, R. N. Lichtenthaler and E. Gomes de Azevedo, in *Molecular Thermodynamics of Fluid-Phase Equilibrium*, Prentice Hall, Upper Saddle River, New Jersey, 1999.

22 Aspen Technology Inc., in *ASPEN PLUS Electrolytes Manual*, Cambridge, MA, 1998.

23 K. S. Pitzer, *J. Am. Chem. Soc*., 1980, **102**, 2902.

24 K. S. Pitzer, *Acc. Chem. Res.*, 1977, **10**, 371.

25 K. S. Pitzer, *Ber. Bunsenges. Phys. Chem.*, 1981, **85**, 952.

26 C. C Chen and L. B.Evans, *AIChE J.*, 1986, **32**, 444.

27 B. Mock, L. B. Evans and C. C. Chen, *AIChE J.*, 1986, **32**, 1655.

28 J. K. Percus and G. Yevick, *Phys. Rev.*, 1964, **136**, B290.

29 J. L. Lebowitz and J. K. Percus, *Phys. Rev.*, 1966, **144**, 251.

30 E. Waisman and J. L. Lebowitz, *J. Chem. Phys.*, 1970, **52**, 4307; *ibid.*, 1972, **56**, 3086.

31 L. Blum, in *Theoretical Chemistry: Advances and Perspectives*, ed. H. Eyring and D. Henderson, Academic Press, New York, 1980, vol. 5, p. 1.

32 J. P. Simonin, O. Bernard and L. Blum, *J. Phys. Chem. B*, 1998, **102**, 4411.

33 T. Sun, J. L. Lénard and A. S. Teja, *J. Phys. Chem.*, 1994, **98,** 6870.

34 J. P. Simonin, *J. Phys. Chem. B,* 1997, **101**, 4313.

35 L. Blum and D. J. Wei, *J. Chem. Phys.*, 1987, **87**, 555.

36 W. G. McMillan and J. E. Mayer, *J. Chem. Phys.*, 1972, **54**, 1523.

37 L. Blum and M. Ubriaco, *Physica A*, 2000, **279**, 224.

38 P. Novotny and O. Sohnel, *J. Chem. Eng. Data*, 1988, **33**, 49.

39 V. Abovsky, Y. Liu and S. Watanasiri., *Fluid Phase Equilibrium*, 1998, **150-151,** 277.

40 H. S. Harned and B. B. Owen, in *The Physical Chemistry of Electrolyte Solutions*, ed. ACS, New York, 1958.

41 K. S. Pitzer, in *Activity Coefficients in Electrolyte Solutions*, ed. CRC, Boca Raton, 1991, 157.

42 P.W. Gurney, *Ionic Processes in Solution*, Dover, New York, 1953.

43 W. J. Hamer and Y.-C. Wu, *J. Phys Chem. Ref. Data*, 1972, **1**, 1047.

44 D. S. P. Koh, K H. Khoo and C.-Y. Chan, *J. Solution Chem.*, 1985, **14**, 635.

45 S. Han, S. H. Pan, *Fluid Phase Equilibrium*, 1993, **83**, 261.

46 L. Mahalias and O. Popovych, *J. Chem. Eng. Data*, 1982, **27**, 105.

47 M. A. Esteso, O. M. González-Diaz, F. F. Hernández-Luis and L. Fernández-Mérida, *J. Solution Chem.*, 1989, **18**, 277.

48 H. S. Harned and J. G. Donelson, *J. Am. Chem. Soc.*, 1938, **60**, 336.

49 H. S. Harned and J. G. Donelson, *J. Am. Chem. Soc.*, 1938, **60**, 2128.

50 H. S. Harned, J. G. Donelson and C. Calmon, *J. Am. Chem. Soc.*, 1938, **60**, 2133.

C. Application of the MSA NRTL Model to high temperatures

As in the case of the MSA model, the extension of the MSA-NRTL to the description of aqueous electrolyte solutions up to high temperatures has been studied.

To that end, different temperature dependencies have been introduced, considering the followingpoints :

- The MSA term is only a small contribution to the thermodynamic coefficients γ and ϕ. Therefore, the introduction of a temperature dependence into the MSA parameters can be neglected. The permittivity and the density of solvent are temperature dependent, as it is known that density and permittivity vary much with temperature. The temperature dependencies of both quantities can be found in the literature.
- In the NRTL term, the introduction of a temperature dependence has been avoided for τ_{cm} and τ_{am} parameters. Since these two parameters are common for salts with ??? (que veux tu dire ?) ions (Procedure II ofthe preceding section), it is not possible at this step of the development to fit ion-specific temperature dependent parameters.

1. Temperature dependence of parameters

Considering these two aspects, only $\tau_{cm,am}$ and α were adjusted in temperature. Three types of temperature dependences have been tried, namely linear, inverse linear and square functions of temperature.

$$X = X^{298} + X^{T}\left(T - 298.15\right) \tag{6. 23}$$

$$X = X^{298} + X^{T}\left(\frac{1}{T} - \frac{1}{298.15}\right) \tag{6. 24}$$

$$X = X^{298} + X^{T}\left(T - 298.15\right)^{2} \tag{6. 25}$$

with X the adjusted parameter, X^{298} the parameter adjusted at 298K as given in the preceding section, and X^{T} the new adjusted parameter.

$\tau_{mc,ac}$, as it has been written in the preceding section (see eqn. (16)), includes an inverse linear temperanture dependence due to the Boltzmann factor. The $\tau_{mc,ac}$ parameter is

also concentration dependent, as it is detailed in eqn. (42) of the preceding section. This leads to

$$\tau_{mc,ac} = \frac{298}{T}\left(\tau^{1}_{mc,ac} + \tau^{2}_{mc,ac} x_w\right) \qquad (6.\ 26)$$

with $\tau^{1}_{mc,ac}$ and $\tau^{2}_{mc,ac}$ adjusted as a function of temperature following eqn. (6.23) to (6.25)

These dependencies have been introduced first in α, then in $\tau_{mc,ac}$, and finally in both parameters.

2. Results

Aqueous LiCl and NaCl solutions have been fitted. Data for the LiCl solutions at high temperatures have been taken from Gibbard et al. [6] and the osmotic coefficients have been fitted from 298 to 373K. Data for the NaCl have been taken from Gibbard et al. [7] in which values for the osmotic coefficients between 273 and 373K are collected.

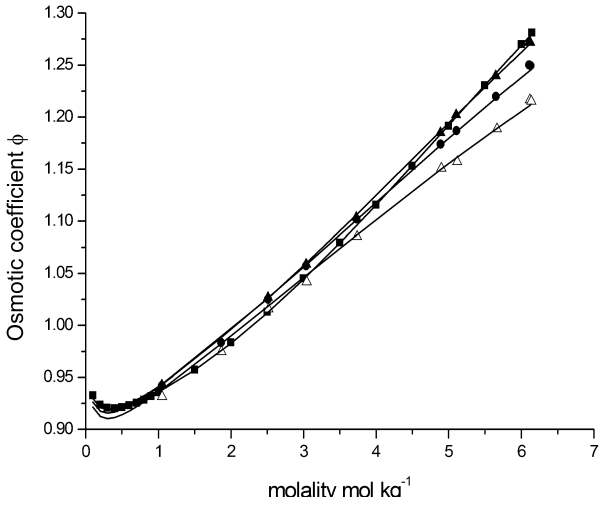

Figure 6.1- Experimental and calculated values of the aqueous NaCl solutions osmotic coefficients at different temperatures. (—): calculated values; (■): 298K; (▲): 323K; (●): 348K; (△): 373K.

The description of LiCl solutions is important since LiCl is soluble in water up to 20 M in the range of temperature 298-373K. Besides, the osmotic coefficients show a monotonous decrease from 298 to 373K, which make it easier to describe. The NaCl does not

[6] H. F. Gibbard Jr. and G. Scatchard, *J. Chem. Eng. Data*, 1973, **18**, 293.
[7] H. F. Gibbard Jr., G. Scatchard, R. A. Rousseau and J. L. Creek, *J. Chem. Eng. Data*, 1974, **19**, 282.

reach concentrations higher than 6M, but exhibits an irregular behaviour between 298 and 373K (see Figure 3.7, chapter III, section 6).

The best compromise between the overall amount of parameters and the accuracy of fit has been found with four parameters. The α and $\tau_{mc,ac}$ parameters have the following temperature dependences:

$$\tau_{mc,ac} = \frac{298}{T}\left[\tau_{mc,ac}^{1,298} + \tau_{mc,ac}^{1,T}\left(\frac{1}{T} - \frac{1}{298.15}\right) + \left(\tau_{mc,ac}^{2,298} + \tau_{mc,ac}^{2,T}\left(\frac{1}{T} - \frac{1}{298.15}\right)\right)x_w\right] \quad (6.\ 27)$$

$$\tau_{mc,ac} = \alpha^{298} + \alpha^{1,T}\left(T - 298.15\right) + \alpha^{2,T}\left(\frac{1}{T} - \frac{1}{298.15}\right) \quad (6.\ 28)$$

Results are collected in Table 6.1. Experimental and calculated osmotic coefficients have been plotted in Figure 6.1 for the NaCl solutions and in Figure 6.2 for the LiCl solutions. Parameters α^{298}, $\tau^{1,298}$ and $\tau^{2,298}$ are given in table 1 in the preceding section. These values of the parameters have been used in order to obtain the best fit.

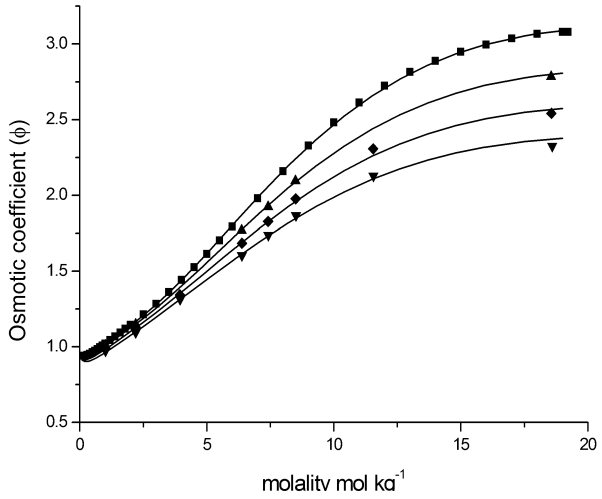

Figure 6.2- Experimental and calculated values of the aqueous NaCl solutions osmotic coefficients at differnet temperatures (—) calculated values (■) 298 K (▲) 323 K. (♦) 348 K (▼) 373 K

Table 6.2- Results from fit of osmotic coefficients at different temperatures.

	T range	m_{max} [a]	$10^4\alpha^{1,T}$ [b]	$\alpha^{2,T}$ [c]	$\tau^{1,T}_{mc,ac}$ [c]	$10^{-5}\tau^{2,T}_{mc,ac}$ [c]	AARD (%)
LiCl	298-373K	18	6.1918	0.8519	1083776.	-10.5465	0.47
NaCl	273-373K	6	4.3704	20.861	563050.4	-4.8506	0.21

[a]: In units of $mol.kg^{-1}$. [b]: In units of K^{-1}. [c]: In units of K.

One observes that the accuracy of the fit is quite satisfactory. For the case of the NaCl solution, the osmotic coefficients at 298, 323, 348 and 373 (see Figure 6.2) are well described.

For the LiCl solutions, the accuracy is poorer. The study of results shows that the deviation is high above 11 mol kg^{-1}. The fit of the data up to 11 mol kg^{-1} yields an AARD of 0.33 %.

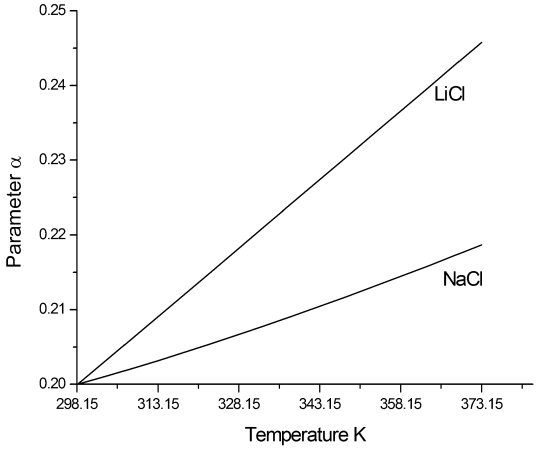

Figure 6.3- Plot of the α parameter for LiCl and NaCl solutions as function of the temperature.

Plots of α and $\tau_{mc,ac}$ as a function of temperature are given in plots 6.3 and 6.4. One observes that for the two salts, the α parameter varies much with temperature, from 0.2 to 0.23, in the temperature range 298-373 K. The general increase of the α parameters for both salts is coherent with the idea that the number of surrounding particles decreases with temperature, since particles will gain in mobility. As a result, the distribution of particles is more random, leading to higher values of α (α=1 corresponds to a complete random distribution of particles).

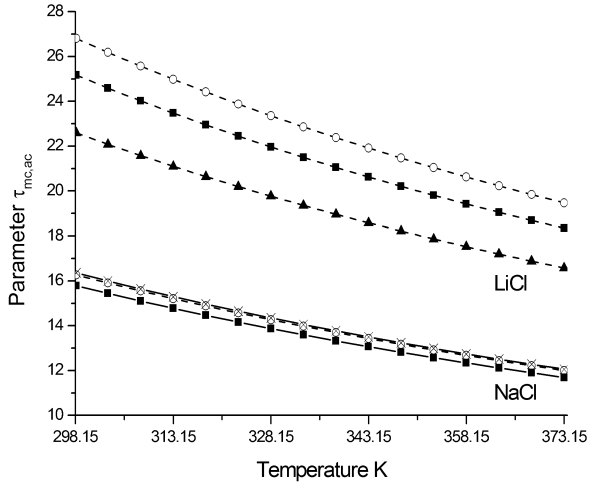

Figure 6.4- Plot of the $\tau_{mc,ac}$ parameter for LiCl and NaCl solutions as function of the temperature and at different molalities of salt. (—): NaCl solutions. (– –): LiCl solutions. (○): 0.1M electrolyte solution. (×): 1M electrolyte solution. (■): 6M electrolyte solution. (▲): 18M electrolyte solution

The study of the values of the α parameters for both systems reveals that the temperature dependence of α in the case of LiCl solutions is, unlike NaCl, nearly linear. Table 6.2 shows that $\alpha^{2,T}$ is high for NaCl and low for LiCl. Figure 6.3 shows that the curve of α as a function of temperature for LiCl is linear, whereas the curve of α for NaCl exhibits a slope that increases slowly with temperature. hyperbolic behaviour. As a result, the neglection of th $\alpha^{2,T}$ parameter in the fit of LiCl osmotic coefficients yield an AARD (0.50%) close to the one obtained with 4 parameters (see Table 6.2).

The $\tau_{mc,ac}$ parameters decreases with temperature for the two systems. Since it has been assumed that τ_{cm} and τ_{am} are independent of temperature (i.e. g_{cm}, g_{am}, and g_{mm} independent of temperature) this implies that g_{ac} decreases with temperature. This behaviour is satisfactory since it is expected that interactions between particles decrease with temperature.

It can be observed from Figure 6.4 that the influence of the concentration on $\tau_{mc,ac}$ is much more important in the case of LiCl solution than in the case of NaCl solutions. That implies that the temperature adjustment of $\tau^2_{mc,ac}$ is more important for LiCl solutions than for NaCl solutions. The neglect of the temperature dependence of $\tau^2_{mc,ac}$ for the NaCl solutions yields to a similar AARD (0.22%), whereas it leads to a loss of accuracy in the case of LiCl (0.67%).

D. MSA-NRTL, e-NRTL and MSA models

As we saw above in section 3, the MSA-NRTL is an accurate model for the description of thermodynamic coefficients of aqueous electrolyte solutions. In order to understand the model, it is interesting to study the importance of long-range MSA and short-range NRTL contributions in the MSA-NRTL model, and also to compare the MSA-NRTL model to other models, such as the e-NRTL and the MSA models.

1. MSA and NRTL contributions to the MSA-NRTL model

Figure 6.3 plots the short-range NRTL and long-range MSA contributions to the osmotic coefficients of LiCl at 298K calculated with the MSA-NRTL model. Worth of note is that the electrostatic term quickly reaches an asymptotic value of –0.2. This shows that the

electrostatic term is only relevant at low concentrations. This is consistent with the two following arguments.

First, electrostatic terms are introduced in free Gibbs energy models for electrolyte solutions so that the resulting equations follow the Deby-Hückel Limiting Law at very low concentrations. Thus, it is coherent to observe that the electrostatic term varies much at low concentrations (according to the DH limiting law), while the short-range NRTL term is very small. Second, the electric charges are shielded at high concentrations, because ions are very close to each other. At short distances, i.e. high concentrations, the electrostatic effects are lowered and tend to a constant value. This yields a low value asymptotic curve at high concentrations.

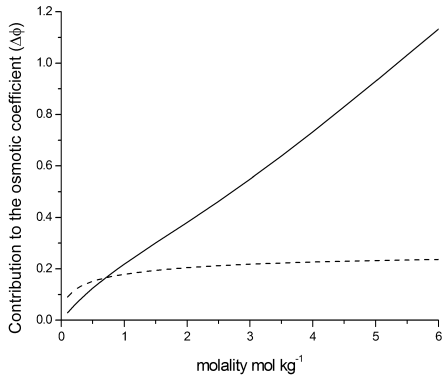

Figure 6.5- MSA and NRTL contributions to excess osmotic coefficient at 298 K. (—): $\Delta\phi^{NRTL}$. (---): $\Delta\phi^{MSA}$. $\phi = -1/(nmM)[\ln(x_w)] + \Delta\phi^{NRTL} + \Delta\phi^{MSA}]$.

Figure 6.5 also shows that the NRTL term is the most important contribution to the osmotic coefficient. This explains the necessary improvement brought to the NRTL term for extending it to highly concentrated electrolyte solutions. The introduction of a concentration dependence in $\tau_{mc,ac}$ and the relaxation of the assumption on τ_{cm} and τ_{am} leaded to a more flexible NRTL term, allowing a better description of thermodynamic coefficients.

2. Comparison between MSA-NRTL and e-NRTL

The e-NRTL model[8] is similar to the MSA-NRTL model, with the two following exceptions. First, the electrostatics are described with the Pitzer-Deby-Hückel equation (PDH). Second, it is assumed that $\tau_{cm} = \tau_{am}$, and that both τ_{cm} (i.e τ_{am}) and $\tau_{mc,ac}$ are concentration dependent.

[8] C. C. Chen, H. I. Britt, J. F. Boston and L. B. Evans, *AIChE Journal*, 1982, **28**, 588

For aqueous solutions, the Pitzer term is similar to our MSA term. In this regard, the less accurate results obtained by Abovsky et al.[9], with a version of the e-NRTL model extended to high concentrations, is only due to the assumptions made in the NRTL model, and not to the PDH term.

The main difference between long-range terms in the e-NRTL and MSA-NRTL models lies in the fact that the MSA better describes the electrostatic effects in non-aqueous solvents. To describe the long-range interactions of electrolytes in solvent mixtures, the e-NRTL model uses the Pitzer term with the parameters defined for the aqueous solution, and add to the latter a Born term, accounting for the variation of the solvent dielectric constant. This is not needed in the MSA term, since it uses the experimental dielectric constant of solvent.

3. Comparison between MSA-NRTL and MSA

Concerning the MSA model, Simonin[10] plotted the different contributions of the MSA model to the osmotic coefficients of LiCl at 298K. To that end, eqn. (3.33) is rewritten as follows

$$\Delta\phi^{MSA} = \Delta\phi_0^{MSA} + \Delta\phi_{corr}^{MSA}$$

$$\Delta\phi^{HS} = \Delta\phi_0^{HS} + \Delta\phi_{corr}^{HS}$$

with $\Delta\phi_0^{MSA}$ the first term of the right-hand-side of eqn. (3.33) and $\Delta\phi_{corr}^{MSA}$ the second and third terms of the right-hand-side of eqn. (3.33). $\Delta\phi_0^{HS}$ is the first term of the right-hand-side of eqn. (3.38) and $\Delta\phi_{corr}^{HS}$ the second term of the right-hand-side of eqn. (3.38)

The different contributions are plotted in Figure 6.6. As in the MSA-NRTL model, one observes the same asymptotic behaviour for the electrostatic MSA contribution when the correction due to the concentration dependence of the MSA parameters is not taken into account (neglect of the second and third term on the right-hand side of eqn. (3.33)).

One also observes that the short-range term is predominant at high concentrations. It is important to note that the successful development of an electrolyte model lays as much in the use of an coherent electrostatic term (in order ot follow the Deby-Hückel Limiting Law), as in the use of an improved short-range term, such as our modified NRTL term, or the concentration dependent HS term.

[9] V. Abovsky, Y. Liu and S. Watanasiri., *Fluid Phase Equilibrium*, 1998, **150-151,** 277.
[10] J. P. Simonin, *J. Phys. Chem. B*, 1997, **101**, 4313

Since it can be observed from Figure 6.6 that the correction "MSA corr" is important at high concentrations, as compared to the "MSA 0" term, an interesting improvement of the MSA contribution to the MSA-NRTL model would be to use the unrestricted version of the MSA model with a concentration dependence in the MSA parameter

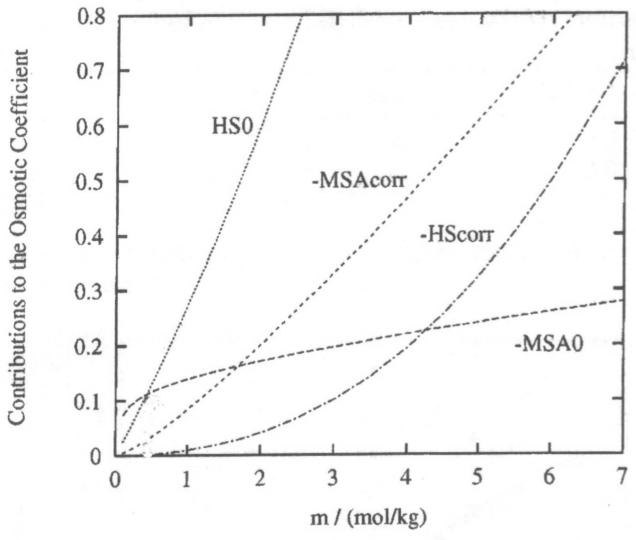

Figure 6.6- Contribution to the osmotic coefficient (at the MM level): HS0 is for Df_0^{HS}, and -HScorr, $-MSA_0$,and -MSAcorr are for the opposites of $\Delta\phi_{corr}^{HS}$, $\Delta\phi_0^{MSA}$ and $\Delta\phi_{corr}^{MSA}$, respectively.

Chapter VII- Conclusion

Two closely related subjects have been studied in this work. First, a physical and statistically consistent model, the MSA model, has been applied to complex solutions. Second, a semi-empirical electrolyte model, the MSA-NRTL model has been developed for the description of industrially relevant systems. The MSA model is a coherent and physical model from the statistical mechanical point of view. However it is a continuous solvent model, with obvious consequences associated to this simplification

.

MSA has been applied to geological systems such as the LiCl hydrates, found in geological layers. These aqueous inclusions in rocks reach very high concentration of LiCl at high temperatures, such as 30 mol/kg at 370K. The MSA model accurately describes the thermodynamic coefficients of such solutions, allowing us to calculate the solubility constant for the LiCl hydrates. The Pitzer model in this case, could not be used for these high solute concentrations.

In a second case, the MSA model has been used for describing solubility pressures of carbon dioxide dissolved in aqueous electrolyte solutions. These systems are complex chemical solutions, in which neutral and charged species coexist. Furthermore, several chemical equilibria occur, relating neutral and charged species. Moreover, vapour-liquid equilibria occur between neutral volatile species, such as carbon dioxide, water or acetic acid. All species could be modelled with the MSA model. In this case, neutral species were taken as hard spheres.

The first success of the model lies in the values of neutral species diameters adjusted with the MSA model, yielding values very close to literature ones, or to that predicted by programs (MOPAC for instance). For instance, the infinite dilution diameter of carbon dioxide is found to be 3.2 Å, whereas the MOPAC package calculate a diameter of 3.1 Å for the carbon dioxide molecule in the vacuum. For the acetic acid, the MSA model finds an optimum value of 6.4 Å , whereas the MOPAC package calculates a diameter of 5.1 Å. Moreover, the MSA model succeeds in describing carbon dioxide pressures with very satisfying precision in the pressure range of 10^5-10^7 Pa.

The MSA parameters adjusted for these systems were binary solute-solvent parameters (NaCl/water or CO_2/water parameters). A few CO_2/salt cross parameters however needed be introduced to improve the quality of fits. The binary salt/water parameters were obtained by fitting aqueous electrolyte solutions. For the neutral species/water parameters, however, the lack of data on binary systems made it impossible to adjust these parameters, so that they were adjusted directly to the ternary salt/CO_2/water systems. The resulting binary CO_2/water parameters were common to all ternary systems studied, and accurately described the available data on aqueous carbon dioxide solutions.

These two studies are the first application of the unrestricted primitive MSA model to such complex solutions. The MSA model is able to describe a variety of chemical ionic solutions.

In contrast to Pitzer, the MSA parameters have a physical meaning. The $\sigma^{(0)}_{Na+}$ corresponds to the diameter of Na^+ in solution, whereas the meaning of the $\beta_{Na\text{-}Na}$ parameter in the Pitzer model is less simple. The number of adjustable MSA parameters is also smaller than the number of Pitzer parameters, especially for the cross parameters, as it has been observed in the description of aqueous electrolyte CO_2 solutions. One can conclude that the MSA model gives results that are at least as good as those obtained with the Pitzer model, but with fewer parameters that have a physical meaning.

The MSA model seems to be a promising model for the development of theoretical models. More systems nevertheless need to be studied in order to valid the model and confirm its interest and ability in describing chemical solutions. This also must be done in order to accumulate parameter values, leading later to the prediction of solution properties.

The second subject studied in this work concerned the development of a molecular semi-empirical electrolyte model. The drawback of the primitive MSA model is that it accounts for the solvent only through its dielectric constant. In a molecular model, the solvent is explicitly taken into account. Most of these models are empirical and the solvent and solute descriptions are simplified, hence limited.

The MSA-NRTL model that was studied here has been successfully applied to aqueous electrolyte solutions up to the saturation concentration for most salts. It has also described ternary mixtures composed of water, organic co-solvent and one salt. The advantage of this model is that it does not require any ternary parameter to model ternary systems. In the case of ternary systems, three types of binary parameters are necessary:

salt/water, water/solvent$_2$ and salt/solvent$_2$ parameters. The first two types of parameters were obtained by fitting aqueous electrolyte solutions data and using literature values obtained from the fit of solvent mixtures data. The salt/solvent$_2$ parameters could not be adjusted in the same way since not enough data were available. Thus, they were adjusted by fitting ternary system data. The problem is that it is not guaranteed that these salt/solvent$_2$ parameters will describe well the binary salt/solvent$_2$ systems.

A preliminary study of the description of aqueous electrolyte solutions at temperature above 298 K with the MSA-NRTL model has been done. The good precision reached with only a few parameters is encouraging. The description of thermodynamic coefficients is important since it allows the description of enthalpies and heat capacities. To reach these quantities, one needs a very accurate representation of the thermodynamic coefficients, especially considering the temperature behaviour of the coefficient curves. The aqueous NaCl solution, for instance, exhibits an osmotic coefficient curve that increases from 298 to 323 K and decreases above 323K (see figure 3.5). This non monotonous behaviour has to be precisely described by the model to get accurate values for the dilution enthalpy of the solution and other quantities obtained by the differentiationof the primary thermodynamical quantities.

This investigation still needs to be carried on in order to make the MSA-NRTL model able to describe enthalpies and calorific capacities of electrolyte systems.

In the meantime, however, this model requires to be extended and modified. The present MSA term in the model can be easily changed to the unrestricted primitive model term, leading to still simple equations, and a more precise description of salt effects at low concentrations.

Besides, the NRTL is an empirical model. This confers him the ability to describe in a simple way solvent species, but with less physical parameters. The NRTL model as it is built does not explicitly take entropic effects (such as steric effects or the influence of molecule shapes) into account, despite the introduction of the α parameter which is related to the number of neighbouring molecules around a particle. The introduction of a hard sphere term, for example, could take the missing effect into account.

In order to further progress, it will also be necessary to find alternatives to the NRTL term. More physical models, including specific ion-solvent interactions (structure-making, structure-breaking effects) and ion-ion interactions (dispersion terms), are to be developed in order to describe the short-range term in a more physical way. First attempts in this direction are currently undertaken.

Models developed in the discrete solvent framework could also represent a good alternative, such as the MSA discrete solvent model. Nevertheless, their complexity and their high sensitivity to parameter values (e.g in the case of the MSA discrete solvent model), makes it difficult to use them for the description of complex solutions.

Diese Arbeit präsentiert Möglichkeiten und Vorteile der thermodynamischen Modellierung komplexer geladener chemischer Systeme, die sowohl in der Natur als auch in industriellen Verfahren zu finden sind. Die Arbeit setzt zwei Schwerpunkte: die Anwendung des statistischen MSA-Modells auf komplexe geladene Systeme, und die Anwendung eines auf industrielle Bedürfnisse ausgerichteten Modells (Modell MSA-NRTL).

Die Errechnung verschiedener thermodynamischer Größen anhand des an hohe Temperaturen angepassten MSA-Modells war im Falle von LiCl-Lösungen mit zufriedenstellender Genauigkeit möglich.

Das Vorhandensein von Salz in wässrigen Lösungen kann die Auflösung von flüchtigen Stoffen beträchtlich beeinflussen. Untersucht wurde der Fall von Kohlendioxid in verschiedenen Elektrolytlösungen. Mit Hilfe des MSA-Modells konnte der Löslichkeitsdruck bei dieser Art von Systemen beschrieben werden.

Was die Entwicklung eines Anwendungsmodells betrifft, wurde das Modell MSA-NRTL erarbeitet. Die teilweise Kombination des MSA-Modells mit dem NRTL-Modell erlaubte die Modellierung von Elektrolytlösungen bei hohen Temperaturen und mit einem oder zwei Lösungsmitteln.

This work present the interests and abilities of the thermodynamic modelling of complex charged chemical systems. These systems are to be found in natural mediums as well as in industrial processes. Two ways of research have been followed here: the application of the MSA model to complex systems, and the development of an applied model oriented towards industrial needs (MSA-NRTL model).

The prediction of thermodynamic quantities with the help of the MSA model, adapted to high temperatures, has been possible in the case of LiCl hydrates, within a satisfactory accuracy.

The presence of salt in aqueous solutions can influence most the solubilisation of volatile species. The case of carbon dioxide in several electrolyte solutions have been studied. The MSA model was able to describe the solubility pressures of such systems.

Concerning the development of applied models, the MSA-NRTL has been elaborated, by combining a part of the MSA model with the NRTL model. This allowed the description of electrolyte solutions with one and two solvents and at high temperatures.